South Atlantic Δ_{47}-based deep sea temperatures reveal underestimation of Early Cenozoic warming and lack of understanding in application of $\delta^{18}O$-temperature proxy

Master Thesis
GEO-4 1520

Brendan Oerlemans
7079303

Supervisors:
Prof. Dr. Lucas Lourens
Dr. Martin Ziegler
MSc Tobias Agterhuis

Utrecht University

Faculty of Geosciences
Utrecht University
The Netherlands
May 27, 2023

Abstract

Climate evolution during the late Paleocene (60 - 56 Ma) might be the best analogue to near-future climate change. At over a 1,000 ppm atmospheric CO_2 levels were similar to what we expect to reach by the end of the century under continued emission and kept rising until the reversal of CO_2 and temperature at the enigmatic Early Eocene Climatic Optimum (EECO, 50 - 52 Ma). Applying clumped isotope thermometry (Δ_{47}) to deep sea sediments in the South Atlantic this study finds robust deep sea temperatures that are 4 to 8 °C higher than previously estimated. These findings put our understanding of the commonly used $\delta^{18}O$-paleothermometer to test. Furthermore, reconstructed $\delta^{18}O_{SW}$ values cast doubt on the assumption that the Cenozoic earth was free of ice until large scale glaciation started at 34 Ma. Elevated South Atlantic deep sea temperatures are corroborated by other deep sea clumped isotope studies that consistently report higher temperatures than previous estimates throughout the entire Cenozoic and across different ocean basins. Because deep sea temperatures are linearly related with global mean surface temperatures this increased temperature puts new estimates of Earth System Sensitivity at the high end (6 to 8 °C temperature increase per doubling of CO_2) of previous projections.

Contents

1 Introduction

Heatwaves, drought, wildfires, storms and floodings become more frequent and more severe. They are the challenges mankind has to face as a consequence of a changing climate (Seneviratne et al., 2021) Both the number of people and the severity with which they are affected by these disasters is dependent on the magnitude of change. First and foremost this magnitude is eventually determined by the cumulative amount of greenhouse gasses (GHG's, most notably CO_2) mankind chooses to emit into the atmosphere (Eyring et al., 2021). However, the exact coupling between GHG emissions and climate response is governed by a number of uncertainties, all of which ultimately depend on our lack of understanding of physical and geochemical processes and long- and short-term feedback mechanisms in the climate system (Anagnostou et al., 2016; Gulev et al., 2021; Tierney et al., 2020).

Among the issues not fully resolved are I) the relationship between global average surface temperatures and atmospheric CO_2 levels , II) the effect of this temperature change on the volume of earth's cryogenic reservoirs and implicitly sea-level and III) the timescales on which these changes take place. Climate models aim to resolve these issues by simulating earths climate system, but their application is yet limited. This is because of our lack of understanding of all mechanisms and processes at play and the lack of computational power required to resolve these simulations on the highest spatial and temporal resolution. For these reasons, climate models require parametrization and constraining boundary conditions that can only be acquired from real world scenarios. As we only have one world to play around with, for these real world scenarios we look back in time and reconstruct climatic changes during episodes of the geologic past that are analogous to future climate change under different emission scenarios.

The Paleocene and Eocene (66 - 34 Ma) are marked by atmospheric CO_2 levels over a 1,000 ppm (Rae et al., 2021) that could well be reached by the end of the 21st century under high growth and low mitigation scenarios (Masson-Delmotte et al., 2021). According to proxies for deep sea temperatures (DSTs), sea surface temperatures (SSTs) and land air temperature (LATs) Global Mean Surface Temperatures (GMSTs) in this period were much warmer than those experienced today (Hansen et al., 2013; Inglis et al., 2020). Although a relationship between temperature and atmospheric CO_2 has been established beyond reasonable doubt, quantification of this relationship has proven to be more difficult (Knutti et al., 2017; Stevens et al., 2016). The latest IPCC AR6 WGI report ranges an Earth Climate Sensitivity (ECS, warming per instantaneous doubling of atmopsheric CO_2) of 2 to 5 °C very likely, but does not exclude a stronger response. Transient Climate Response (TCR) and Earth System Sensitivity (ESS) are nowadays coined as more suitable parameters for climate change on a longer term as these provide for a gradual increase of atmospheric CO_2 and allow ocean buffering capabilities (10^1 - 10^2 years) and long-term feedback mechanism like ice-sheet growth, changes in vegetation cover and deep-sea temperature variations (10^3 years) to kick in respectively. Because the mechanisms that are believed to have led to early Cenozoic warm temperatures are not determined by atmospheric CO_2 forcing only, Earth System Sensitivity in this high-emission analogous climate system is poorly constrained. Deep ocean temperatures serve as good indicator for climate variability on the longer term (>10^3 years) due to their sluggish response to atmospheric forcing. Moreover, as physical property, DSTs across multiple basins can be compared to assess potential deep water exchange, which in turn can provide clues to deep water formation sites and the extent of oceanic overturning systems.

For decades, bottom water temperatures have been reconstructed from the ratio of oxygen isotopes ($\delta^{18}O$) in seafloor dwelling carbonate shell-forming organisms: benthic foraminifera. Applying this method in deep time, however, requires a series of assumptions that influence reliability. A novel approach, clumped isotope thermometry (Δ_{47}), quantifies the excess abundance of the rare oxygen and rare carbon isotope in the same

carbonate molecule with respect to a stochastic distribution of its constituents. This method requires less assumptions and thus provides more robust temperature estimates. Recent efforts at establishing a Cenozoic deep sea temperature record based on primarily North Atlantic benthic foraminiferal Δ_{47}-values provide disconcertingly higher and more variable temperatures than previously observed (Meckler et al., 2022).

By establishing a Paleogene South Atlantic Δ_{47}-record and comparing this with the North Atlantic temperatures, this study aims to verify the global applicability of these data and discern a global temperature signal from potential inter-basin deep sea temperature variations. Along providing insight into the mechanisms leading to the hot late Paleocene and early Eocene climates, these comparative records may severely affect our understanding of the roles of CO_2 and the connectivity between the different Atlantic basins in the early Cenozoic climate.

2 Background

The sections in this chapter serve to provide a reference framework for understanding the methodology outlined and results discussed in this study. Though each of these subjects is worthy of a library at its own but outside the scope of this study, the information provided here was intentionally kept at bare minimum. Sources cited in text provide further reading.

2.1 Cenozoic climate

After a dominantly constant warm Paleozoic (541 - 252 Ma) and Mesozoic (252 - 66 Ma) the Cenozoic (66 - 0 Ma) is marked by long-term secular cooling, interrupted by a shorter episode of global warming during the late Paleocene-early Eocene (58 – 48 Ma) (Rohling, 2017) leading to the Early Eocene Climatic Optimum (EECO; 52 – 50 Ma). Temperatures peaked during the EECO and additional short-lived hyperthermal events occurred superimposed on the warming trend. The most pronounced of these is the Paleocene Eocene Thermal Maximum (ETM1, commonly PETM, 56.0 Ma), which marked the start of the Eocene. The PETM is followed by hyperthermals ETM2 at 54.0 Ma and ETM3 at 52.9 Ma (Westerhold et al., 2020). Overprinted on the entire Cenozoic record is the climatic response to variations in astronomical forcing that operates on timescales of 10^4 to 10^6 years (see figure 2.1).

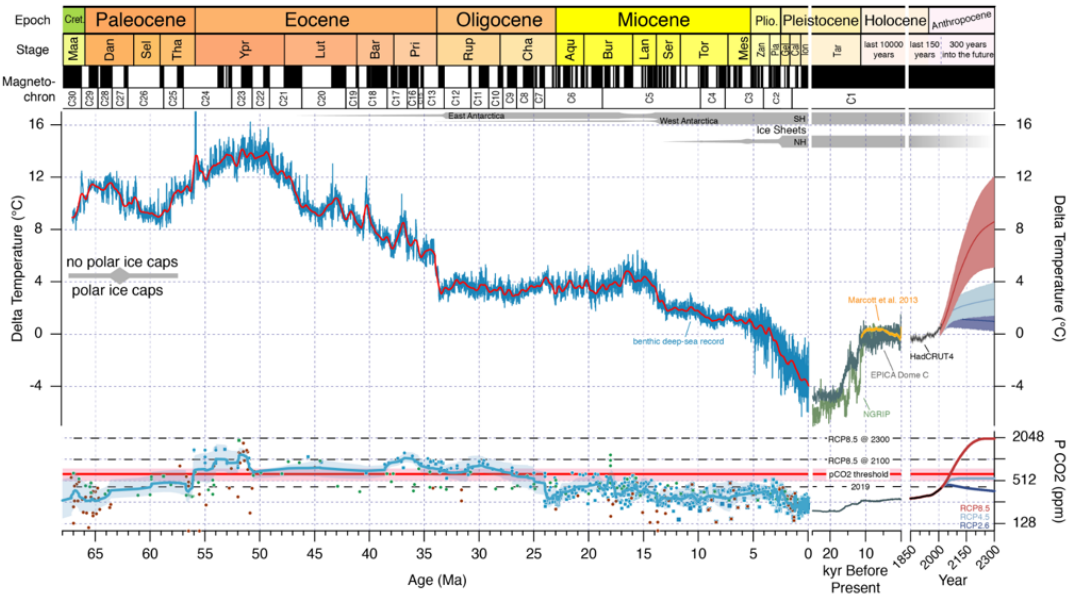

Figure 2.1: Temperature reconstruction for the entire Cenozoic (66 - 0 Ma), based on $\delta^{18}O_B$-values. Bottom panel shows CO_2-values reconstructed over the same interval. Adapted from Westerhold et al. (2020).

Knowledge on climate evolution for this period rests on temperature reconstructions for different parts of the climate system, each based on their individual proxies. For example, SSTs can be reconstructed using

the bio-organic proxies $U^{k'}_{37}$ and TEX_{86}, indexes of the ratios of different species of unsaturated alkenones from haptophyte algae and the different species of membrane lipids from marine thaumarchaeota respectively (Brassell et al., 1986; Schouten et al., 2002). LATs are determined from the ratios of cyclisation and methylation in branched tetraethers of soil bacteria (Weijers et al., 2007) and finally DSTs are commonly inferred from oxygen isotope values or the ratio of magnesium to calcium in benthic foraminifera (Barker et al., 2005; Epstein et al., 1951; McCrea, 1950). Although each of these proxies has its own uncertainties and limitations (e.g. Evans and Müller (2012) and de Bar et al. (2019)), they are generally in broad agreement when applied to early Cenozoic sedimentary archives and find that temperatures in all parts of the climate system are estimated to be in the range of 10 to 20 °C warmer than today (Caballero & Huber, 2013; Cramer et al., 2011; Cramwinckel et al., 2018; Peterse et al., 2012; Westerhold et al., 2020).

The causes of both the long-term cooling over the Cenozoic as well as the shorter-lived reversal leading to the EECO are not firmly established. For both developments, hypotheses lean on changes in continental configuration that influence either global heat redistribution by ocean currents, changes in latitudinal land and sea distribution affecting planetary albedo or fluctuating atmospheric CO_2 levels related to changes in weathering rates induced by changes in global orography and sea-floor spreading rates. These are further explained in sections 2.1.1 and 2.1.2.

As a result of different mechanisms proposed, Earth System Sensitivity, the long-term response to a doubling of CO_2 expressed as a change in GMST, remains poorly determined. To discern climate changes caused by changes in continental configuration from those caused purely by atmospheric carbondioxides increases, further quantitative constraints on both mechanisms are required.

2.1.1 Carbon-dioxide

Changes in atmospheric carbon dioxide levels are the main driver of changes in climate. The mechanism responsible for increasing temperatures with increasing CO_2 levels is now commonly referred to as the *greenhouse* effect. The processes responsibly were already described over a hundred years ago by Arrhenius (1896). This coupling is also observed in the long term Cenozoic cooling that runs in concert with a decrease in atmospheric carbondioxide concentrations (figure 2.1). Yet what drives the changes in atmospheric CO_2 in a natural system in the first place is harder to understand. Atmospheric CO_2 plays a role both in the short organic and long inorganic carbon cycles and alterations in operations of either of these cycles affects the other. The short organic carbon cycle describes the draw-down of atmospheric carbon into organic matter by biological productivity on land and in the oceans and its release back into the atmosphere after decay.

The inorganic carbon cycle concerns the long-term burial of carbon into sediments compacting to sedimentary rock or fossil reservoirs. This carbon only returns to the atmosphere during volcanic out-gassing, sea-floor spreading or by combustion of the fossil organic material (coal, oil and gas). The latter currently returns carbon to the atmosphere at over 100 times the rate of volcanic out-gassing (Gerlach, 2011). Weathering of exposed silicate rock takes up CO_2 from the atmosphere, which gets transported as bicarbonate (HCO_3^-) to the ocean by surface run-off and rivers where it continues in either of the explained carbon cycles. The *weathering thermostat* is the negative feedback mechanism that regulates how much weathering takes place. A warmer and wetter climate causes more weathering of silicate rock, thus more CO_2 uptake, in turn cooling down the climate and reducing further weathering. The baseline value of that thermostat is determined by the surface area of erodible minerals which in turn is determined by earth's orography. The collision of tectonic plates responsible for the uplift of the Himalayas, Rocky Mountains and Andes mountain chains is believed to have lowered the setting of that thermostat during the Cenozoic and thus leading to lower CO_2 levels reconstructed (France-Lanord & Derry, 1997; Raymo et al., 1988; Wallmann, 2001).

2.1.2 Tectonics and Ocean currents

Global geodynamics is responsible for setting the *weathering thermostat*, but also set the dimensions of and the connections between the ocean basins in which ocean currents find their way. This influences climate because the ocean currents redistribute heat over the globe, and also transport nutrients and minerals both laterally and vertically, affecting the global carbon cycles. Tectonic reconstructions over the late Cretaceous and Cenozoic indicate that several major reconfigurations have taken place that have potentially considerably altered Cenozoic climate evolution.

The spreading of the African and South-American continent started at approximately 120 Ma, but the connecting of the North and South Atlantic basins through deep sea opening at the equatorial region which would allow for heat transport across the hemispheres is only believed to have started at the latest Cretaceous or early Cenozoic and is still discussed (Batenburg et al. (2018), Pérez-Díaz and Eagles (2017), and Uenzelmann-Neben et al. (2017)). The opening of the Drake Passage between South-America and Antarctica, the separation of Australia from Antarctica and the formation of the Tasman Strait during the Oligocene allowed for the onset of the Antarctic Circumpolar Current (ACC) that is believed to have led to large scale Antarctica glaciation (DeConto & Pollard, 2003; Kennett, 1977; Pérez-Díaz & Eagles, 2017) and simultaneously halting a southern hemisphere deep water formation site (Zhang et al., 2020). A closure of the Mediterranean - Indian Ocean in the then Tethys ocean is approximated to have taken place at the late Oligocene to early Miocene and restricted circumglobal equatorial currents, leading to more latitudinal heat transport and diminishing of a possible evaporation-driven low-latitude deep water formation site (Agterhuis et al., 2022; Hotinski & Toggweiler, 2003; Torfstein & Steinberg, 2020).

Furthermore, latitudinal reconfiguration of land and sea surfaces has the potential to considerably alter earth's planetary albedo by allowing for increased accumulation of highly-reflective snow on high-latitude landmasses (Rohling, 2017).

2.2 Oceans of the past

Deep sea sediments are an invaluable resource for information on past climates. Slow settling (sedimentation rates in the order of a centimetre per 1000 years) of clastic and biogenic sediments over geologic time-scales have turned the seabed into a layered archive of oceanic conditions of the past. As the oceans are intrinsically connected with earth's global climate these past ocean conditions in turn provide information on past climates.

First, the ocean plays an important role in both the inorganic and organic carbon cycles. At the sea-surface-atmosphere interface carbon dioxide is exchanged until equilibrium conditions are reached. Since 1850, this process is estimated to have taken up approximately 25% of all anthropogenic emissions (Friedlingstein et al., 2019; Watson et al., 2020). Without this sink, atmospheric CO_2 levels would by now have risen from a pre-industrial 280 ppm to approximately 470 ppm instead of the present-day 420 ppm. Conversely, if atmospheric CO_2 levels drop, the ocean will start its outgassing and slow down atmospheric CO_2 decrease. Furthermore, the ocean is a facilitator for organic productivity: Water column productivity (mostly in the surface layer) takes up inorganic carbon in dissolved form and exports parts of this as sinking particles (faecal pellets, organic detritus) to the deep water where again a part of it exits the organic carbon cycle and enters the inorganic carbon cycle as sediment and later sedimentary rock.

Secondly, the ocean both takes up and redistributes heat. Water has a much higher heat capacity than air. The total heat-uptake of the upper 2000 meters of the ocean since 1955 resulted in an average warming of these waters by 0.09 °C. Although a seemingly small number, if it were not for this uptake, atmospheric temperatures - the usual benchmark when we talk about climate change - would have risen by 36 °C (Levitus et al., 2012). Temperatures in the tropics are higher than those in polar regions due to higher incoming solar radiation at the equator compared to the higher latitudes. The difference between these two, the temperature gradient, is determined by latitudinal heat transport by ocean currents and atmospheric circulation. This poleward heat transport greatly affects land- and sea-ice and snow cover at high latitudes that in turn alter earth's radiation budget via its reflective properties, an effect amplified by the albedo-feedback mechanism. Considering this intertwined nature of climate and oceans one must conclude that we cannot understand past climate without understanding past oceans.

Throughout earths 4.5 billion year existence the oceans have known three distinct phases, known as the Strangelove Oceans (Precambrian, before 542 Ma), Neritan Oceans (Paleozoic, 542 - 253 Ma) and Cretan Oceans (Mesozoic and Cenozoic, 253 Ma onwards) (Rohling, 2017). As a result of great changes in ocean biota each of these phases is marked by distinct interactions between the ocean-atmosphere carbon reservoir and the longer term biosphere mediated sedimentary carbon reservoir. The implication here is that to learn about the modern Cretan ocean-climate system we can look no further back then 253 million years ago. In this 253 million year interval the earth has gone from a constantly warm Mesozoic to long term secular

cooling starting at the beginning of the Cenozoic (see section 2.1).

The deep ocean is a the largest and most stable heat reservoir in our climate system. Studies on long term climate evolution therefore aim to reconstruct deep sea temperatures of the past. Deep sea temperatures are determined at the areas where the deep water was formed. In the modern ocean these formation sites are the polar waters of the North Atlantic (forming North Atlantic Deep Water, NADW) or the water surrounding Antarctica (forming Antarctic Bottom Water, AABW). Deep sea temperatures are believed to correlate with global average surface temperatures. For this assumption, two effects that influence polar surface water temperatures are estimated to offset each other. Polar amplification would register an amplified change in deep water temperature changes, but this is compensated for by the moderating effect of ocean surface temperatures on land surface temperatures (Hansen et al., 2013). Recently this assumption has found quantitative support from a multi-model comparison study (Goudsmit-Harzevoort et al., 2023).

Deep ocean temperature reconstructions have primarily been obtained through analysis of microfossils and their chemistry found buried in the seafloor: foraminifera.

2.3 Foraminifera as paleoclimate tracer

Foraminifera are mineralized test (shell) forming unicellular aquatic eukaryotic organisms. Their tests can be made from a multitude of materials, but the calcareous ($CaCO_3$) foraminiferal tests are the most abundant, best preserved and of most interest as they provide a fossil record for the Cambrian (538.8 Ma) to present (Binczewska et al., 2014). Foraminifera are either of the planktonic type (living in the surface or mixed layer of the oceans) or benthic type (living at or in the sea floor). Over their lifetime, as they grow their calcareous tests, they incorporate the isotopic signature of used source material in their tests. This includes the isotopic composition of the water (H_2O) in which they grow and the dissolved carbonate (CO_3^{2-}) used for their tests. Because the ratio of oxygen isotopes in water is determined by processes related to the global cryo- and hydrosphere and the ratio of carbon isotopes in dissolved carbonate by that related to the global carbon cycle, the foraminifera indirectly register climate information. Once the organism dies, no further incorporation of any material or isotopes takes place and the calcareous test remains as the only preserved part. To a large extent, ocean floors are made up of layer upon layer of these calcareous microfossils , each layer deposited during a a specific period of the geologic past at rates in the order of a centimetre per 1000 years (Broecker, 1982). Thus, if retrieved from below the sea floor, dated correctly and analysed for isotopic composition, these foraminfera are able to provide information on paleoclimates.

Additionally, in the middle of the 20th century it was observed by McCrea (1950) that the abundance of the rare heavier oxygen isotope in foraminifera tests relative to the abundance of this isotope in the waters in which it formed is determined by ambient temperature. Consequently, one can use these fossil benthic foraminifera as a paleothermometer and infer past bottom water temperatures by measuring their isotopic composition. Because absolute quantities of rare isotopes are not easily measured these are commonly expressed in reference to a standard. This resulted in the $\delta^{18}O$ definition, as first practised by Epstein et al. (1951):

$$\delta^{18}O = \left(\frac{\left(\frac{^{18}O_{sample}}{^{16}O_{sample}} \right)}{\left(\frac{^{18}O_{standard}}{^{16}O_{standard}} \right)} - 1 \right) \times 1000‰ \tag{2.1}$$

Likewise, the carbon isotope composition is defined as:

$$\delta^{13}C = \left(\frac{\left(\frac{^{13}C_{sample}}{^{12}C_{sample}} \right)}{\left(\frac{^{13}C_{standard}}{^{12}C_{standard}} \right)} - 1 \right) \times 1000‰ \tag{2.2}$$

Various standards are used in different laboratories, but these are all calibrated to international reference standards to allow for interlaboratory comparison of data. Nowadays, $\delta^{18}O$ is usually reported to Vienna Standard Mean Ocean Water, noted as $\delta^{18}O_{\text{VSMOW}}$ and $\delta^{13}C$ to Vienna PeeDee Belemnite, noted as $\delta^{13}C_{\text{VPDB}}$.

A $\delta^{18}O$-temperature calibration was established (Epstein et al., 1951) and has gone through numerous revisions and updates over the decades, but the primary relationship never changed significantly (Epstein et al., 1953; Marchitto et al., 2014; Shackleton, 1974). Ever since, compiled benthic $\delta^{18}O_B$- and $\delta^{13}C_B$-records (the so-called stacks) have formed the backbone of Cenozoic paleoclimate studies (Lisiecki & Raymo, 2005; Westerhold et al., 2020; J. Zachos et al., 2001).

From just the information provided here an issue with using $\delta^{18}O_B$ as a paleoproxy readily arises. To establish either of the two unknowns: I) the seawater oxygen isotopic signal ($\delta^{18}O_{SW}$) or II) the temperature from measured $\delta^{18}O_B$-values, it is required that the other is already known. Even though $\delta^{18}O_{SW}$-values are poorly constrained for the geologic past (Ravelo & Hillaire-Marcel, 2007), by making some assumptions $\delta^{18}O_B$-based temperature records have been constructed (e.g. Hansen et al. (2013) and Westerhold et al. (2020)). Other complicating factor are that foraminiferal fractionation rates are sensitive to seawater pH and can vary between species (Katz et al., 2003; Uchikawa & Zeebe, 2010).

2.4 Clumped Isotope Thermometry

Clumped isotope thermometry is the study of the abundance of multiply substituted isotopologues relative to what one would expect assuming a stochastic distribution of the rare isotopes. Multiply substituted isotopologues are molecules where two or more conventional isotopes have been replaced by their rarer isotopic counterparts: the so-called clumping of rare isotopes. Clumping can occur in all molecules that are composed of at least two atoms of which at least two stable isotopes exist. Given the scope of this study, the explanation here is limited to the application on carbonates.

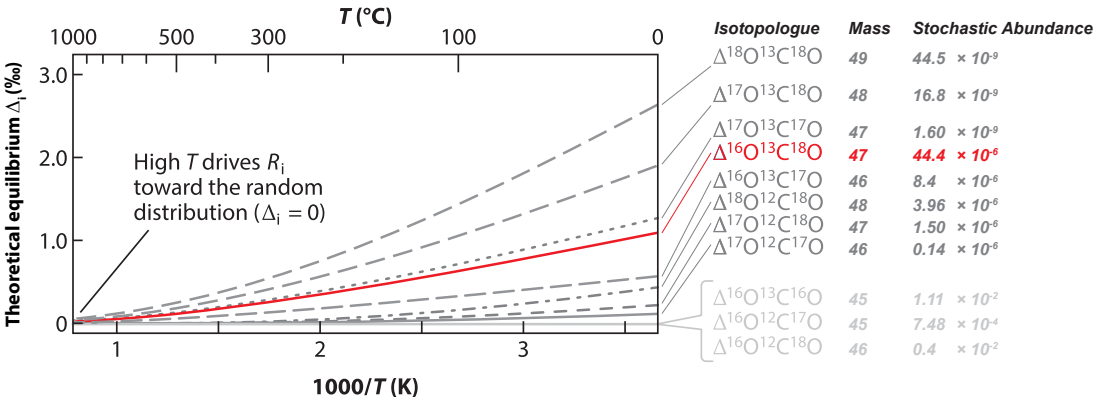

Figure 2.2: The deviation from the stochastic distribution of the different CO_2 isotopologues is temperature dependent. At 0 °C approximately 1.1 ‰ more clumping occurs for $^{13}C^{18}O^{16}O$ (displayed in red) compared to a stochastic distribution of oxygen and carbon-isotopes. With increasing temperatures less clumping occurs and the distribution approaches the stochastic, i.e. 0 ‰ clumping. The single substituted isotopologues (displayd in lighter gray) do not exhibit any clumping as that is impossible by definition. Modified from Huntington and Petersen (2023) following theory and calculations from (Wang et al., 2004), stochastic abundances for isotopologues from Eiler (2007).

The thermometric possibilities arise from the temperature dependency of the clumping of ^{13}C and ^{18}O (see figure 2.2) and its promises for paleoclimate applications on the fact that clumping is not influenced by any other factor (Eiler, 2007). In applying clumped isotope thermometry to foraminifera carbonates, the $^{13}C^{18}O^{16}O$ abundance in the CO_2 from processed carbonates is measured and put in ratio to the stochastic abundance calculated from the same samples bulk isotopic composition (the chance of that isotopologue occurring given a random distribution of all isotopes). This is expressed as the Δ_{47} value (the 47-subscript indicating the total mass of the clumped isotopologue) and calculated as follows:

$$\Delta_{47} = \left(\frac{R^{47}}{R^{47*}} - 1 \right) \times 1000‰ \tag{2.3}$$

In which R^{47} is the abundance ratio of mass 47 relative to mass 44 (i.e. conventional CO_2) as measured and R^{47*} the calculated stochastic abundance ratio of mass 47 relative to mass 44. The latter is calculated as:

$$R^{47*} = 2 \times \left(\frac{^{13}C}{^{12}C} \right) \times \left(\frac{^{18}O}{^{16}O} \right) + 2 \times \left(\frac{^{17}O}{^{16}O} \right) \times \left(\frac{^{18}O}{^{16}O} \right) + \left(\frac{^{13}C}{^{12}C} \right) \times \left(\frac{^{17}O}{^{16}O} \right)^2 \tag{2.4}$$

Where $^{18}O/^{16}O$ and $^{13}C/^{12}C$ are derived from measured $\delta^{18}O_{\text{VSMOW}}$ and $\delta^{13}C_{\text{VPDB}}$ respectively, which in turn ultimately result from the abundance ratio of mass 46 (primarily $^{12}C^{18}O^{16}O$) over 44 and mass 45 (primarily $^{13}C^{16}O_2$) over 44, but which need to corrected for ^{17}O interference (Brand et al., 2010). Finally, $^{17}O/^{16}O$ is calculated from $^{18}O/^{16}O$, assuming that the samples lies on a specific mass dependent fractionation line (Eiler, 2007).

Note that the R^{46} and R^{45} terms as previously included in the Δ_{47} definition (Eiler, 2007) have been omitted following the InterCarb community consensus (Bernasconi et al., 2021) after having been deemed statistically insignificant (Daëron et al., 2016).

As there is a preference for clumping of heavier isotopes under lower temperatures (figure 2.2), the Δ_{47} can be translated into ambient temperatures using an empirically established calibration (Meinicke et al., 2021). Furthermore, with an independent proxy for temperature, these data can be used to deconvolute the temperature signal from the combined $\delta^{18}O_B$ value, isolating the $\delta^{18}O_{SW}$ value (see equation 3.6 in section 3.3.3).

3 Method

3.1 Site and Samples

The Walvis Ridge is an approximately 3000 km long aseismic hotspot seamount chain stretching from the African continental shelf to the Tristan da Cunha hotspot at the Mid-Alantic Ridge. The ocean ridge separates the Eastern South Atlantic to the Angola Basin in the North and the Cape Basin in the South. The Rio Grande Rise is its less pronounced counterpart mirrored in the Mid-Atlantic ridge, located in the Western South Atlantic with the Brazil basin to the North and the Argentine Basin to the South (Pérez-Díaz & Eagles, 2017). See figure 3.1 for bathymetric impressions of the basin and the Walvis Ridge.

First sampling of the area took place in 1980 (DSDP Leg 74) and resulted in recovery of pelagic oozes and chalk from the Cretaceous / Paleogene (K/Pg), across the Paleocene / Eocene (PETM) boundary all through to the Eocene / Oligocene transition (EOT). The site was revisited during IODP expedition leg 208 (2004) to recover intact composite sequences of these transitions from multiple depths at six different locations. Site 1262 (27°11.15'S, 1°34.62'E) is the expeditions deepest site at 4755 meters depth and was drilled for the purpose of recovering sections suitable for study on water chemistry and circulation at abyssal depths (J. Zachos et al., 2004). Over the Cenozoic, the site has consistently lied in close proximity to the Calcite Compensation Depth (CCD, present day at 4.8 - 5.0 km) and lysocline, with local subsidence staying in pace with long-term deepening of the CCD. Microfossils in the Late Paleocene and Early Eocene are preserved particularly well. Three holes were drilled and the recovered intervals were spliced together into a single stratigraphic section with a total length of 236 meters composite depth (mcd).

The most recent age model for this splice is synthesized in Westerhold et al. (2020), using astronomical tuned stable isotope and x-ray fluorescence (XRF) data from Westerhold et al. (2008), Westerhold et al. (2018), Littler et al. (2014) and Dinarès-Turell et al. (2014), all updated to orbital solution La2010b (Barnet et al., 2019; Laskar et al., 2011; Westerhold et al., 2017).

Table 3.1: Details of grouped intervals used to generate four binned datapoints. Each interval spans between 110 and 150 Kyr. The samples were taken at Bremen Core Repository (BCR) on the 12th of January 2022 for the 57.9 Ma bin and the 12th and 13th of April 2022 for the other three bins.

Age (Ma)	Site	Hole	Core	Section	Interval (cm)	Resolution (cm)	Samples (N)	Replicates (N)
56.7	1262	A	14	4 5	0 - 150 5 - 40	2 - 3	55	75
57.0	1262	B	16	4 5	93 - 146 3 - 124	3	60	91
57.9	1262	B	17	4 5	33 - 148 0 - 73	3	58	57
60.2	1262	A	17	5	20 - 125	3	33	101

From this site a number of consecutive samples were taken at four different intervals, see table 3.1. These intervals were chosen such as to provide coeval data to the record from Meckler et al. (2022) while taking into account the level of preservation of foraminifera as indicated by the coarse fraction for these cores and

avoiding hyperthermal peaks following the stable-istopes analysis from Littler et al. (2014). As data from each of these intervals will be grouped together (binned) for the purpose of this study these will be referred to as bins from now on.

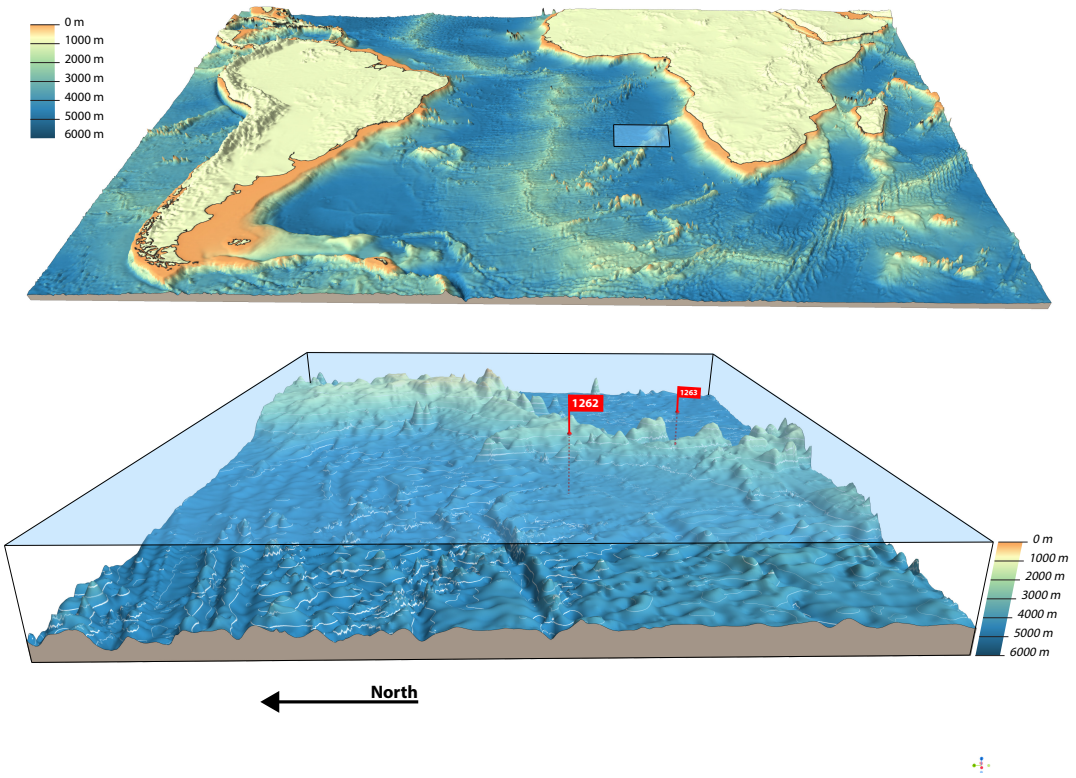

Figure 3.1: Locations of sites 1262 and 1263 of IODP expedition leg 208 on the Walvis Ridge in the Southern Atlantic. Vertical exaggeration of 50x on the South Atlantic basin overview map and 20x on the Walvis Ridge map. Bathymetric data from Gebco Compilation Group (2022).

3.2 Preparation

After retrieval all samples were freeze-dried and their bulk composition was weighed for later determination of coarse fraction. The samples were washed with lukewarm tap-water and separated into three fractions (>38 µm, >63 µm and >150 µm) by means of sieves. The fractions where transferred from the sieves into glass bowls using demineralized water and left to dry out in an oven (40 °C) overnight. Consecutively, all fractions were transferred to glass storage jars (20 ml) and weighed individually.

The largest fraction (>150 µm) was then dry-sieved to >212 µm and picked for the species *Nuttallides truempeyi*, as this allowed for the most direct comparison with the stable isotope record from the same site (Littler et al., 2014) and other Eocene clumped data (Agterhuis et al., 2022; Meckler et al., 2022). *Nuttallides truempeyi* form a lobulate outlined lenticular trochospiral test. The cross-section is unequally biconvex to planoconvex, with an involute umbilical side that is more convex than the evolute spiral side. Crescentic chambers increase slowly in size throughout four to five whorls that are all visible on the spiral side (Holbourn et al., 2013). See figure 3.2 for their morphology.

The foraminifera were typically 300 - 600 µm in size, with some exceptions reaching up to 1.5 - 2 mm. Generally, between 5 and 25 specimens were found in each sample with the 57.9 Ma bin on the lower end and the 60.2 Ma on the higher end of this range (see the relationship between number of samples and number of replicates in table 3.1). To obtain sufficient material for measurements, consecutive samples were grouped together in slightly larger intervals if required.

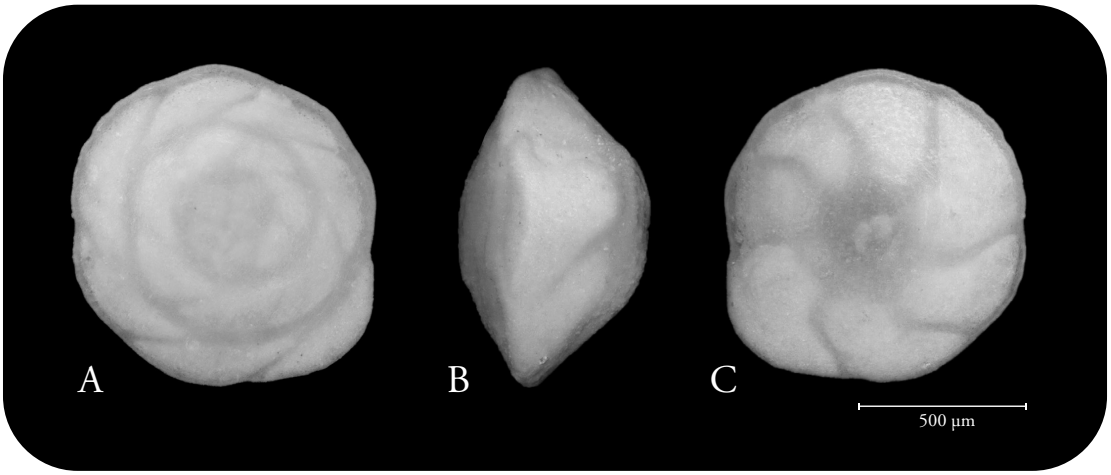

Figure 3.2: *Nuttallides truempeyi* morhpology. (A) spiral view, (B) apertural view, (C) umblical view. From IODP site 1262, hole B, core 16, section 4W, interval 138 - 139 cm. Dated at 57.02 Ma (Westerhold et al., 2020). Photographed using the Nikon Keyence VHX-5000 series digital microscope.

To open up the foraminifera chambers for cleaning, all specimens were cracked between glass plates and transferred to Eppendorf tubes (0.5 mL) using demineralized water. After pipetting off excess water the cracked specimens were subjected to ultrasonic cleaning for 30 seconds. Afterwards, potentially present undesired materials (organic matter and foreign calcareous ooze) were brought in suspension by means of an appropriately strong jet of demineralized water, which was again pipetted off. The suspending and pipetting was done twice. The ultrasonic cleaning procedure was repeated at least two times until foraminiferal parts were deemed free of foreign matter and displayed a glassy look under the microscope. After the cleaning procedure, the samples were let to dry to ambient room temperature under cover.

3.3 Measurements

3.3.1 Instruments

The isotope ratio mass spectrometry (IRMS) measurements were conducted between November 2022 and January 2023 at Utrecht University Geolab. The setup consists of a *Thermo Scientific Kiel IV Carbonate Device* for dissolving the carbonate samples and purification of the resulting carbon-dioxide gas. Thereafter, the gas entered the *Thermo Scientific 253 Plus 10 kV IRMS* for measurement of relative intensities of masses 44 to 49. See the schematic in figure 3.3 for a more elaborate description of the steps and processes.

To avoid any temporal biases between and within runs and within the range of each interval all samples were evenly distributed both over the total number of and within the individual runs. Each run consisted of 36 or 46 measurements. For the runs of 36 measurements 19 slots were reserved for standards (ETH-1, ETH-2 or ETH-3), 2 for check-standards (IAEA-C2, Merck) and 15 were samples. For the longer run of 46 measurements these numbers are 22, 2 and 22 respectively. In the runs of 46 total measurements, the ratio of standards versus samples as recommended in Kocken et al. (2019) has been followed, whereas for the shorter runs relatively more standards were used. Adopting further recommendations, ETH-1 and ETH-2 were measured only three times each in every run, allowing ETH-3 to be measured more often, resulting in smaller margins of error as the Δ_{47}-values of ETH-3 best reflect those of the target samples. The benefit of the longer run is the higher sample-to-standard efficiency, while the shorter runs fit in better with the day-to-day schedule of operations in the laboratory. The international check-standards IAEA-C2 and Merck are used to monitor long-term reproducibility of the instrumental setup (see also figure A.1 in the appendix).

Finally, the Long Integration Dual Inlet (LIDI) workflow as proposed by Hu et al. (2014) and materialized by Müller et al. (2017) was embraced to minimize gas losses associated with multiple switches of the changeover

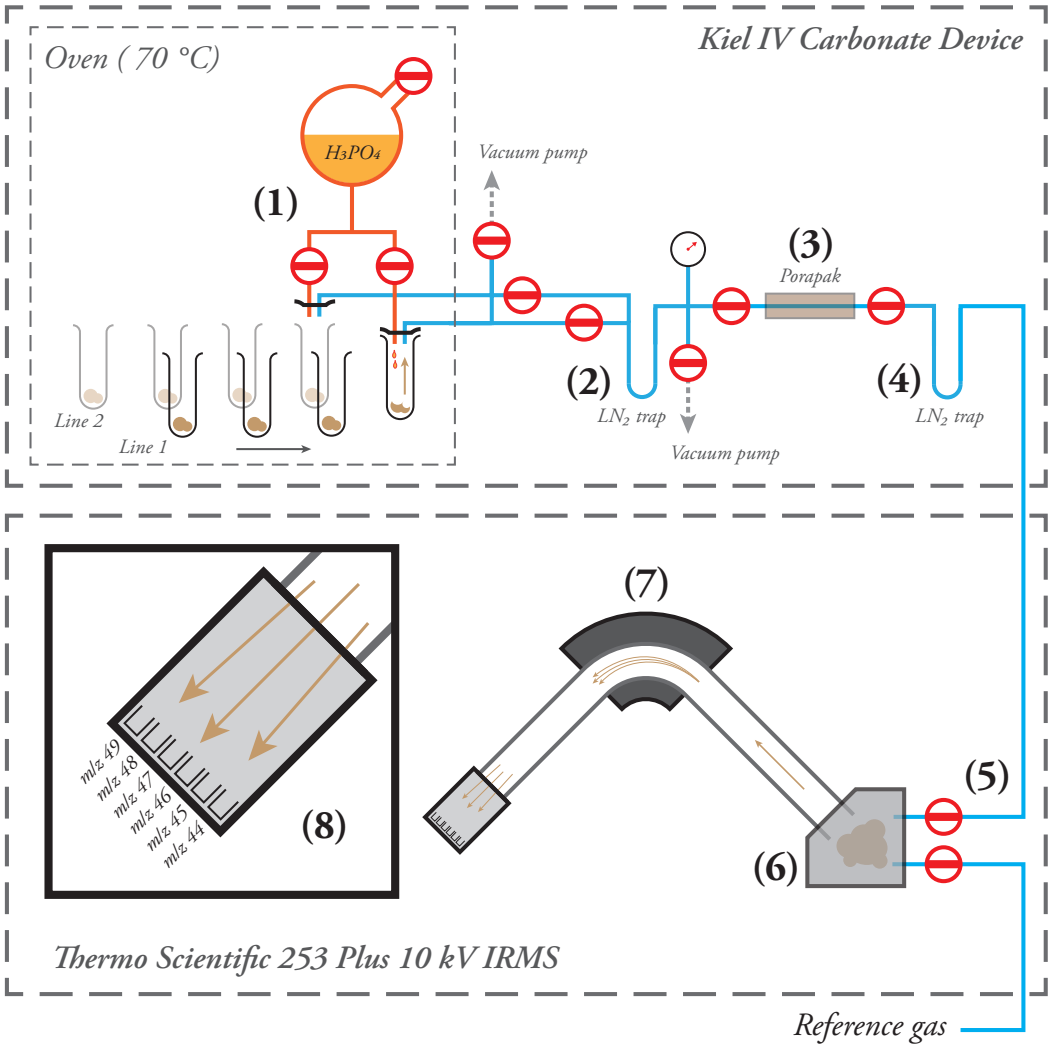

Figure 3.3: Simplified schematic of the Clumped Isotope Mass Spectrometry set-up at Utrecht University GeoLab. (**1**) Acid digestion of carbonate samples. (**2**) Liquid nitrogen (-196 °C) watertrap. (**3**) Porapak Mesh Trap for organic matter. (**4**) Second liquid nitrogen trap. (**5**) Alternating input between sample gas and reference gas. In LIDI methodology the entire sample is measured before the reference gas measurement takes place. (**6**) Ionization of gas particles in ionization chamber. (**7**) The amount of deflecting by the electromagnet is determined by combined particle mass/charge (m/z). (**8**) Faraday cups measure incoming charge. The positions of the cups is set such that the signal they capture is specific to a single mass, thus a combined set of isotopologues. Schematic image modified after (Spencer & Kim, 2015).

valve and pressure adjustment at the beginning of the acquisition process.

3.3.2 Complications and corrections

Clumped isotopes

Over the past decades, a number of factors have shown to complicate clumped isotope measurements. In essence, these either have to do with (1) the influence of impurities and contamination in the gas, (2) the re-distribution of isotopes across the isotopologues between the moments of dissolution and final measurements of cup intensities (acid fractionation, redistribution in capillaries and redistribution in ion-source) and (3) a non-linearity between δ^{47} and Δ_{47} due to incorrect determination of cup pressure base lines used to correct for background noise (Spencer & Kim, 2015).

To prevent possible cross-sample contamination the Porapak (see figure 3.3) was heated to 150 °C for 1.5 hours between each run. Then, to monitor potential contamination in the sample CO_2 gas the intensity of mass 49 over mass 44 (R^{49}_{sample}) is compared to that of the working gas (R^{49}_{WG}). Because mass 49 in pure CO_2 would indicate presence of the extremely rare triply substituted $^{13}C^{18}O_2$ (44.5 ppb, see figure 2.2), a large difference between these two values would indicate contamination by foreign compounds that could also influence the measurements at mass 47 (e.g. the chlorocarbon derivative $^{12}C^{35}Cl^+$). In this study, only measurements that fitted the following criterion where considered for further analysis:

$$\left(R^{49}_{sample} - R^{49}_{WG}\right) \times 10^4 < 0.1 \tag{3.1}$$

Furthermore, samples with high internal standard deviations (> 0.15 ‰) and $\delta^{18}O$ values lower than -0.5 ‰ or higher than 1.5 ‰ were omitted from the record as these are most likely to be contaminated. From a total of 324 measurements, 5 were dismissed as outliers.

Fragmentation and re-combination of isotopes among the isotopologues which pushes the analytice gas towards a more stochastic distribution, and thus warmer temperatures, can take place at the ion source (Huntington et al., 2009). This can partially be remedied by decreasing the pressure and residence time of the analyte gas in the ion-source, but that comes at the cost of lower internal precision due to lower beam intensities (Cui & Wang, 2014). Alternatively and more preferable higher internal precision can be maintained by placing the measured samples in a reference frame with standards from the same analytical sessions, see section on Empirical Transfer Functions (ETFs).

Finally, the issue with δ^{47} - Δ_{47} non-linearity is a result of using pressure baselines (PBLs) established without analyte gas entering the ion-source. The background noise therefore did not include the beam-intensity dependent production of secondary electrons causing a negative offset in some Faraday cups (He et al., 2012). In the Utrecht University GeoLab this is solved by establishing intensity-dependent PBLs for m/z 44 intensities 5, 10, 15, 20 and 25 V and accelerating voltages of 9.38 - 9.54 kV using the working gas on a daily basis in the so-called *background scans* and using these for corrections (Meckler et al., 2014).

The measured Δ_{47}-values of all samples and (check)standards in a run are first corrected for an offset based on run-mean difference between the measured ETH-3 Δ_{47}-values and the accepted Δ_{47}-values. To place the offset-corrected measured *raw* Δ_{47} values into an internationally recognized standard reference frame used across laboratories, ETFs are established. This is a relationship based on a linear regression between measured (*raw*) and internationally accepted (*true*) values of all measurements on ETH standards within an analytical session (see table A.1 in the appendix for data on standards). Such an analytical session is loosely defined as the period in which changes in external factors (source instability, changes in working gas, laboratory conditions and sample preparation) do not yet result in a drift in measurement reproducibility (Kocken et al., 2019; Meckler et al., 2014). Throughout this study, the ETFs were constructed based on the ETH-standards within a running window of 250 measurements before and 250 after each measurement. In practice, that implied an approximate 35 ETH-1 and ETH-2 measurements and 180 ETH-3 measurements used for establishing a linear regression. Using the slope and intercept of the regression lines the ETF is now constructed to place the Δ_{47}-values into the Intercarb Carbon Dioxide Equilibrium Scale (Bernasconi et al., 2021):

$$\Delta_{47(I-CDES90°C)} = slope \times \Delta_{47-RAW} + intercept \tag{3.2}$$

A temperature-dependent acid fractionation factor to correct for fractionation between the abundance of $^{13}C^{18}O^{16}O$ in liberated CO_2 (Δ_{47}) and the abundance of $^{13}C^{18}O^{16}O_2{}^{2-}$ (Δ_{63}) in carbonates as previously applied (Ghosh et al., 2006) is now redundant as this would equally affect samples and standards and is therefore incorporated in the ETF (Bernasconi et al., 2021). Now, with all corrections applied the Δ_{47}-values are fit to be used in temperature reconstructions.

Stable isotopes

Stable oxygen and carbon isotope abundances ($\delta^{18}O$ and $\delta^{13}C$) of samples derive from intensities on cups m/z 46 and 45 respectively. Because the natural abundances are much higher these require a much less rigorous correction scheme. Since acid fractionation on $\delta^{18}O$-values is not corrected for by transforming to

an accepted reference frame, a manual correction is applied using a temperature-dependent acid fractionation factor (AFF) as described by Kim et al. (2007):

$$\alpha_{CO_2(ACID)-Calcite} = e^{(3.59\times T^{-1}-1.79\times 10^{-3})} \tag{3.3}$$

With an acid digestion temperature of 70 °C (343.15 K) this leads to an AFF of 1.00871 which is thenceforth applied to establish $\delta^{18}O_B$-values:

$$\delta^{18}O_B = \frac{\delta^{18}O_{CO_2} + 1000}{1.00871} \times 1000 \tag{3.4}$$

Finally, both the $\delta^{18}O$ and $\delta^{13}C$ values are offset-corrected based on a running window (15 measurement before, 15 after) mean offset between ETH-3 measured and accepted $\delta^{18}O$ and $\delta^{13}C$-values.

3.3.3 Temperature and $\delta^{18}O_{SW}$ calculations

From the corrected Δ_{47}-values mean Δ_{47}-values and standard deviations for each bin were calculated using empirically established calibrations. Latest available calibrations include one using biogenic, abiogenic and synthetic carbonates from Anderson et al. (2021) and one using foraminifera data from Peral et al. (2018)). The calibration from Meinicke et al. (2020) includes a reprocessing of these data and is favoured due to the best fit of linear regression on the temperature interval concerned (Kocken, 2022). Bin mean-temperatures and maximum and minimum temperatures associated with 68% (1σ) and 95% (2σ) for each bin were reconstructed following the foraminifera based calibration established in Meinicke et al. (2020) and recalculated for the I-CDES scale (Meinicke et al., 2021):

$$\Delta_{47} = 0.0397 \times \frac{10^6}{T^2} + 0.1518 \tag{3.5}$$

Here, temperature (T) is expressed in Kelvin (K). Note that the uncertainties on slope and intercept as originally established have been omitted, following the notion that these uncertainties when propagated for the analytical errors only have a minor effect to confidence intervals (<0.1 °C) on reconstructed temperatures (Agterhuis, personal communication, 2022).

An evaluation of the sensitivity of reconstructed temperatures as a function of the number of replicates per bin is included in figures A.3 and A.2 of the appendix.

Using mean $\delta^{18}O_B$-values and Δ_{47}-based temperature of each bin, the seawater isotopic signal can be inferred by solving the [$\delta^{18}O_{SW}$ - $\delta^{18}O_B$] to temperature calibration from Marchitto et al. (2014) for $\delta^{18}O_{SW}$:

$$\delta^{18}O_{SW} = (0.245) \times T - (0.0011) \times T^2 - (3.31) + \delta^{18}O_B \tag{3.6}$$

Again, note the omission of uncertainties in the calibration. Since above calibration was derived from *Cibicidoides* the $\delta^{18}O_B$-values were first corrected for vital effects in *Nuttallides* according to Katz et al. (2003):

$$\delta^{18}O_{Cibicidoides} = \frac{\delta^{18}O_{Nuttallides} + 0.1}{0.89} \tag{3.7}$$

4 Results

In the top panel of 4.1 the mean Δ_{47} values for four Late Paleocene time intervals (56.7, 57.0, 57.9 and 60.2 Ma) are plotted on the I-CDES90 scale to allow for inter-laboratory analysis. The number of replicates per data-point are displayed as labels above the data points. The solid and dashed lines display the 68% and 95% confidence intervals respectively. Numerical results are included in table A.2 of the appendix. Values are plotted on a time series using the Westerhold et al. (2020) age model for site 1262, with sample depths (mcd) converted to age by linear interpolation between the age models tie points. Mean ages for each bin are calculated as weighted average of individual replicates. All measurements have been conducted on well preserved *Nutallides truempyi* (see figure 3.2) with approximately 15 specimens per aliquot and each aliquot allowing for two to six measurements, depending on total aliquot size.

The second and third panel show $\delta^{13}C$- and $\delta^{18}O_B$-values respectively for individual replicates used for each bin. $\delta^{18}O_B$-values are corrected to *Cibicidoides* following Katz et al. (2003). The gray lines (background) are records established from the same species and the same core and serve as long-term reference and verification here (Littler et al., 2014).

Deep sea temperatures reconstructed from Δ_{47}-values using equation 3.5 are displayed in the fourth panel (confidence intervals as before) along the temperatures reconstructed from $\delta^{18}O_B$-values using equation 3.6 rewritten for temperature and assuming a constant $\delta^{18}O_{SW}$-value of approximately -1 ‰, following the canonical view of an ice-free earth prior to the onset of Antarctic glaciation (Hansen et al., 2013; J. Zachos et al., 2001). The gray line reflects a global temperature signal using CENOGRID $\delta^{18}O_B$-values (Westerhold et al., 2020) with the same Marchitto-calibration (equation 3.6). Here, Δ_{47}-derived bottom water temperatures are 4 °C (57.0 Ma), 5 °C (56.7 Ma), 7 °C (60.2) Ma and 8 °C (57.8 Ma) warmer than those reconstructed using the $\delta^{18}O_B$-paleothermometer.

The bottom panel finally shows reconstructed $\delta^{18}O_{SW}$-values in each binned time interval using the Δ_{47}-derived temperatures and the independently measured $\delta^{18}O_B$-values in the same samples to solve equation 3.6 for $\delta^{18}O_{SW}$. The horizontal lines display reference $\delta^{18}O_{SW}$-values for an ice-free earth, the Modern, and Pleistocene glacial maxima under the assumption that the isotopic composition of seawater is determined solely by ice-volume.

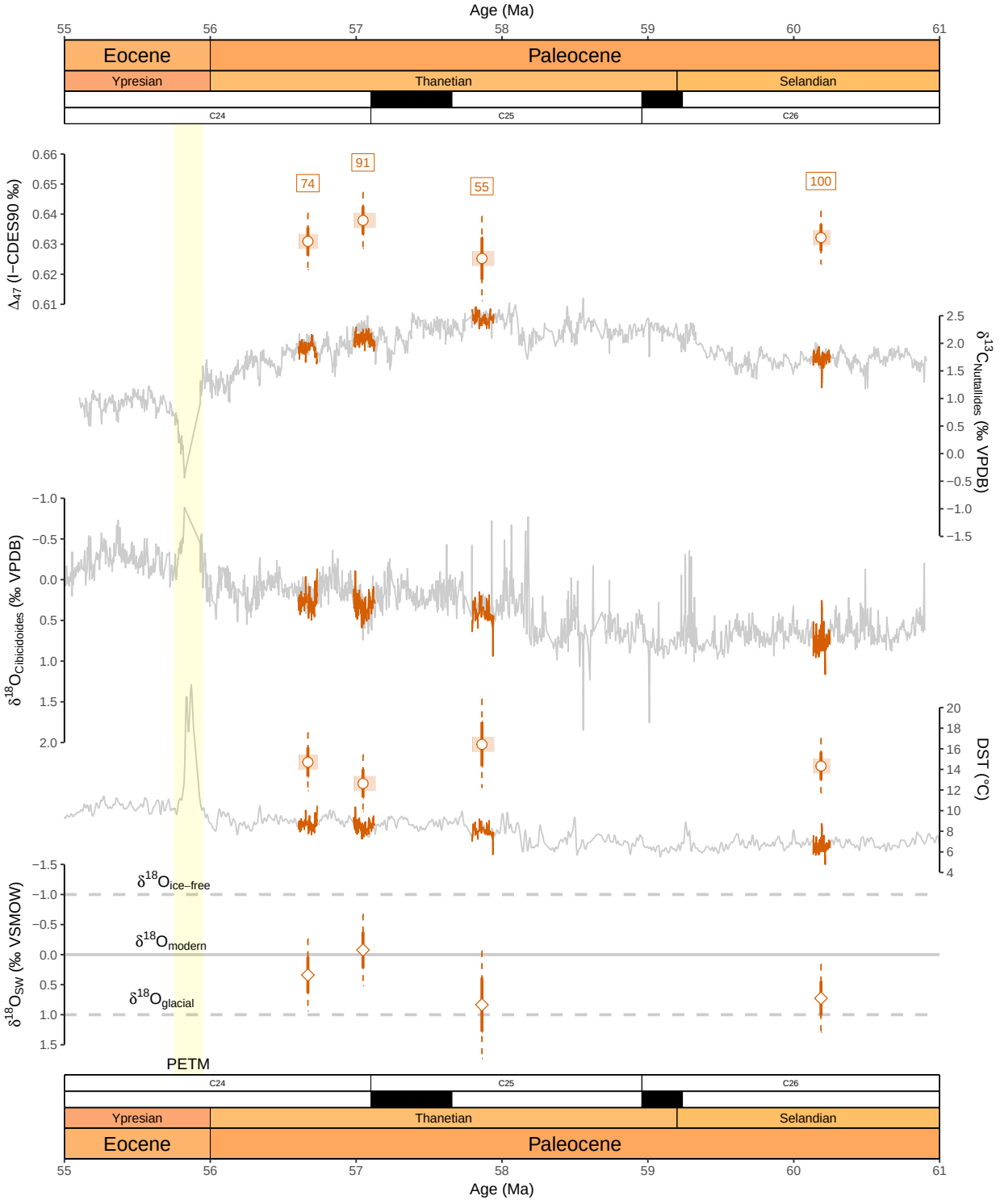

Figure 4.1: A) Δ_{47} values for the four time intervals (bins) in the Late Paleocene. Solid errorbars show the 68% confidence interval, dashed lines 95% confidence. Horizontal shading indicates time interval for which samples have been binned and labels on top show number of replicate measurements used. B) and C) $\delta^{13}O_C$ and $\delta^{18}O_B$ values for individual measured samples of each bin, $\delta^{18}O_B$-values corrected to Cibicidoidess following Katz et al. (2003). Grey line displays a continuous late Paleocene records from the same site (Littler et al., 2014). D) Reconstructed temperatures from Δ_{47}-values and $\delta^{18}O_B$-values. E) Reconstructed $\delta^{18}O_{SW}$ using Δ_{47} derived bottom water temperatures.

5 Discussion

5.1 Late Paleocene and Early Eocene Deep Sea Temperatures

In recent decades, different proxies have been proposed to assess deep sea temperatures in the geologic past. In figure 5.1 deep sea temperatures based on site 1262 $\delta^{18}O_B$ values from Littler et al. (2014), using the calibrations from Hansen et al. (2013) (light gray) and Marchitto et al. (2014) (dark gray) are displayed along the Δ_{47}-based temperatures for the same site (red circles, this study), nearby site 1263 (red circles after PETM; Agterhuis, in preparation) and for sites 1407 and 1409 in the North Atlantic (blue circles Meckler et al. (2022)). The green dots display benthic foraminifera Mg/Ca derived bottom water temperatures for site 1209 in the Pacific (see figure 5.2) with the green line a smoothed fit and shaded 90% confidence intervals (Cramer et al., 2011).

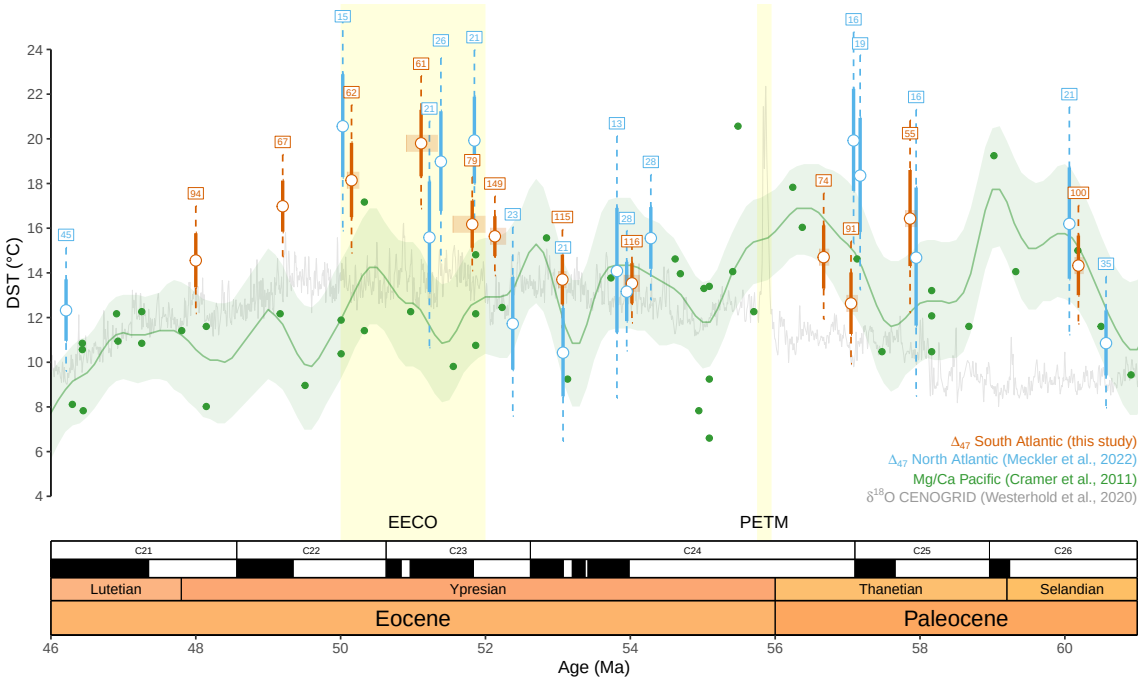

Figure 5.1: Gray lines: $\delta^{18}O_B$-based temperatures for site 1262 (South Atlantic) with Hansen et al. (2013) (light) and Marchitto et al. (2014) (dark) calibrations. Red open circles: Δ_{47}-based temperatures in late Paleocene (site 1262, this study) and early Eocene (site 1263, Agterhuis, in preparation). Blue open circles: Δ_{47}-based temperatures for sites 1407/1409 (North Atlantic, Meckler et al. (2022)). Green line: Mg/Ca based temperatures with trend and shaded 90% confidence intervals for site 1209 (Pacific, Cramer et al. (2011), calibrated following Lear et al. (2010)).

First of all, a marked offset between the temperatures from clumped isotopes and the stable oxygen isotope record is visible (+ 2-4 °C (57.0 Ma), + 3-5 °C (56.7 Ma), + 5-7 °C (60.2) Ma and + 6-8 °C (57.9 Ma)). These elevated Δ_{47}-derived temperatures compared to previous estimates are found consistently throughout

the Cenozoic and in multiple ocean basins (Meckler et al., 2022). Furthermore, the absolute temperature-variability from the Δ_{47}-record is larger (3.2 °C corresponding to 0.011 ‰) than that found from $\delta^{18}O_B$-values (2.1 °C corresponding to 0.474 ‰), when considering the averages of the four bins, see figure 4.1. The large variability that is visible for the North Atlantic prior to the PETM is also observed in the Pacific Mg/Ca record, but is less distinct in the South Atlantic reconstruction. The Δ_{47}-derived temperatures are corroborated by the Mg/Ca temperatures in the Late Paleocene, whereas the Mg/Ca temperatures during the Eocene seem to align better with the conventional $\delta^{18}O$ temperature reconstructions.

The lower temperature variability found from oxygen isotopes only, may be attributed to non-thermal $\delta^{18}O_B$-dampening factors like seawater pH and $\delta^{18}O$-values (Meckler et al., 2022; Zeebe, 2001). Under acidifying ocean conditions, thus decreasing pH, the rate of incorporation of the heavier ^{18}O-isotope in foraminifera shells increases (Uchikawa & Zeebe, 2010). This effect is a direct result of carbon speciation in seawater that is governed by pH. As the major component of total dissolved inorganic carbon changes from CO_3^{2-} to HCO_3^- when pH lowers the isotopic composition of the oxygen-bearing substrate for calcification increases. This is because HCO_3^- is isotopically heavier than CO_3^{2-}. If not corrected for, these elevated $\delta^{18}O_B$-values would be interpreted as colder bottom waters (assuming no changes in $\delta^{18}O_{SW}$). Thus, increased atmospheric CO_2 levels, associated with warmer climates, are registered as lower $\delta^{18}O_B$-values and higher temperatures, while at the same time the induced acidification by increased pCO_2-levels, is registered as a higher $\delta^{18}O_B$-value and presumed lower temperature; hence the *dampening-effect*.

The influence of seawater pH on benthic foraminifera remains however poorly studied. Uchikawa and Zeebe (2010) report a $\Delta\delta^{18}O_B$ of +0.9 ‰ (ΔT of $\sim$ -3.5 °C for typical late Paleocene $\delta^{18}O_B$-values) for a ΔpH of -1 inferred from a study on the planktic non-symbiont bearing *Globigerina bulloides*. Another study found an effect of + 0.65 ‰ per -1 ΔpH based on a core top *Oridorsalis umbonatus* study off the Namibian coast (Rathmann & Kuhnert, 2008). Inorganic calcite precipitation experiments put the effect at + 1.42 ‰ per ΔpH of -1 (McCrea, 1950; Usdowski & Hoefs, 1993; Zeebe, 2001). Best estimate reconstructions place late Paleocene pH at 7.8 (interpolated from Rae et al. (2021)). This is 0.4 lower than the pre-industrial oceans with a pH of 8.2, on which the temperature calibration in equation 3.6 is based (Marchitto et al., 2014). Hence, approximately 2 to 3 °C of the difference between the Δ_{47}- and $\delta^{18}O_B$-derived temperatures could potentially be explained by this pH-effect.

Furthermore, as opposed to the CENOGRID-based temperature reconstruction, no global warming trend is discernible from the South-Atlantic clumped isotope temperature reconstruction over the period 60 - 54 Ma. From a long-term perspective, the temperatures are variable around the 14 °C level, with only a sharp temperature rise at $\sim$ 53 Ma.

5.2 South Atlantic $\delta^{18}O_{SW}$ values

Over the geologic past, the total amount of water on earth has remained constant, as has the total budget of ^{18}O and ^{16}O stable isotopes contained within. However, the distribution of the different oxygen-related isotopologues of water (most notably $H_2{}^{16}O$ and $H_2{}^{18}O$) has differed between different reservoirs due to fractionation processes. Evaporation and precipitation fractionate against the heaver and lighter isotopes respectively, leading to isotopically lighter water stored on land after precipitation (as ice, surface or ground-water) and heavier water remaining in the oceans, where the evaporation occurred. The magnitude of this effect ultimately depends on the governing hydrological regime. Because the heavy oxygen isotopes largely behave similar to dissolved salts, this is often referred to as *the salinity effect*, even though the relationship is not direct and has not always held to the same extent in climates of the past (Rohling & Bigg, 1998).

Figure 5.3 shows reconstructed $\delta^{18}O_{SW}$ for the Early Eocene (site 1263, Agterhuis, in preparation) and Late Paleocene (site 1262) using independent Δ_{47}-derived bottom water temperatures to de-convolute the seawater isotopic signal from the isotopic signal recorded in the benthic foraminifera. The filled diamonds indicate the values found when the pH correction according to Zeebe (2001) is applied to the $\delta^{18}O_B$-values prior to reconstruction. This correction, the highest of the three independent calibrations (+ 1.42 ‰ per ΔpH of -1), was chosen to display the entire range over which pH possibly affects the reconstructed $\delta^{18}O_{SW}$. Deep sea pH values for the Paleogene have been estimated by linear interpolation between values obtained from boron isotopes ($\delta^{11}B$) by Rae et al. (2021). Note that as no data is available for the Paleocene, pH-values for

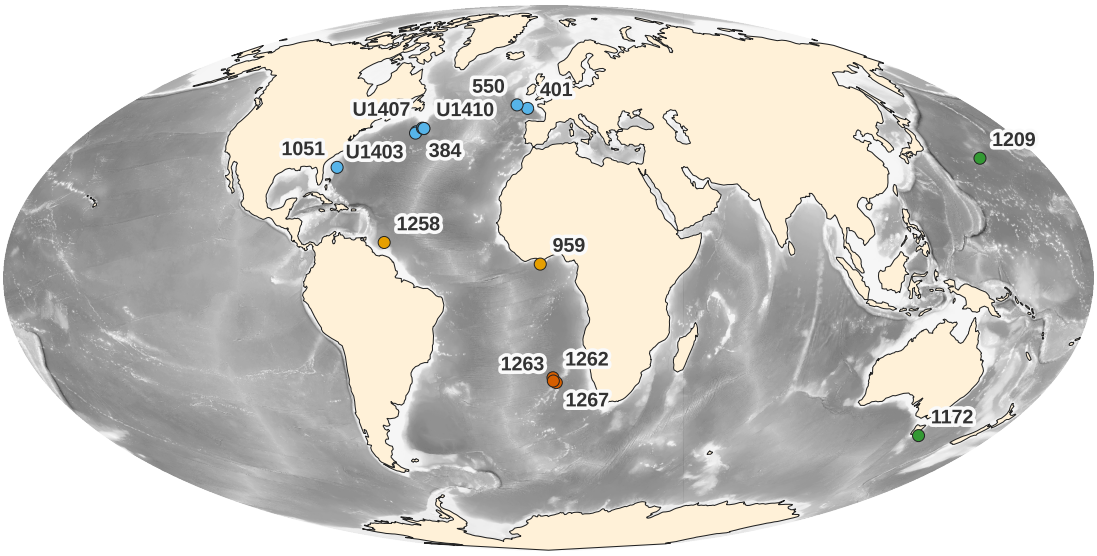

Figure 5.2: Modern location of sites used in comparison of records. Bathymetric data from Gebco Compilation Group (2022).

---

this period are a result of interpolation of a 10 Myr interval spanning the K/P-boundary to PETM. Similarly, using the Mg/Ca-temperature model from Cramer et al. (2011), the $\delta^{18}O_B$-record from Littler et al. (2014) and the same pH correction as before a continuous $\delta^{18}O_{SW}$ model can be generated (solid and dashed lines in figure 5.3).

In contrast with a presumed ice-free world in the early Cenozoic (J. Zachos et al., 2001), datapoints at 60.2 and 57.9 Ma show $\delta^{18}O_{SW}$-values that reflect conditions found between present-day glaciation and that during the glacial maxima of the pleistocene. Two datapoints from the latest Paleocene (57.0 and 56.7 Ma) show $\delta^{18}O_{SW}$ resembling the modern ocean. The larger variability in Paleocene $\delta^{18}O_{SW}$ (0.79 ‰) compared to $\delta^{18}O_B$ (0.47 ‰), averaged per bin, is chiefly explained by realizing that the larger temperature variability found from Δ_{47} compared to $\delta^{18}O_B$ (see section 5.1) is translated into $\delta^{18}O_{SW}$-variations using equation 3.6. Explained alternatively, the *dampening* induced by lower pH hindered registration of the full range of the seawater isotopic variation in the benthic foraminifera. $\delta^{18}O_{SW}$ at 60.2, 57.0 and 56.7 Ma are in line between the two different approaches, here hinging on the good correlation between Δ_{47}- and Mg/Ca-derived temperatures (figure 5.1). In the North Atlantic (blue diamonds, Meckler et al. (2022)), the estimated variability in $\delta^{18}O_{SW}$ is even larger, in line with greater temperature variability (see figure 5.1) and limited variation in $\delta^{18}O_B$ (see figure 5.4). In the Eocene, the most depleted seawater is observed at 53 Ma, than increases towards glacial values at 50 Ma and decreases thereafter. This bulge is readily explained by observing a peak in Δ_{47}-derived temperatures at the EECO while $\delta^{18}O_B$-derived temperatures remain relatively constant over 50 - 52 Ma (figure 5.1).

Because of the uncertainties associated with analytical precision (Mg/Ca- and Δ_{47}-temperatures), applied corrections (ocean pH) and the assumptions made (linear interpolation of ocean pH values over the entire Paleocene), these resulting values should be treated as indicative rather than definite, but do help investigating possible mechanisms at work. However, in terms of relative changes within each basin over time these uncertainties and corrections are irrelevant as they apply a more or less constant offset. A possible partial explanation for this variability is a fluctuation in atmospheric CO_2 levels, thus pH and consequently $\delta^{18}O_{SW}$, that is not caught in the early Cenozoic part of the $\delta^{11}B$-record (Meckler et al., 2022). As an indication, a 0.11 shift in pH corresponds to 500 ppm shift in atmospheric CO_2 (Rae et al., 2021). According to the pH correction from Zeebe (2001) this is reflected as a 0.15 ‰ change in fractionation. If corrected for interpolated pH values from the long-term trend, $\delta^{18}O_{SW}$-values that were coeval to extremes in a hypothetical shorter term CO_2 and pH variability, would be over or under compensated and the variability maintained. However, to explain the full variability in $\delta^{18}O_{SW}$, short-term pH fluctuations would have to exceed the

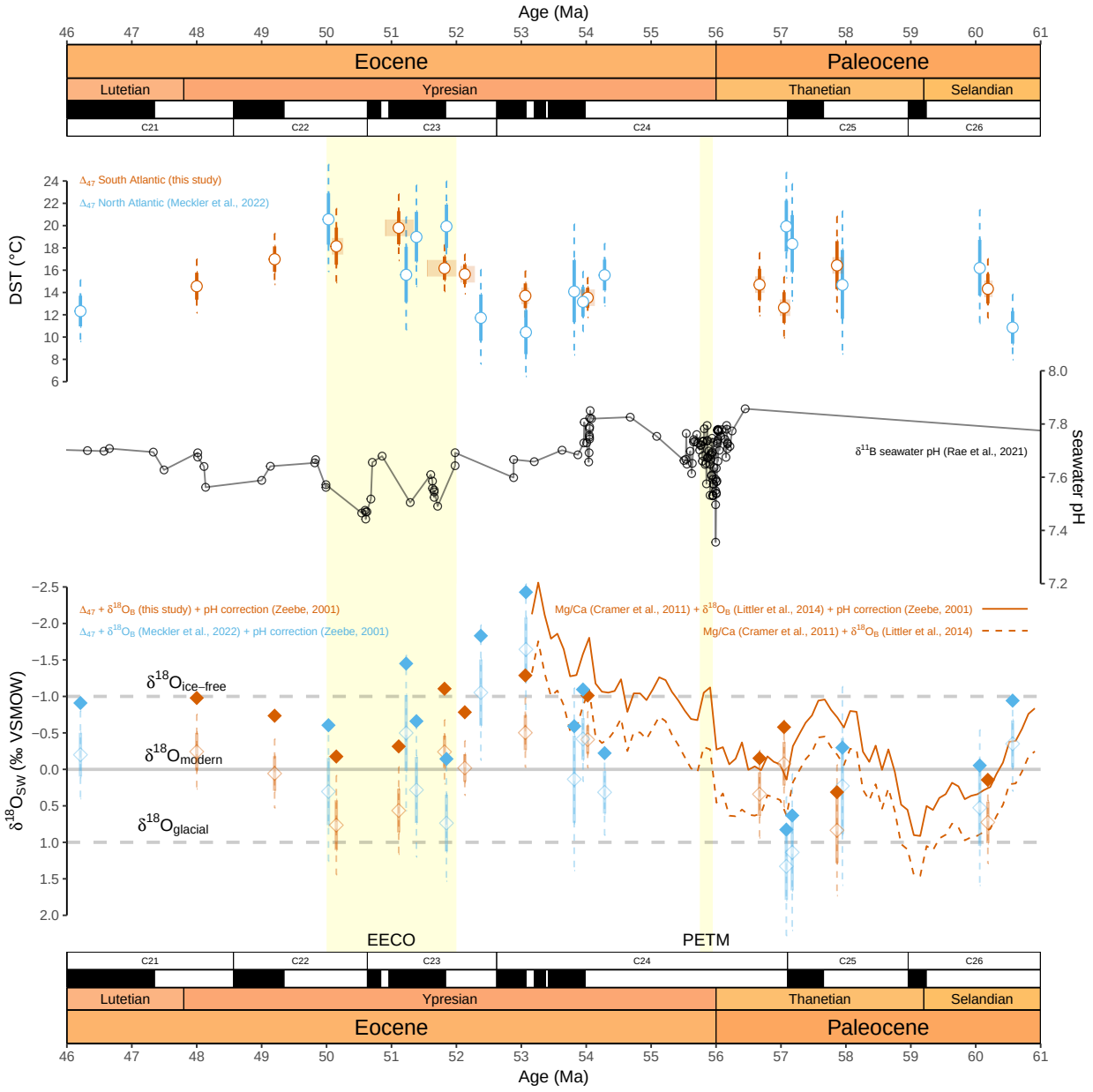

Figure 5.3: Top panel shows Δ_{47}-derived temperatures as before. Middle panel shows reconstructed seawater pH from boron isotopes ($\delta^{11}B$) by Rae et al. (2021), note that no data is available for the Paleocene. Bottom panel shows reconstructed $\delta^{18}O_{SW}$ values using Δ_{47}-derived temperatures are shown as faded open diamonds (Red: South Atlantic / Walvis Ridge sites 1263 and 1262, Blue: North Atlantic sites 1407/1409 from Meckler et al. (2022). Confidence intervals as before). Solid diamonds are values using pH correction as in Zeebe (2001). Solid red line display reconstructed $\delta^{18}O_{SW}$-values based on the South Atlantic $\delta^{18}O_B$-record (Littler et al., 2014) using a Mg/Ca derived global deep sea temperature signal (Cramer et al., 2011). The dashed line is corrected for pH according to Zeebe (2001)

magnitude of change observed over the entire Cenozoic, which is rather unlikely.

To explain the conundrum of absolute $\delta^{18}O_{SW}$-values a number of possible hypotheses exist, which can be grouped in three approaches. I) The average isotopic composition of the seawater is different from what is calculated for the global oceans in a presumed ice-free world (approximately -1.2 ‰). This includes variations in ice volume, ground- and surface waters, input related to tectonic activity (e.g. hydrothermal vents,

volcanic activity, seafloor spreading) affecting ocean $\delta^{18}O_{SW}$ on a global scale, as well as hydrological and hydrographical influences that affect seawater isotopic composition on a localized level. II) There is a stronger gradient in oxygen isotope distribution among watermasses, or III) The rate of incorporation of ^{18}O over ^{16}O in benthic foraminifera is affected by other factors than just temperature. This includes the pH-effect mentioned in 5.1, but potentially also other not well understood species-dependent physiological factors (Katz et al., 2003).

When looking solely at ice-volume as a possible explanation 56 to 94 meter sea-level equivalent of ice would be required to warrant the lowest to highest Paleocene $\delta^{18}O_{SW}$-values at 57.0 and 57.8 Ma respectively. When considering the value corrected for pH following Zeebe (2001), 31 to 50 meters would suffice. Though in stark contrast with the often assumed ice-free early Cenozoic, corroborating evidence for sea-level changes of 15 to 30 meter on 10^6 years time-scales is found from backstripping studies on the New Jersey plain (K. G. Miller, Kominz, et al., 2005). This study suggests that glacio-eustatic changes only can explain these sea-level changes in terms of magnitude and speed and thus ephemeral small ice-sheets must have existed in the Antarctic interior. Sames et al. (2020) argues that the ^{18}O depleted meteoric waters (precipitation) needs not necessarily be stored as ice, but can be locked as surface- and groundwater in humid greenhouse climates and discharged in arid times, thereby omitting the prerequisite of an ice-sustaining climate. However, this aquifer-eustasy does most likely not exceed decimetre scale sea-level changes and is thus not considered a likely driver of the sea-level changes required here (Davies et al., 2020).

Agterhuis et al. (2022) argue that low-latitude highly evaporative areas of salinity-dominated deep water formation can cause relatively high deep water $\delta^{18}O_{SW}$-values. This would however require much lighter $\delta^{18}O_{SW}$-values, and in this case fresher, water-masses elsewhere, which is hard to reconcile with the homogeneity found in $\delta^{18}O_B$ and $\delta^{13}C$-values found in the different ocean basins (see figure 5.4 and Cramer et al. (2009)).

Instead of mechanisms depleting the oceans from ^{16}O, the high $\delta^{18}O_{SW}$ values can also be interpreted as an addition of ^{18}O to the ocean reservoirs. Sea-floor spreading, hydrothermal activity, continental and submarine weathering all have the possibility of altering $\delta^{18}O_{SW}$, yet these processes operate on 10^7 to 10^8 years times-scales and hence are unable to explain the 10^6 year variability observed here (Coogan et al., 2019; Jaffrés et al., 2007).

Taking these possible explanations, the most likely contender that fits the magnitude and variability of the $\delta^{18}O_{SW}$ signal during the late Paleocene and early Eocene is that of small ephemeral ice-sheets on the Antarctic interior, (K. Miller et al., 2011; K. G. Miller, Wright, & Browning, 2005). Combining the effect of a lower seawater pH on the signal registration by benthic foraminifera and a sealevel decrease of up to 30 meters due to the formation of such an Antarctic interior icesheet (DeConto & Pollard, 2003), a possible explanation for the early Cenozoic $\delta^{18}O_{SW}$-values arises.

The assumption of a constant seawater $\delta^{18}O$-value of -1 ‰(i.e. ice-free) clearly does not hold. To reconstruct $\delta^{18}O_{SW}$ from benthic foraminifera in deep time, more constraint on individual influencing factors are required. Using clumped isotope thermometry the factor temperature is now constrained. Further knowledge on Paleocene seawater pH and its effect on fractionation of oxygen isotopes in foraminifera is imperative.

5.3 Watermasses, Circulation and Overturning

In an oceanic overturning system, physical and chemical properties of deep water masses are set at the time and place of deep water formation (Broecker, 1982). Therefore, when deep water masses at different locations carry a similar physical and chemical profile this can be interpreted as having a common area of deep water formation and thus being part of the same overturning circulation.

The oxygen isotope value of seawater is a characteristic commonly used in tracing and assessing the origin of water-masses, on the notion that $\delta^{18}O_{SW}$ values reflect the salinity (the *salinity effect* explained before) as determined in the area of deep water formation by processes of brine rejection in sea-ice formation or strong evaporation (Frew et al., 2000). In this study, $\delta^{18}O_{SW}$-values are derived from combining $\delta^{18}O_B$-values and Δ_{47}-based temperatures. Because $\delta^{18}O_B$-values evolve similarly at the North and South Atlantic sites

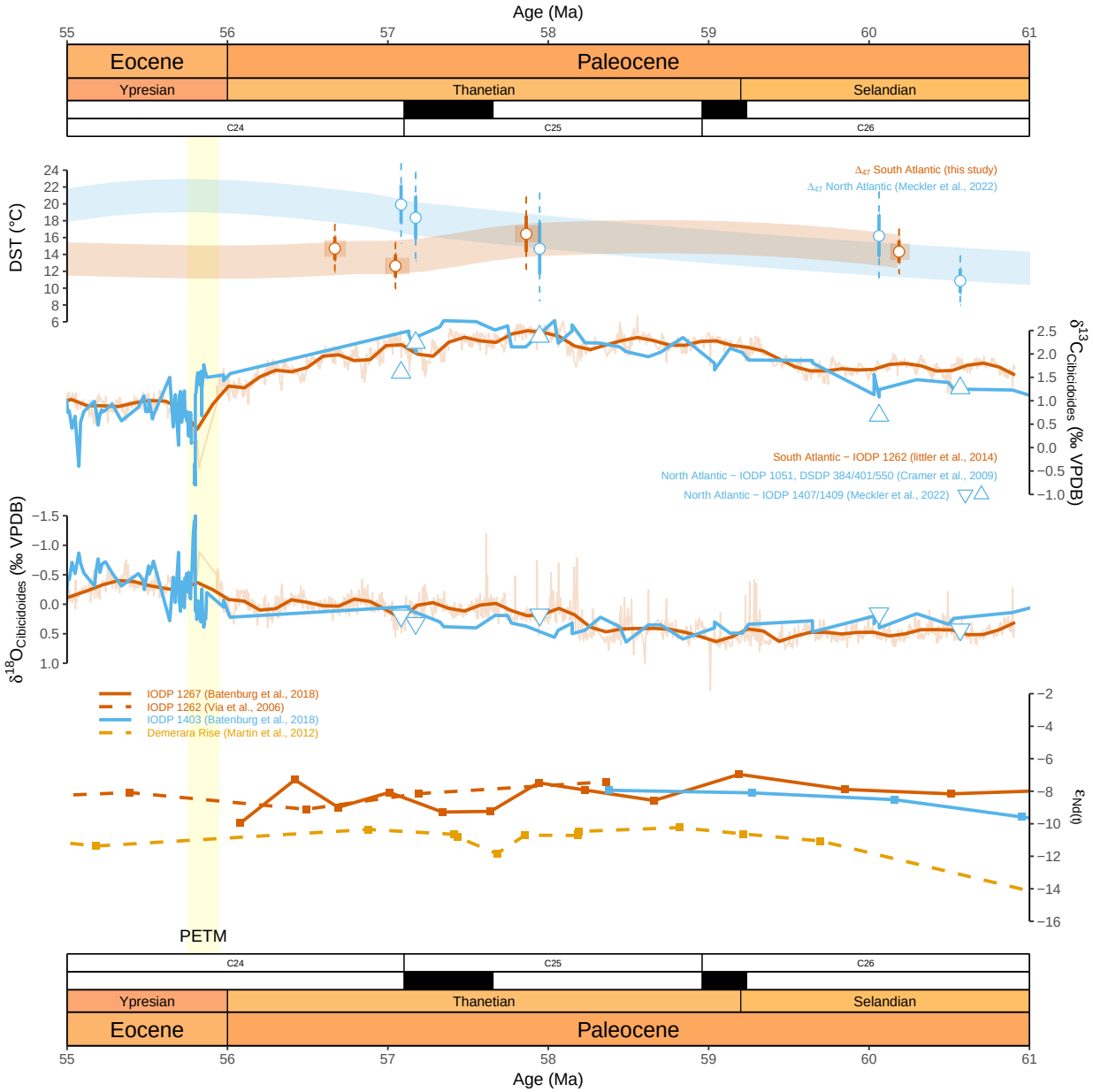

Figure 5.4: Top panel shows Δ_{47}-derived temperatures as before with a smoothing applied not so much as to interpolate values but to guide the eye for long term development of bottom water temperatures. Second and third panel show $\delta^{13}C$- and $\delta^{18}O_B$- values from North- and South Atlantic sites with colours as before. Continuous record for North Atlantic are from ODP site 1051 and DSDP sites 384/401/550 (Cramer et al., 2009). Open triangles are data from (Meckler et al., 2022). South Atlantic record from (Littler et al., 2014). Bottom panel shows Neodymium isotope record for North Atlantic (site 1403 solid blue, Batenburg et al. (2018)), South Atlantic (site 1267 solid red, Batenburg et al. (2018); site 1262 dashed red, Via and Thomas (2006)) and equatorial Atlantic (site 1258, Demerara Rise, orange, Martin et al. (2012)).

(see figure 5.4 panel C), the variation in $\delta^{18}O_{SW}$ is governed by Δ_{47} values. Therefore, temperatures from clumped isotopes are favoured here over inferred $\delta^{18}O_{SW}$-values to assess similarities between deep waters among basins. While the Δ_{47}-derived DSTs of the North- and South-Atlantic show more similar values at 60 and 58 Ma (< 2 °C difference) a strong diverging trend (7 °C difference at $\sim$ 57 Ma) is observed at the latest Paleocene (top panel figure 5.4).

Changes in $\delta^{13}C$ provide a constraint on carbon-transfer between ocean, atmosphere and sediments and differences in carbon isotope values reflect nutrient contrasts and thereby tell about homogeneity between basins. Over the Cenozoic, basin-averaged multi-site $\delta^{13}C$-stacks for North- and South Atlantic shows a maximum gradient of $\sim$ 0.9 ‰, while values at 58 Ma are highly homogeneous (Cramer et al., 2009). The strong divergence between DSTs in these basins at $\sim$ 58 Ma is not reflected in changing $\delta^{13}C$-values when comparing a record from nearby site 384 in the North Atlantic and the same site (1262) in the South Atlantic sites (second panel figure 5.4).

The ratio of Neodymium isotopes in sedimentary coatings or fish debris is the most direct proxy for water origins that is currently available. The ratio of ^{143}Nd to ^{143}Nd is acquired from continental contributions (fluvial and aeolian input). As this ratio differs from one continental crust to the other, the values found in seawater can thus be linked to the different ocean basins that are surrounded by these continents. A convergence of neodymium isotope records spanning the Maastrichtian and Paleocene (72 - 56 Ma) from various Atlantic sites was interpreted by Batenburg et al. (2018) as a homogenisation of Atlantic water related to an intensified Atlanting overturning system with Southern source waters as a result of continental rifting. A modelling study by Zhang et al. (2020) corroborates this and points to a common area of deep water formation source in high Southern latitudes that was driven by convection at the center of subpolar gyres that were constrained by closed Drake and Tasmanian passage providing a Western boundary for gyre build up. Zeebe and Zachos (2007) find additional support in [CO_3^{2-}] gradients between the North and South Atlantic basins that are reversed compared to present day, also suggesting a reversed deep ocean circulation.

Although the coarse resolution record provided by Batenburg et al. (2018) does allow for interpretation of changes in ocean circulation in terms of multi-million year processes like continental drift an openings of oceanic passages, sub-million year variations in ocean circulation from climatic forcing are not resolved in this record. Late Paleocene sections of these records are shown in the last panel in figure 5.4 (Batenburg et al. (2018) and references therein) and serve to illustrate this limitation. Most importantly, available data from site 1403 is only available till 58 Ma, just when a presumed divergence (based on Δ_{47}-temperatures in this study) between bottom water sources at nearby sites 1407/1409 and site 1262 takes place.

Clumped isotope derived bottom water temperatures (and indirectly $\delta^{18}O_{SW}$-values) do not endorse the conclusion of a pan-Atlantic deep water homogenisation.The convergence described in Batenburg et al. (2018) hinges mostly on North Atlantic $\varepsilon_{Nd(t)}$-changes while values in the South Atlantic remain relatively constant. Because the Paleocene North Atlantic was marked by high levels of tectonic activity (Hansen et al., 2009) alternative inputs of Neodymium can not be ruled out as being responsible for this convergence. To further constrain the evolution of North- and South Atlantic deep-water exchange higher resolution coeval records for both sites on multiple independent proxies (i.e. $\varepsilon_{Nd(t)}$ and Δ_{47}) are essential. Additionally, another approach would be to apply clumped isotope thermometry to deconvolute the $\delta^{18}O_{SW}$ signal from the $\delta^{18}O$ of planktic foraminfera and compare that to the deep water $\delta^{18}O_{SW}$-values for evaluating potential sites of deep water formation. For this method however, good preservation of the foraminifera to avoid the overprinting of a deep water temperature signal is important, which commonly is the case in areas with high sedimentation rates (e.g. van der Ploeg et al. (2023)).

5.4 Earth System Sensitivity

Earth System Sensitivity (ESS) is the expression of long term climate evolution in response to atmospheric forcing, i.e. CO_2 increase. This is expressed as a change in Global Mean Surface Temperature (GMST) per doubling of atmospheric CO_2. Deep Sea Temperatures (DSTs) are believed to reflect GMSTs (Goudsmit-Harzevoort et al., 2023; Hansen et al., 2013; Inglis et al., 2020), thus the elevated Δ_{47}-derived temperatures may have severe implications for our understanding of ESS in the early Cenozoic.

To assess whether the relationship between DSTs and GMSTs also holds in climate systems with a different

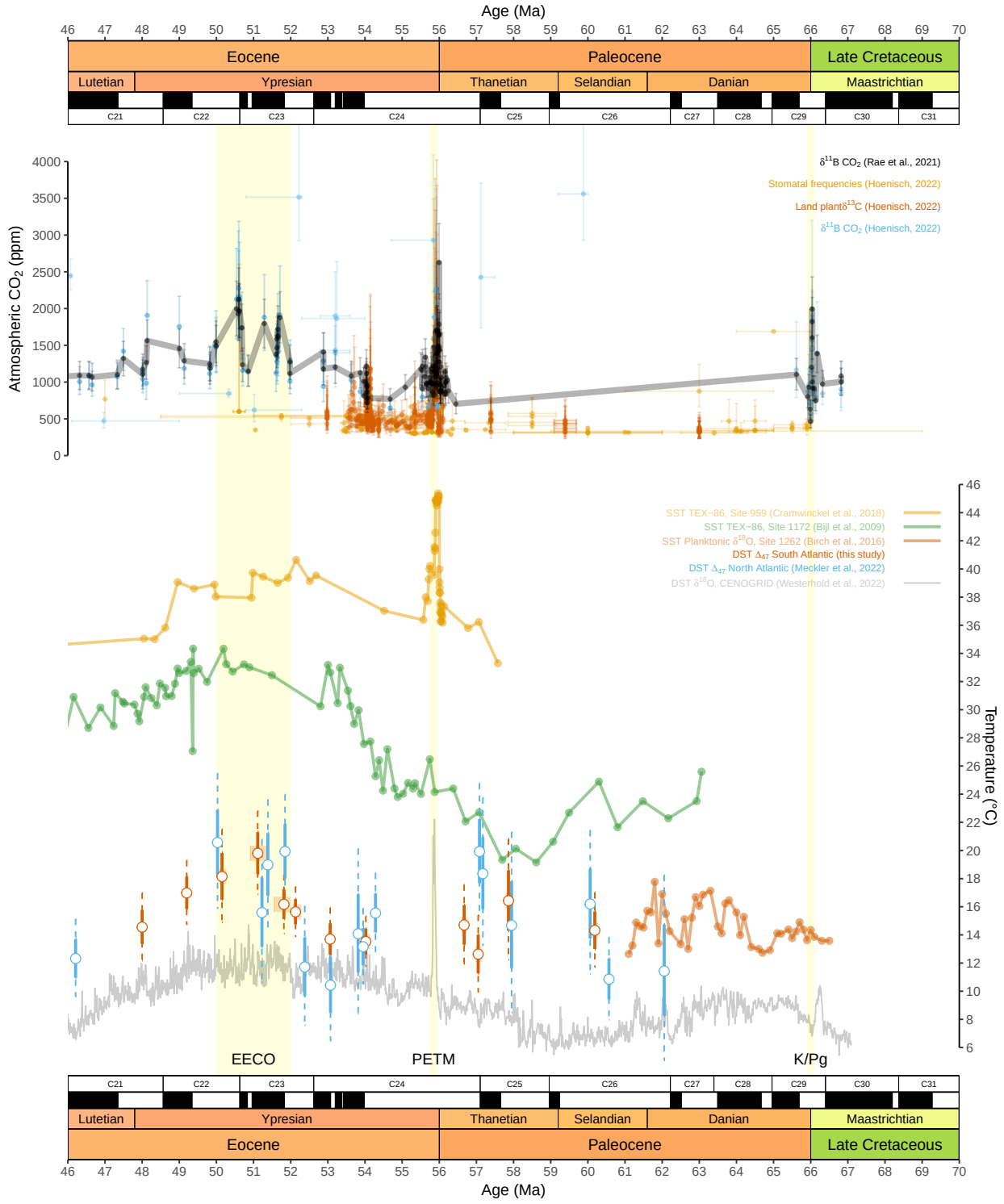

Figure 5.5: Top panel shows atmospheric CO_2 from different proxies. Orange dots are from stomatal frequencies, red dots are derived from Land Plant $\delta^{13}C$-values and blue dots from boron isotopes (Hoenisch, 2022). The most recent reconstruction based on boron isotopes in benthic foraminfera is displayed as black line, but does not contain data between K/Pg and PETM (Rae et al., 2021). Bottom panel shows deep sea temperatures as before and is supplemented with TEX_{86}-based SST reconstructions for equatorial site 959 (orange, Cramwinckel et al. (2018)) and East Tasmanian site 1172 (green, Bijl et al. (2009) and planktonic $\delta^{18}O$-based Walvis Ridge site 1262 (red, Birch et al. (2016)). See figure 5.2 for locations.

modus of operandi from what is described in Hansen et al. (2013) the sparsely available Paleocene SST reconstructions are compared against trends in DSTs established in this study in figure 5.5. Both SSTs at sites 959 and 1172 show higher values after the PETM than before, while Δ_{47}-based DSTs for the South Atlantic show a reversed trend across this boundary. This reversal could be interpreted as a reconfiguration of Southern Hemisphere overturning in this interval. In the conceptual framework where a coeval change in both SSTs and DSTs reflect a change in the global climate and the change in gradient between DSTs and SSTs at a given location as an alteration in the overturning systems, the deep-sea to surface temperature gradient being larger post-PETM would imply a change to deep-water formation at higher latitudes. Alternatively, the larger gradient could indicate a more vigorous overturning post-PETM, which is in line with modelling studies from Zhang et al. (2020).

An early Paleocene temperature reconstruction based on planktic foraminfera $\delta^{18}O$-values from site 1262 shows SST values as low as same site Δ_{47}-based deep sea temperatures. This is hard to reconcile with the TEX_{86} records, but could be explained by the overprinting of a deep sea temperature signal on the planktonic forams as indicated by relatively poor preservation described in Birch et al. (2016).

The debate on what was the primary driver for Paleocene and Eocene climate evolution is still ongoing. For example, Batenburg et al. (2018) strongly suggest the opening of the Atlantic gateway towards the onset of the EECO as the main driver for Early Eocene high temperatures, while Cramwinckel et al. (2018) conclude that DSTs and tropcial SSTs evolving in concert proves atmospheric CO_2 levels to be the primary cause. Ruling out the likelihood of a major intensification of pan-Atlantic overturning in the Late Paleocene by DSTs established in this study and thus establishing a level background against which the CO_2-driven climate operates, ESS can be assessed by relating atmospheric forcing to GMST changes. However, as there is a big hiatus in CO_2 reconstructions for the late Paleocene (see figure 5.5), these assessments lean on long-term interpolation. Paleo-CO_2 data from land plant $\delta^{13}C$-values and stomata count is deemed unreliable (summarized in Berends et al. (2021)), especially further back in time. Earlier $\delta^{11}B$-based CO_2 reconstructions from Pearson and Palmer (2000) are erratically high, therefore the assessment is made base on interpolation of the record synthesized in Rae et al. (2021).

Figure 5.6 shows estimates of Paleocene climate sensitivity to be approximately 8 °C degrees from South Atlantic data and a more variable 6 - 10 °C based on the North Atlantic data (Meckler et al., 2022). Because global mean DSTs catch the long-term (10^3< years) changes in climate that ESS means to reflects and the South Atlantic was most likely better connected to a greater part of the global oceans, the more stable Southern Atlantic based value is favourable when estimating global climate sensitivity. This South-Atlantic value is consistent with the high end of previous estimates (Cramwinckel et al., 2018; Rohling et al., 2012). This, in turn, implies that climate models that have hitherto been validated using lower estimates on ESS, could structurally underestimate future global warming under elevated CO_2 levels.

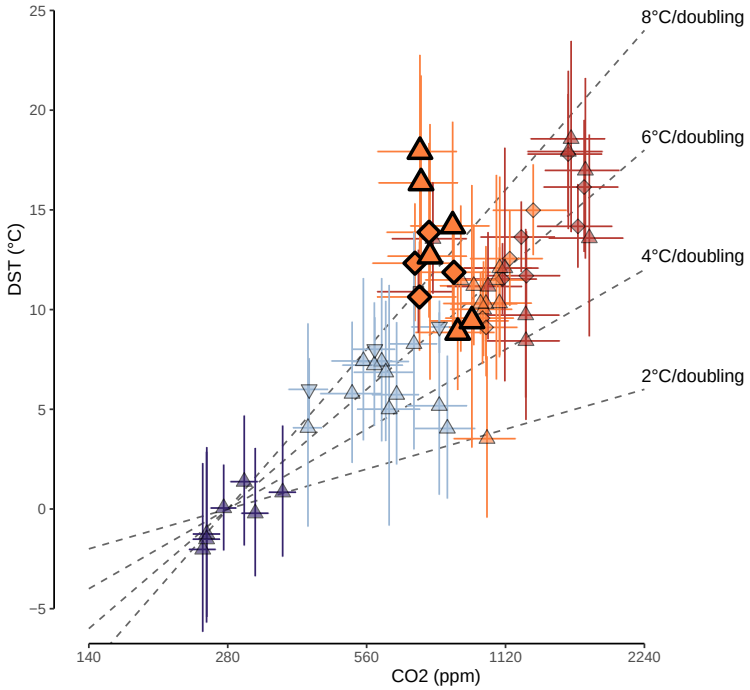

Figure 5.6: Projection of paleo-temperature and paleo-CO_2 reconstructions in an Earth System Sensitivity framework. Shapes indicate ocean basins from which DSTs are reconstructed, colours follow the classification of ages in ice-, cool-, warm- and hothouse states (dark blue to dark red respectively) as used in Westerhold et al. (2020). Paleocene data is displayed in larger symbols with triangles for North Atlantic sites (Meckler et al., 2022) and diamonds for South Atlantic sites (this study).

6 Conclusion and Outlook

Conclusion - New robust Walvis Ridge deep sea temperature estimates based on clumped isotope thermometry (Δ_{47}) in the late Paleocene complement same-site data into an ever more complete Cenozic South Atlantic DST record. The late Paleocene to early Eocene data presented here reveals significantly higher temperatures than from hitherto applied $\delta^{18}O$ paleothermometry. This is in line with recent studies applying clumped isotope thermometry in a variety of deep water basins over the entire Cenozoic that finds the same discrepancy. The difference in temperatures is partially explained by the omission of a correction for the lower pH value of the early Cenozic oceans to the $\delta^{18}O$-temperature calibration. Additionally, the $\delta^{18}O_B$ are measured relative to an assumed global $\delta^{18}O_{SW}$-value of -1 ‰, reflecting an ice-free world. The independently derived temperature estimates in this study challenge that assumption. Deconvoluting the seawater oxygen isotope signature from $\delta^{18}O_B$-values using Δ_{47}-based temperatures exposes values over the entire range from those in an ice-free world to those during the glacial maxima of the Pleistocene. Storage of meteoric water on land in any form, spatial heterogeneity of $\delta^{18}O_{SW}$-values and foreign input of heavy oxygen are proposed as possible mechanisms explaining this conundrum, yet none of these can explain the magnitude and variability of the mismatch entirely. The use of $\delta^{18}O$-thermometry to establish DSTs in deep time is best re-assessed before further applications and existing temperature records need re-evaluation.

A 7 °C difference between North and South Atlantic deep waters at 58 Ma puts hypotheses of an early Paleocene opening of an Atlantic equatorial gateway to test. A required coeval similar temperature signal is only observed at the onset of the EECO at 53 Ma. Southern hemisphere sea surface temperatures show a reversed trend across the PETM compared to South Atlantic deep sea temperatures, which might indicate a reconfiguration of Southern Ocean overturning circulation. Increased understanding of the characteristics of Atlantic overturning across the Paleocene, up to the onset of the EECO, can be acquired by improving the resolution of the Δ_{47} and $\varepsilon_{\mathrm{Nd(t)}}$ records in the North and South Atlantic.

A rough assessment puts late Paleocene Earth System Sensitivity at 6 - 8 °C warming per doubling of atmospheric CO_2, which is at the high-end of previous estimates for the early Cenozoic. To refine this assessment further constraints on Paleocene atmospheric CO_2 levels are imperative. To observe earth's climate response under a regime of *increasing* atmospheric carbon-dioxide from present-day to near future CO_2 levels the late Paleocene may prove to be the best analog we have.

Outlook - A continuous South Atlantic (Walvis Ridge) DST record based on clumped isotope thermometry is continuously getting closer to completion at Utrecht University and will aid the interpretation of the primarily North Atlantic Δ_{47}-DST record from Meckler et al. (2022) . Over the last 20 years, community efforts have accelerated the applicability of clumped isotopes as a paleothermometer (e.g. Bernasconi et al. (2021)). Although great precision and reproducibility has already been obtained in IRMS, the field of clumped isotope thermometry at large is still in its infancy and exciting developments are ahead. Isotope Ratios Laser Spectrometry (IRLS) is a novel development that allows for distinction between different isotopologues of the same mass, is less hampered by potential contamination and has the potential to achieve greater reproducibility on smaller sample sizes (Huntington & Petersen, 2023).

Acknowledgements

I would like to thank my supervisors, Tobias Agterhuis, Martin Ziegler and Lucas Lourens for provoking my enthousiasm in deep-time paleoceanography and their guidance during the course of this research. Additionally, I would like to thank those who have worked on - and are still working on - the reconstruction of the Walvis Ridge clumped isotope record. Specifically for the late Paleocene and early Eocene discussed in this study: Saike Ke, Bas Koene, Lea de Vries, Meya Kersten, Sanne Posthuma and Anne Roozendaal. I am much obliged to Arnold van Dijk and Desmond Eefting for putting in tremendous effort to keep the IRMS facilities running continously at the Utrecht University GeoLab. Natasja Wolters and Giovanni Dammers are thanked for their assistance and patient explanations on sample preparation. Furthermore, my gratitude goes out to everyone at the Utrecht University clumped isotope working group for their worthwhile feedback and contributions during our weekly discussions. Lastly, a final word of appreciation to Elena Domínguez Valdes for taking the time and effort to get me kick-started on data-analysis and plotting in *R* and answering any of my follow-up questions.

A Appendix A: Tables and Figures

Table A.1: Accepted values for standards used in applied corrections in this study. Data from Bernasconi et al. (2021) and Müller et al. (2019).

Standards	Δ_{47} (I-CDES 90°C)	$\delta^{18}O$ (‰ VPDB)	$\delta^{13}C$ (‰ VPDB)
ETH-3	0.6132 ± 0.0014	-1.78 ± 0.06	1.71 ± 0.02
ETH-2	0.2085 ± 0.0015	-18.69 ± 0.11	-10.17 ± 0.06
ETH-1	0.2052 ± 0.0016	-2.19 ± 0.04	2.02 ± 0.03
IAEA-C2	0.6445 ± 0.0021	-8.94 ± 0.04	-8.25 ± 0.02
Merck	0.5151 ± 0.0034	-15.62 ± 0.01	-41.91 ± 0.02
UU reference gas		-2.82	-4.67

Table A.2: Numerical results for measured Δ_{47}-values (I-CDES scale), carbonate oxygen and carbon stable isotope values, reconstructed temperatures and reconstructed sewater isotope values.

Bin	Δ_{47} (I-CDES 90°C) (± 1SE)	SD	Temperature (°C) (± 95% CI)	$\delta^{13}C_{Cib}$ (‰ VPDB)	$\delta^{18}O_{Cib}$ (‰ VPDB)	$\delta^{18}O_{SW}$ (‰ VSMOW)
56.7	0.6309 ± 0.0047	0.0405	14.7 ± 2.8	2.25	0.29	0.34
57.0	0.6379 ± 0.0047	0.0447	12.6 ± 2.7	2.42	0.31	-0.08
57.9	0.6252 ± 0.0070	0.0519	16.4 ± 4.3	2.79	0.42	0.83
60.2	0.6322 ± 0.0045	0.0446	14.3 ± 2.6	2.06	0.75	0.73

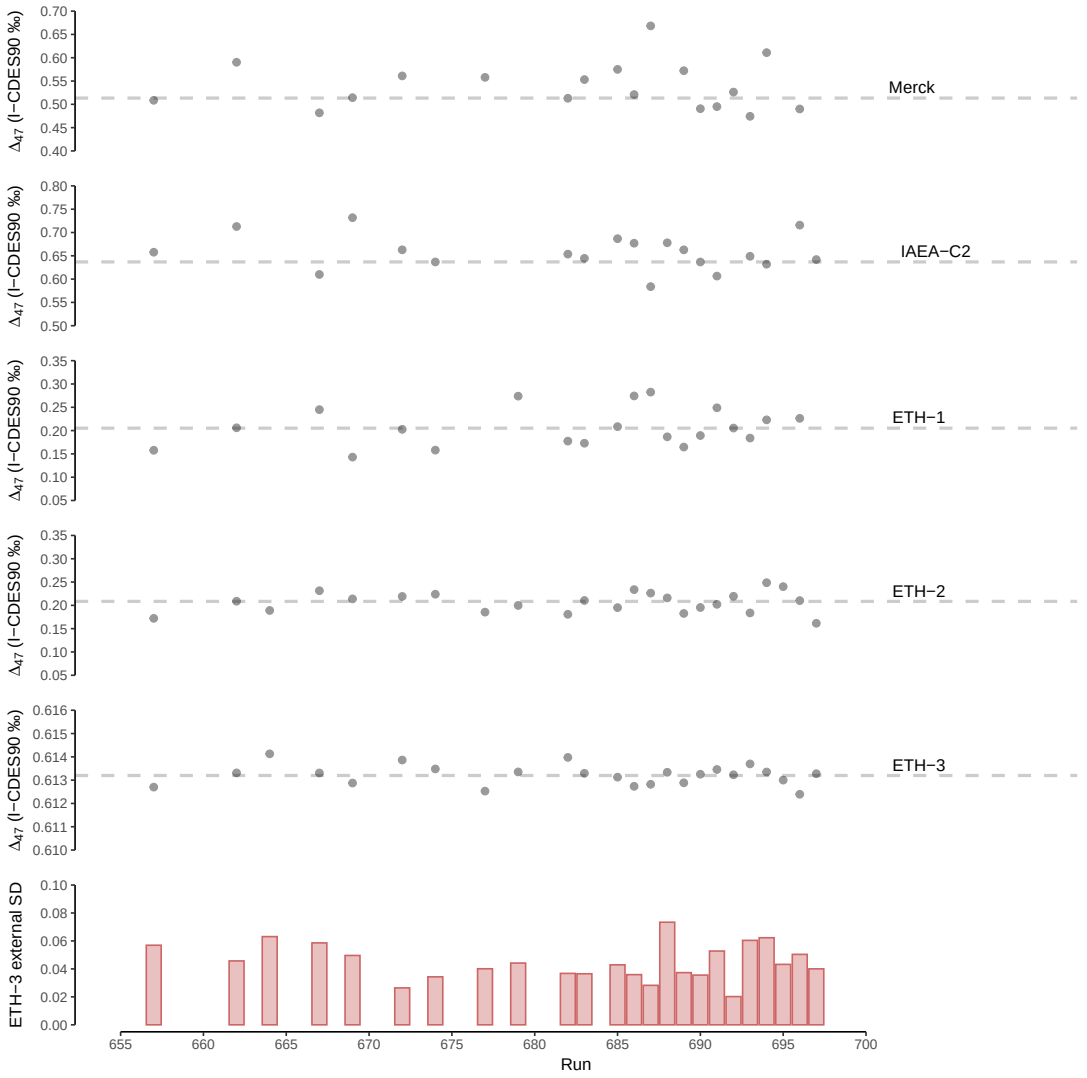

Figure A.1: Reproducibility of check-standards IAEA-C2 and Merck over the course of measuring period. Measuring runs 657 to 697 took place between 27-10-2022 and 19-01-2023 at Utrecht University GeoLab. variations in ETH-1, ETH-2 and ETH-3 are also included but provide less insight in long-term reproducibility as they are corrected by their own long-term averages. Bottom panel shows standard deviations for the ETH-3 per run based on 13 to 16 replicate measurements.

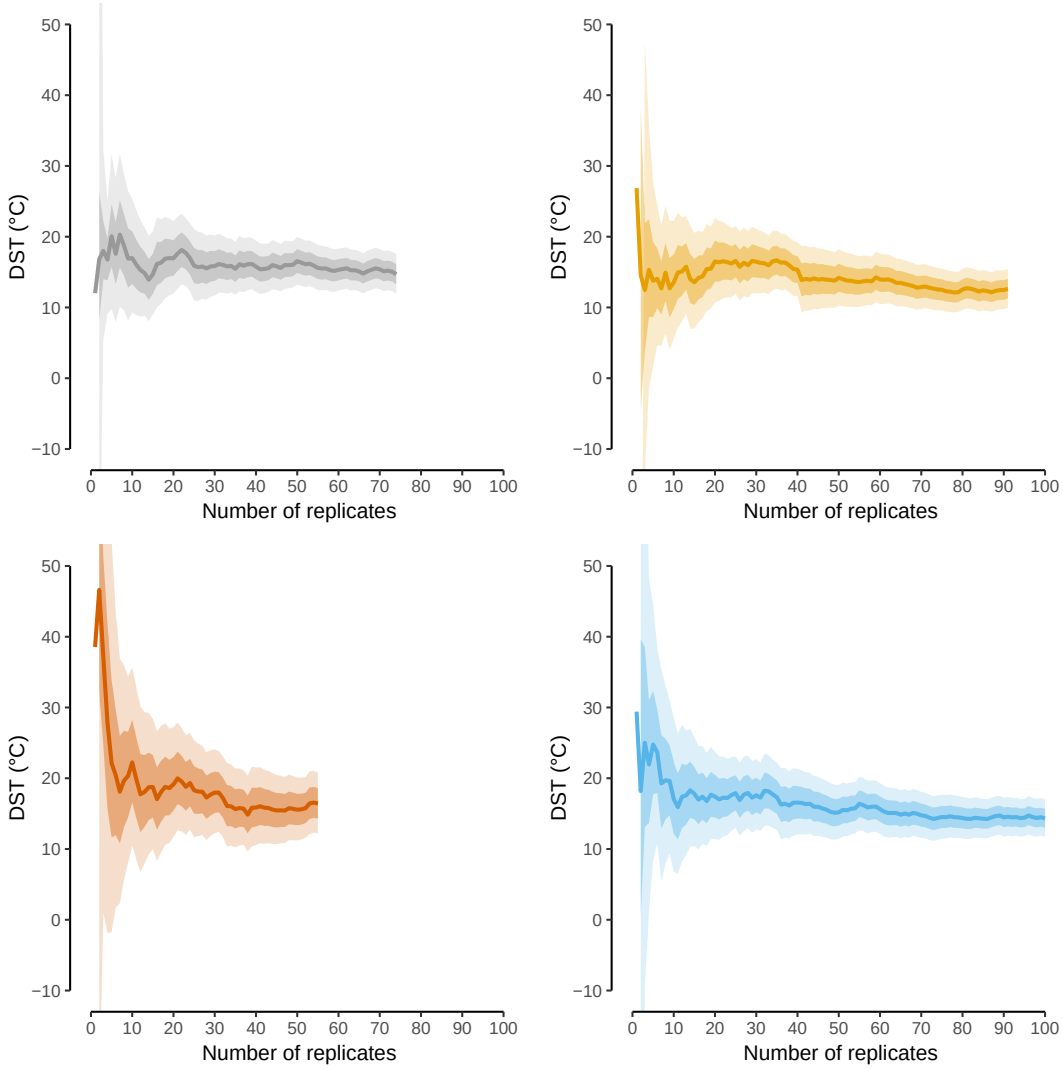

Figure A.2: Evolution of mean temperature and 68% and 95% confidence intervals with the iterative addition of single sample measurements. Top left to bottom right: 56.7, 57.0, 57.9 and 60.2 Ma bins.

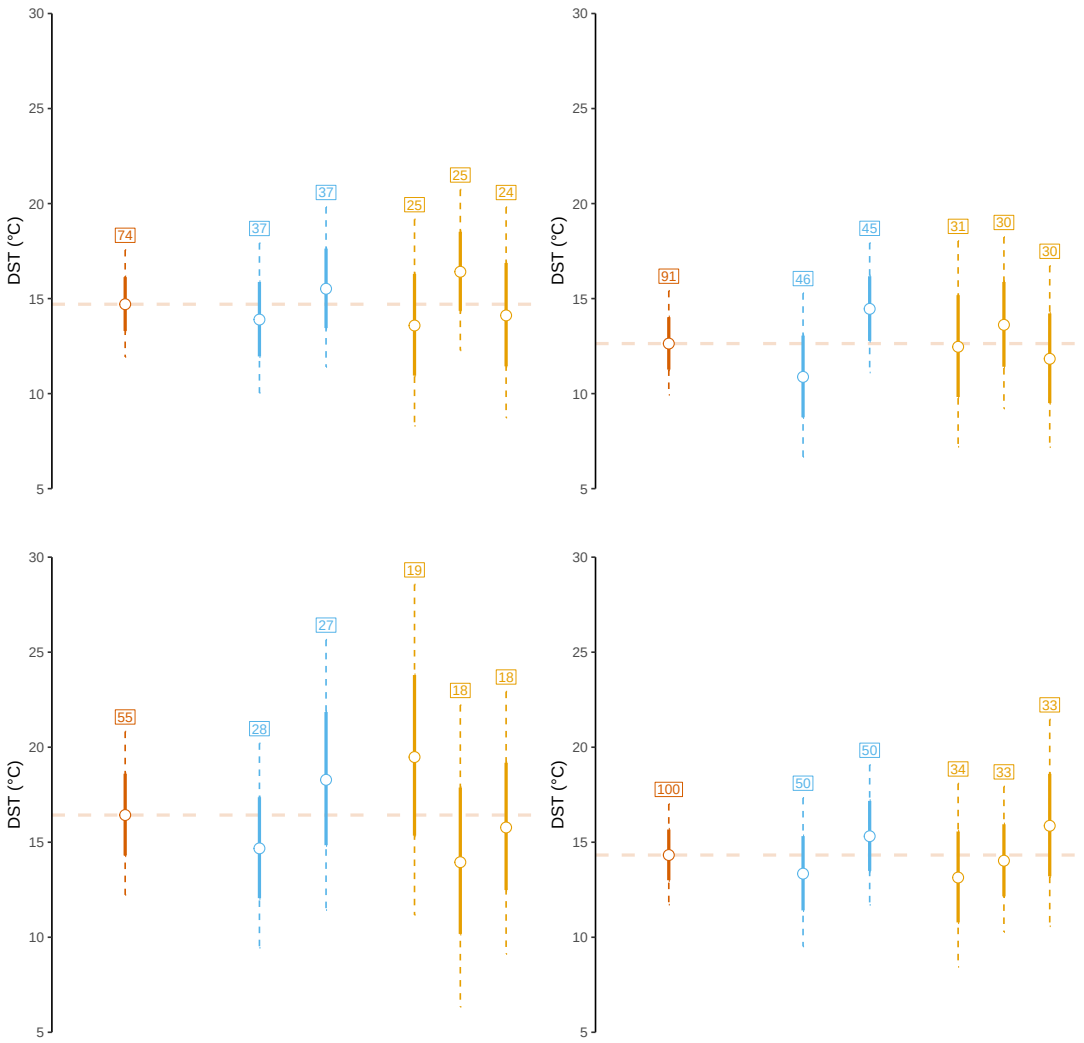

Figure A.3: A visual analysis on even sub-setting of bins. Each bin (red) was subdivided into two (blue) or three (orange) bins. Bins were arranged on age (core-depth) of samples and subdivided such that every *n*-th sample was included in sub-bin *n*. Thus all sub-bins span the same interval as the main bin. Top left to bottom right: 56.7, 57.0, 57.9 and 60.2 Ma bins.

B Appendix B: R Code

The following pages contain the annotated R-script used for data-analysis and plotting the figures in this thesis. Most code has been duplicated for each figure so that each of these pieces of script can be used on its own without being dependent on earlier definitions.

```r
# This R script was created for clumped isotope data analysis using the output archive file (xlsx) from the Clumped Isotope IRMS setups at the UU GeoLab Stable Isotope Laboratory winter 2022-2023.

# Author: Brendan Oerlemans (b.oerlemans@uu.nl)

# Import required packages

library(readxl)
library(tidyverse)
library(ggpubr)
library(patchwork)
library(deeptime)
library(ggh4x)
library(ggrepel)

# Set working directory to local drive and folder
setwd("~/Studie/MarineSciences/Clumped_MSCresearch/R")

# constants for D47-Temperature calculations
slope <- 39700 # meinicke et al. (2021)
int <- 0.1518 # meinicke et al. (2021)
C <- 273.15 # Kelvin to Celsius

# other constants
d18Oicefree <- -1 # d18O seawater values in an ice free world
d18Omodern <- 0
d18Oglacial <- 1
pHpi <- 8.2 # ocean pH for pre-industrial

##    IMPORTING DATA FROM REFERENCED STUDIES
#     - All data is available from DOI's referenced.
#     - Unless otherwise stated, import and processing happens on unaltered original datafiles as named and published by respective authors.

# CENOGRID (Westerhold et al., 2020) https://doi.org/10.1126/science.aba6853
westerhold <- read.table("data/Westerhold-etal_2020/datasets/TableS34.tab", sep="\t", skip=23, header=FALSE)
colnames(westerhold) = c("age","d13Ccount","d13C","d13Cinterp","d18Ocount","d18O","d18Ointerp","d13Cloess","d18Oloess","comment","d13Cloesslt","d18Oloesslt","comment2")
westerhold <- westerhold |>
  mutate(
    T_Hansen = case_when(
      age >= 0 & age <= 3.66 ~ 1-4.4*((d18Oloess-3.25)/3),
      age > 3.66 & age <= 34.025 ~ 5-8*((d18Oloess-1.75)/3),
      age > 34.025 ~ (-4*d18Oloess)+12, # Hansen et al. (2013), Supplementary Material Westerhold 2020
      TRUE ~ as.numeric(NA)),
    T_Marchitto = case_when(
      age >= 34.025 ~ (0.245 - sqrt(0.045461 + 0.0044*(d18Oloess-d18Oicefree)))/0.0022, # Calibration from Marchitto et al. (2014), eq. 9 in https://doi.org/10.1016/j.gca.2013.12.034
      TRUE ~ as.numeric(NA)))

# Mg/Ca deep sea temperature trend (Cramer et al., 2011) https://doi.org/10.1029/2011JC007255
cramer <- read.table("data/cramer_2011/jgrc12191-sup-0013-ts03.txt", sep="\t", header=TRUE)

cramer <- cramer |>
  drop_na(Mg.Ca) |>
  mutate(
    T_MgCa_lear = (Mg.Ca - 1.36)/0.106, # Using the calibration from Lear et al. (2010) https://doi.org/10.1029/2009PA001880
    T_MgCa_lear_min = (Mg.Ca.min - 1.36)/0.106,
    T_MgCa_lear_max = (Mg.Ca.max - 1.36)/0.106)

# Mg/Ca deep sea temperature datapoints (Cramer et al., 2011) https://doi.org/10.1029/2011JC007255
cramerall <- read.table("data/cramer_2011/jgrc12191-sup-0011-ts01.txt", sep="\t", skip=1, header=FALSE)
colnames(cramerall) <- c("Site", "Depth", "Age", "MgCa", "MgCa_adj", "Taxa", "Paleodepth", "ref")
cramerall <- cramerall |>
  mutate(
    T_MgCa_lear = (MgCa - 1.36)/0.106,
    T_MgCa_lear_adj = (MgCa_adj - 1.36)/0.106)

# Boron isotope based Cenozoic pH record (Rae et al., 2021) https://doi.org/10.1016/j.gca.2013.12.034
rae <- read_xlsx("data/rae_2021/ea49_rae_suppl_data1.xlsx", sheet="d11B_pH")
rae <- rae |>
  mutate(age = age/1000) |>
  drop_na(xco2)

# IODP site 1262 stable isotope data (Littler et al., 2014) https://doi.org/10.1016/j.epsl.2014.05.054
littler <- read.table("data/Littler_2014/datasets/208-1262_CF_benthic_stable_isotope.tab", sep="\t", header=TRUE, skip=26)
colnames(littler) = c("sample","depth","depthcomp","age","CF","d13C","d18O","REF")

# Apply Westerhold et al. (2020) age model to Littler (2014) data (DOI's as before)
WHage1262 <- read.table("data/Westerhold-etal_2020/datasets/TableS28.tab", sep="\t", header=TRUE, skip=19)
WHage1263 <- read.table("data/Westerhold-etal_2020/datasets/TableS29.tab", sep="\t", header=TRUE, skip=19)

littler <- littler |>
  mutate (
    WHage = (approx(WHage1262$Depth.cr..rmcd., WHage1262$Tuned.time..Ma., depthcomp)$y),
    T_MgCa_lear = (approx(cramer$Age, cramer$T_MgCa_lear, WHage)$y),
    age = age/1000,
    pH = (approx(rae$age, rae$pH, age)$y),
    d18Ocib = (`d18O` + 0.1)/0.89, # correct Nutallides to Cibicoides (Katz et al., 2013) https://doi.org/10.1029/2002PA000798
    d18Ocib_zeebe = d18Ocib + (pH-pHpi)*(1.42), # correct d18Ocib for pH according to Zeebe et al., 2001 https://doi.org/10.1029/2002PA000798
    d18Ocib_rathmann = d18Ocib + (pH-pHpi)*(0.65), # correct d18Ocib for pH according to Rathmann et al., 2008 https://doi.org/10.1016/j.marmicro.2007.08.001
    d18Osw_MgCa = d18Ocib + 0.245*T_MgCa_lear - 0.0011*T_MgCa_lear^2 - 3.31, # calculate seawater d18O using Marchitto (2014)
    d18Osw_MgCa_zeebe = d18Ocib_zeebe + 0.245*T_MgCa_lear - 0.0011*T_MgCa_lear^2 - 3.31, # calculate seawater d18O using Marchitto (2014) and Zeebe pH corrections
    d18Osw_MgCa_rathmann = d18Ocib_rathmann + 0.245*T_MgCa_lear - 0.0011*T_MgCa_lear^2 - 3.31, # calculate seawater d18O using Marchitto (2014) and Rathmann pH corrections
    T_hansen = (-4*d18Ocib)+12) #Hansen et al., 2013
```

```r

# Stable isotope data for North Atlantic sites (Cramer et al., 2009) https://doi.org/10.1029/2020JC016970 (*Data has reformatted prior to import*)
cram09NA <- read.table("data/cramer_2009/datacramer2009NA.csv", sep=",", header=TRUE)

# Neodymium isotopes data (Batenburg et al., 2018) https://doi.org/10.1038/s41467-018-07457-7
batenburg1267 <- read.table("data/batenburg_2018/1267.txt", sep="", header=TRUE)
batenburg1403 <- read.table("data/batenburg_2018/1403.txt", sep="", header=TRUE)

# Neodymium isotopes DR sites (Martin et al., 2012) https://doi.org/10.1016/j.epsl.2012.01.037
martin1258 <- read_xls("data/martin_2012/1-s2.0-S0012821X12000660-mmc1.xls", sheet="1258")
martin1260 <- read_xls("data/martin_2012/1-s2.0-S0012821X12000660-mmc1.xls", sheet="1260")

martinDR <- bind_rows(martin1258, martin1260)

martinDR <- martinDR |>
  rename(
    Age = Age1,
    eNdt = `εNd(t)4`) |>
  transform(Age = as.numeric(Age)) |>
  drop_na(Age)

# Neodymium isotopes IODP site 1262 (Via et al., 2006) https://doi.org/10.1130/G22545.1
via1262 <- read.table("data/via_2006/1262.txt", sep="", header=TRUE)

via1262 <- via1262 |>
  rename(
    Age = Age.Ma.,
    eNdt = εNd.t.)

# Additional Cenozoic CO2 data (PaleoCO2.org / Hoenisch et al., 2022) https://zenodo.org/record/7348638
paleoCO2 <- read.table("data/paleoco2/age_co2_plot_data.csv", sep=",", header=TRUE)

paleoCO2 <- paleoCO2 |>
  mutate(
    age = age/1000,
    age_l = age - (age_uncertainty_younger/1000),
    age_h = age + (age_uncertainty_older/1000),
    co2_l = co2 - co2_uncertainty_lower,
    co2_h = co2 + co2_uncertainty_higher) |>
  filter(grepl('Boron|Stomata|Land Plant', proxy))

# SST data site 959 (Cramwinckel et al., 2018) https://doi.org/10.1038/s41586-018-0272-2
cramwinckel18_tex <- read_xlsx("data/cramwinckel_2018/41586_2018_272_MOESM1_ESM.xlsx", sheet="Tropcomp_1", range="A2:G250")

cramwinckel18_tex <- cramwinckel18_tex |>
  rename(
    age = `Age (Ma, GTS2012)`)

# SST data site 1209 (Bijl et al., 2009) https://doi.org/10.1038/nature08399
bijl09_tex <- read_xls("data/bijl_2009/41586_2009_BFnature08399_MOESM285_ESM.xls", sheet="Sheet1")

# Additional SST data https://www.paleo-temperature.org/
phanSST <- read_xlsx("data/PhanSST/PhanSST_v001.xlsx")

phanSST <- phanSST |>
  filter(between(Age, 40, 75))

phanSST1262 <- phanSST |>
  filter(grepl("1262", SiteName)) |>
  filter(Age > 60) |>
  mutate(
    Age = round(Age, digits=1)) |>
  group_by(Age) |>
  summarise(
    Age = mean(Age),
    d18O = mean(ProxyValue)) |>
  mutate(
    SST = 17 - 4.52*(d18O - d18Oicefree) + 0.03*(d18O - d18Oicefree)^2)

# Clumped isotope data (Meckler et al., 2022) https://doi.org/10.1126/science.abk0604
meckler_2022 <- read_xlsx("data/meckler_2022/science.abk0604_data_s1.xlsx", skip=1)

# select relevant data, drop empty lines, add interpolated pH values from Rae et al.
meckler_2022 <- meckler_2022 |>
  select( "Age (Ma, CENOGRID)", "Site", "D47 avg     I-CDES (‰)", "N", "D47 SE (‰)", "d18O Cibicidoides (‰ VPDB)", "d13C Cibicidoides (‰ VPDB)") |>
  dplyr::rename(
    binage = `Age (Ma, CENOGRID)`,
    D47 = `D47 avg     I-CDES (‰)`,
    SE = `D47 SE (‰)`,
    d18Ocibavg = `d18O Cibicidoides (‰ VPDB)`,
    d13Ccibavg = `d13C Cibicidoides (‰ VPDB)`)|>
  drop_na(Site) |>
  transform(binage = as.numeric(binage)) |>
  mutate(
    bin_id = paste("MCKLR_", formatC(binage, digits = 2, format = "f"), sep = ""),
    extSD = SE*sqrt(N),
    pH = (approx(rae$age, rae$pH, binage)$y),
    location = case_when(
      Site == 1406 | Site == 1407 | Site == 1409 | Site == 1410 ~ "North Atlantic",
      Site == 690 ~ "Southern Ocean",
      Site == 761 ~ "Indian Ocean",
      TRUE ~ "South Atlantic")) |>
  filter(bin_id != "MCKLR_54.00") |> # filter out ETM2 datapoint that consists of background values and hyperthermals combined
  filter(bin_id != "MCKLR_51.11") # filter out duplicate datapoint with agterhuisEECO dataset

# Clumped isotope data Walvis Ridge - Eocene (Agterhuis et al., 2022 - unpublished)
agterhuisEECO <- read_xlsx("data/agterhuis_eeco853.xlsx", sheet="data")
```

```r
agterhuisEECO_data <- agterhuisEECO |>
  mutate(
    `Final AFF` = as.numeric(`Final AFF`),
    d18Ocib = as.numeric(`d18Ocorr`),
    d13Ccib = case_when(
      Species == "Cib" ~ as.numeric(`Final d13C`),
      Species == "Ntr" ~ as.numeric(`Final d13C`) + 0.34, # Katz et al. (2003)
      Species == "Ou" ~ as.numeric(`Final d13C`) + 0.72),  #Katz et al. (2003)
    pH = (approx(rae$age, rae$pH, `Age (Ma)`)$y),
    bin_id = case_when(
      `Age (Ma)` >= 52.60 ~ "EECO53",
      `Age (Ma)` >= 52.00 ~ "EECO52.1",
      `Age (Ma)` >= 51.45 ~ "EECO51.8",
      `Age (Ma)` >= 49.50 ~ "EECO51.2",
      `Age (Ma)` >= 48.15 ~ "EECO49.2",
      TRUE ~ "EECO48",)) |>
  drop_na(`Age (Ma)`) |>
  group_by(bin_id)

agterhuisEECO_data <- agterhuisEECO_data |>
  summarise(
    D47 = mean(`Final AFF`),
    extSD = sd(`Final AFF`),
    N = n(),
    SE = extSD/sqrt(N),
    pH = mean(pH),
    d18Ocibavg = mean(d18Ocib, na.rm = TRUE),
    d13Ccibavg = mean(d13Ccib, na.rm = TRUE),
    binage = mean(`Age (Ma)`),
    binagemin = min(`Age (Ma)`),
    binagemax = max(`Age (Ma)`),
    #binduration = binagemax - binagemin,
    location = "South Atlantic",
    Site = "1263")

# Additional Clumped isotope data Walvis Ridge ETM2 (Agterhuis et al., 2022) https://doi.org/10.1038/s43247-022-00350-8
agterhuisETM <- read_xlsx("data/agterhuis_2022.xlsx", sheet="D47 & d18O-T sorted on d18O", skip=6)

agterhuisETM_data <- agterhuisETM |>
  select("Site", "Age (Ma)", "d13C all corrected to Cib (‰ VPDB)", "d18O all corrected to Cib (‰ VPDB)", "D47 (‰ I-CDES)", "Bin")
  |>
  rename(
    d13Ccib = `d13C all corrected to Cib (‰ VPDB)`,
    d18Ocib = `d18O all corrected to Cib (‰ VPDB)`,
    bin_id = Bin) |>
  mutate(
    Site = str_remove(Site, "ODP Site "),
    bin_id = case_when(
      bin_id == "Hyperthermal peak" ~ "ETM2_HT",
      bin_id == "Slope" ~ "ETM2_SL",
      bin_id == "Background" ~ "ETM2_BG",
      TRUE ~ NA),
    pH = (approx(rae$age, rae$pH, `Age (Ma)`)$y)) |>
  group_by(bin_id)

agterhuisETM_data <- agterhuisETM_data |>
  summarise(
    D47 = mean(`D47 (‰ I-CDES)`),
    extSD = sd(`D47 (‰ I-CDES)`),
    N = n(),
    SE = extSD/sqrt(N),
    pH = mean(pH),
    d18Ocibavg = mean(d18Ocib),
    d13Ccibavg = mean(d13Ccib),
    binage = mean(`Age (Ma)`),
    binagemin = min(`Age (Ma)`),
    binagemax = max(`Age (Ma)`),
    location = "South Atlantic" ) |>
  filter(bin_id == "ETM2_BG") # only use background value

# read in and filter archive file from UU GeoLAB
archive <- read_xlsx("ARCHIVE_2022_October_CORR.xlsx", sheet="Archive", skip=2573) #CORR refers to file that was corrected for
mislabeled samples
archive <- archive |>
  select("Date", "SA/STD", "Run", "Sa m44", "Weight...24", "49 parameter", "D47 SD", "Final AFF", "Temperature", "Final d18O",
  "Final d13C") |>
  rename(weight = Weight...24)


# treshold value for outliers
high49 <- 0.1
lowintensity <- 10000
d18Olo <- -0.5
d18Ohi <- 1.5

# Selecte relevant samples for this study from archive and remove outliers
archive_filter <- archive |>
  filter(grepl("SK|BO|TA_EECO50", `SA/STD`)) |>
  filter(`49 parameter` < high49) |>
  filter(`Sa m44` > lowintensity) |>
  filter(between(`Final d18O`, d18Olo, d18Ohi)) |>
  mutate(
    Species = case_when(
      grepl("Ou", `SA/STD`) ~ "Ou",
      TRUE ~ "Ntr"))

# Load DISDATA from Bremen Core Repository, append MCD depths to sample-list based on self-created LOOKUP code
DIS_depths <- read_xlsx("samples/DIS_DATA.xlsx")
samples <- read_xlsx("samples/Sample_list.xlsx")
```

```r
samples <- samples |>
  select("LOOKUP", "SA/STD", "Core") |>
  left_join(DIS_depths, by="LOOKUP")

# Apply WESTERHOLD 2020 age-model to sample-list based on MCD_TOP
samples <- samples |>
  mutate(
    age = case_when(
      Core == 1262 ~ (approx(WHage1262$Depth.cr..rmcd., WHage1262$Tuned.time..Ma., MCD_TOP)$y),
      Core == 1263 ~ (approx(WHage1263$Depth.cr..rmcd., WHage1263$Tuned.time..Ma., MCD_TOP)$y),
      TRUE ~ as.numeric(NA)))

# Apply LITTLER 2014 age-model (alternative) to sample-list based on MCD_TOP
Lage <- read.table("data/Littler_2014/datasets/208-1262_age_model.tab", sep="\t", header=TRUE, skip=17)
samples <- samples |>
  mutate (Lage = (approx(Lage$Depth..m., Lage$Age.model..ka., MCD_TOP)$y)/1000)

# Append agemodels (Westerhold, Littler) to archive (selection)
archive_filter <- left_join(archive_filter, samples, by = "SA/STD")

## Create Clumped Dataset from filtered archive ----
# Binning archive (selection) samples
bins <- c("LP_56.7", "LP_57.1", "LP_58.0", "LP_60.3", "EECO50", "ETH-4", "ETH-3", "ETH-2", "ETH-1", "Merck", "IAEA-C2")

archive_filter <- archive_filter |>
  mutate(
    d18Ocib = (`Final d18O` + 0.1)/0.89, # correct Nutallides to Cibicoides # Katz et al., 2013
    d13Ccib = case_when(
      Species == "Cib" ~ as.numeric(`Final d13C`),
      Species == "Ntr" ~ as.numeric(`Final d13C`) + 0.34, # Katz et al. (2003)
      Species == "Ou" ~ as.numeric(`Final d13C`) + 0.72),  #Katz et al. (2003)
    pH = (approx(rae$age, rae$pH, age)$y), # look up pH value (interpolate) from Rae et al., 2021
    d18Ocib_zeebe = d18Ocib + (pH-pHpi)*(1.42), # correct d18Ocib for pH according to Zeebe et al., 2001
    d18Ocib_rathmann = d18Ocib + (pH-pHpi)*(0.65), # correct d18Ocib for pH according to Rathmann et al., 2008
    T_marchitto =  (0.245 - sqrt(0.045461 + 0.0044*(d18Ocib-d18Oicefree)))/0.0022, # Marchitto et al. (2014), eq. 9
    T_march_zeebe = (0.245 - sqrt(0.045461 + 0.0044*(d18Ocib_zeebe-d18Oicefree)))/0.0022,
    T_march_rathmann = (0.245 - sqrt(0.045461 + 0.0044*(d18Ocib_rathmann-d18Oicefree)))/0.0022,
    bin_id = str_extract(`SA/STD`, str_c(bins, collapse = "|"))) |>
  group_by(bin_id)

# summarize and calculate values per bin
Clumped_data <- archive_filter |>
  summarise(
    D47 = mean(`Final AFF`),
    extSD = sd(`Final AFF`),
    N = n(),
    SE = extSD/sqrt(N),
    pH = mean(pH),
    d18Ocibavg = mean(d18Ocib),
    d13Ccibavg = mean(d13Ccib),
    binage = mean(age, na.rm = TRUE),
    binagemin = min(age, na.rm = TRUE),
    binagemax = max(age, na.rm = TRUE),
    location = "South Atlantic",
    Site = as.character(min(Core, na.rm = TRUE)))

# Merging all clumped datasets in one dataframe
ALL_clumped <- bind_rows(Clumped_data, agterhuisEECO_data, agterhuisETM_data, meckler_2022)

# Apply the same calculations to all D47 values from different studies:
ALL_clumped <- ALL_clumped |>
  mutate(
    binduration = binagemax - binagemin,
    T_d18Oavg = (0.245 - sqrt(0.045461 + 0.0044*(d18Ocibavg-d18Oicefree)))/0.0022, # calculate d18Ocib based temps for each bin - Marchitto et al. (2014), eq. 9
    CI95upper = D47 + qt(0.975, N-1) * SE, # 4 lines: Calculate upper and lower values for 95% and 68% CI
    CI95lower = D47 - qt(0.975, N-1) * SE,
    CI68upper = D47 + qt(0.840, N-1) * SE,
    CI68lower = D47 - qt(0.840, N-1) * SE,
    T47_meinicke = sqrt(slope/(D47-int))-C, # calculate D47 based temps using Meinicke (2021)
    d18Osw = d18Ocibavg + 0.245*T47_meinicke - 0.0011*T47_meinicke^2 - 3.31, # calculate seawater d18O using Marchitto (2014)
    d18Ocibavg_zeebe = d18Ocibavg + (pH-pHpi)*(1.42), # correct d18Ocib for pH according to Zeebe et al., 2001
    d18Ocibavg_rathmann = d18Ocibavg + (pH-pHpi)*(0.65), # correct d18Ocib for pH according to Rathmann et al., 2008
    d18Osw_zeebe = d18Ocibavg_zeebe + 0.245*T47_meinicke - 0.0011*T47_meinicke^2 - 3.31, # calculate seawater d18O using Marchitto (2014)
    d18Osw_rathmann= d18Ocibavg_rathmann + 0.245*T47_meinicke - 0.0011*T47_meinicke^2 - 3.31, # calculate seawater d18O using Marchitto (2014)
    T_CI95upper = sqrt(slope/(CI95lower-int))-C, # 4 lines: Calculate upper and lower temperatures associated with lower and upper CI's
    T_CI95lower = sqrt(slope/(CI95upper-int))-C,
    T_CI68upper = sqrt(slope/(CI68lower-int))-C,
    T_CI68lower = sqrt(slope/(CI68upper-int))-C,
    d18Osw_CI95upper = d18Ocibavg + 0.245*T_CI95lower - 0.0011*T_CI95lower^2 - 3.31, # 4 lines: CI values for d18Osw
    d18Osw_CI95lower = d18Ocibavg + 0.245*T_CI95upper - 0.0011*T_CI95upper^2 - 3.31,
    d18Osw_CI68upper = d18Ocibavg + 0.245*T_CI68upper - 0.0011*T_CI68upper^2 - 3.31,
    d18Osw_CI68lower = d18Ocibavg + 0.245*T_CI68lower - 0.0011*T_CI68lower^2 - 3.31,
    T95CIpm = ((T_CI95upper-T47_meinicke)+(T47_meinicke-T_CI95lower))/2
  )

# PLOTTING

# colorblind palette used throughout plots
cbPalette <- c("#56B4E9", "#D55E00", "#E69F00", "#999999", "#009E73", "#0072B2", "#F0E442", "#CC79A7")

# colour used for highlighting EECO, PETM etc.
episodecolor <- "#FFFFDD"

# x-axis boundaries for all plots are set here:
xlimplots_lo <- 46
```

```r
xlimplots_hi <- 70

# Set boundaries for hyperthermals:
EECO_min <- 50
EECO_max <- 52
ETM2_min <- 0
ETM2_max <- 0
PETM_min <- 55.75
PETM_max <- 55.95
KPG_min <- 65.9
KPG_max <- 66.1

# Structure of all plots:
# - Markers: plots hyperthermals as rectangular shapes in background
# - Data: data to be plotted
# - Labels: labels to be plotted with data
# - Key: Annotation or legend style explanation
# - Visually: add geological timescales, applies themes, sets transparancy

# Select data from all clumped data to be plotted (filter can be changed and additional filters can be applied):
data_sel <- ALL_clumped |>
  filter(grepl("Atlantic", location))

ylimplots_lo <- 2
ylimplots_hi <- 30

plot_clumped_temps <- ggplot() +
  scale_x_continuous(limits=c(xlimplots_lo-5, xlimplots_hi+5), breaks=seq(xlimplots_lo,xlimplots_hi,2)) +
  scale_y_continuous(limits=c(ylimplots_lo, ylimplots_hi), breaks=seq(ylimplots_lo+2, ylimplots_hi-6,2), position="left") +
  labs(x="Age (Ma)", y="DST (°C)")+
  # Markers
  annotate("rect", xmin = EECO_min, xmax = EECO_max, ymin = ylimplots_lo, ymax = ylimplots_hi, fill=episodecolor) +
  annotate("text", x = (EECO_min + EECO_max)/2, y = ylimplots_lo, vjust=-1, label = "EECO") +
  annotate("rect", xmin = ETM2_min, xmax = ETM2_max, ymin = ylimplots_lo, ymax = ylimplots_hi, fill=episodecolor) +
  annotate("text", x = (ETM2_min +ETM2_max)/2, y = ylimplots_lo, vjust=-1, label = "ETM2") +
  annotate("rect", xmin = PETM_min, xmax = PETM_max, ymin = ylimplots_lo, ymax = ylimplots_hi, fill=episodecolor) +
  annotate("text", x = (PETM_min +PETM_max)/2, y = ylimplots_lo, vjust=-1, label = "PETM") +
  # cenogrid
  geom_line(data=westerhold, aes(x = age, y=T_Hansen), alpha=0.1, linewidth=0.3) +
  # cramer Mg/Ca
  geom_line(data=cramer, aes(x = Age, y = T_MgCa_lear), color="#339933", linewidth=0.5, alpha=0.5) +
  geom_ribbon(data=cramer, aes(x = Age, ymin = T_MgCa_lear_min, ymax = T_MgCa_lear_max), fill="#339933", alpha=0.1) +
  geom_point(data=cramerall, aes(x = Age, y=T_MgCa_lear_adj), alpha=1, size=1.5, color="#339933", shape=21, fill="#339933") +
  # Data this study
  geom_errorbar(data=data_sel, aes(x = binage, ymax = T_CI95upper, ymin = T_CI95lower, color=location), alpha=1, width=0, linetype="dashed") +
  geom_errorbar(data=data_sel, aes(x = binage, ymax = T_CI68upper, ymin = T_CI68lower, color=location), alpha=1, width=0, size=1, linetype="solid") +
  geom_errorbarh(data=data_sel, aes(xmin = binagemin, xmax = binagemax, y = T47_meinicke, color=location), alpha=.2, size=5, height=0, linetype="solid") +
  geom_point(data=data_sel, aes(x = binage, y = T47_meinicke, color=location), size=3, shape=21, fill="white") +
  # labels (replicate N)
  geom_label_repel(data=data_sel |> filter(between(binage,xlimplots_lo,xlimplots_hi)),
                   aes(x = binage, y = T_CI95upper, label=N, color=location),
                   nudge_y=.5, direction="y", segment.color = NA, size=2, label.padding = unit(0.1, "lines"),label.r = unit(0, "lines")) +
  # key
  annotate("text", x = 61, y = 6.4, label = expression(paste(Delta["47"], " South Atlantic (this study)")), color="#D55E03", hjust=1, size=3) +
  annotate("text", x = 61, y = 5.6, label = expression(paste(Delta["47"], " North Atlantic (Meckler et al., 2022)")), color="#56B4E3", hjust=1, size=3) +
  annotate("text", x = 61, y = 4.8, label = "Mg/Ca Pacific (Cramer et al., 2011)", color="#339933", hjust=1, size=3) +
  annotate("text", x = 61, y = 4, label = expression(paste(delta^{18},"O CENOGRID (Westerhold et al., 2020)")), color="#999999", hjust=1, size=3) +
  # visually
  theme_classic() +
  guides(y ="axis_truncated") +
  theme(legend.position = "none") +
  scale_colour_manual(values=cbPalette, guide=FALSE) +
  scale_fill_manual(values=cbPalette, guide=FALSE) +
  coord_geo(dat = list("Geomagnetic Polarity Chron", "Geomagnetic Polarity Subchron", "stages", "epochs"),
            xlim = c(xlimplots_lo,xlimplots_hi), ylim = c(ylimplots_lo, ylimplots_hi-4),
            pos = list("b", "b", "b", "b"),
            lab = list(TRUE ,FALSE, TRUE, TRUE),
            height=list(unit(0.8, "line"), unit(0.8, "line"), unit(1.0, "line"), unit(1.5, "line")),
            fill=list("white", c("black", "white"), NULL, NULL),
            abbrv = list(FALSE, TRUE, FALSE, FALSE),
            size = list(2, 1, 3, 5),
            center_end_labels = TRUE,
            skip = "C19")

print(plot_clumped_temps)

# FIGURE 5.4 (NA/SA watermasses, T47, d18O, d13C, Nd-isotopes)

plot_T47_ymin <- 4
plot_T47_ymax <- 28

plot_T47 <- ggplot() +
  scale_x_continuous(limits=c(xlimplots_lo-15, xlimplots_hi+5), breaks=seq(xlimplots_lo,xlimplots_hi,1), position="top") +
  scale_y_continuous(limits=c(plot_T47_ymin,plot_T47_ymax), breaks=seq(plot_T47_ymin+2,plot_T47_ymax-4,2)) +
  labs(x="Age (Ma)", y="DST (°C)") +
  # Markers
  annotate("rect", xmin = EECO_min, xmax = EECO_max, ymin = plot_T47_ymin, ymax = plot_T47_ymax, fill=episodecolor) +
  annotate("rect", xmin = ETM2_min, xmax = ETM2_max, ymin = plot_T47_ymin, ymax = plot_T47_ymax, fill=episodecolor) +
  annotate("rect", xmin = PETM_min, xmax = PETM_max, ymin = plot_T47_ymin, ymax = plot_T47_ymax, fill=episodecolor) +
  # data
  geom_line(data=data_sel, aes(x = binage, y = T47_meinicke, color=location), stat="smooth", method="loess", alpha=0.2, size=10, level=0.7, span=0.4) +
```

```
    geom_errorbar(data=data_sel, aes(x = binage, ymax = T_CI95upper, ymin = T_CI95lower, color=location), alpha=1, width=0, linetype="dashed") +
    geom_errorbar(data=data_sel, aes(x = binage, ymax = T_CI68upper, ymin = T_CI68lower, color=location), alpha=1, width=0, size=1, linetype="solid") +
    geom_errorbarh(data=data_sel, aes(xmin = binagemin, xmax = binagemax, y = T47_meinicke, color=location), alpha=.2, size=5, height=0, linetype="solid") +
    geom_point(data=data_sel, aes(x = binage, y = T47_meinicke, color=location), size=3, shape=21, fill="white") +
    # key
    annotate("text", x = 60.8, y = 24, label = expression(paste(Delta["47"], " South Atlantic (this study)")), color="#D55E03", hjust=1, size=2.5) +
    annotate("text", x = 60.8, y = 22, label = expression(paste(Delta["47"], " North Atlantic (Meckler et al., 2022)")), color="#56B4E3", hjust=1, size=2.5) +
    # visually
    theme_classic() +
    guides(y ="axis_truncated") +
    theme(legend.position = "none") +
    scale_colour_manual(values=cbPalette) +
    coord_geo(dat = list("epochs", "stages", "Geomagnetic Polarity Subchron", "Geomagnetic Polarity Chron"),
              xlim = c(xlimplots_lo,xlimplots_hi), ylim = c(plot_T47_ymin,plot_T47_ymax),
              pos = list("t", "t", "t", "t"),
              lab = list(TRUE, TRUE, FALSE, TRUE),
              height=list(unit(1.5, "line"), unit(1.0, "line"), unit(0.8, "line"), unit(0.8, "line")),
              fill=list(NULL, NULL, c("black", "white"), "white"),
              abbrv = list(FALSE, FALSE, TRUE, FALSE),
              size = list(5, 3, 1, 2),
              center_end_labels = TRUE)

plot_d13C_NASA_ymin <- -1.5
plot_d13C_NASA_ymax <- 3

plot_d13C_NASA <- ggplot() +
  scale_x_continuous(limits=c(xlimplots_lo-2, xlimplots_hi+2), breaks=seq(xlimplots_lo,xlimplots_hi,1), position="top") +
  scale_y_continuous(limits=c(plot_d13C_NASA_ymin,plot_d13C_NASA_ymax), breaks=seq(plot_d13C_NASA_ymin+0.5,plot_d13C_NASA_ymax-0.5, 0.5), position="right") +
  labs(x="Age (Ma)", y=expression(paste(delta^{13},"C"["Cibicidoides"]," (\u2030 VPDB)"))) +
  # Markers
  annotate("rect", xmin = EECO_min, xmax = EECO_max, ymin = plot_d13C_NASA_ymin, ymax = plot_d13C_NASA_ymax, fill=episodecolor) +
  annotate("rect", xmin = ETM2_min, xmax = ETM2_max, ymin = plot_d13C_NASA_ymin, ymax = plot_d13C_NASA_ymax, fill=episodecolor) +
  annotate("rect", xmin = PETM_min, xmax = PETM_max, ymin = plot_d13C_NASA_ymin, ymax = plot_d13C_NASA_ymax, fill=episodecolor) +
  # cramer 2009 + Meckler 2022 North Atlantic || Littler South Atlantic
  geom_line(data=littler |> drop_na(d13C), aes(x=WHage, y=d13C), color="#D55E00", alpha=.2, size=.5) +
  geom_smooth(data=littler |> drop_na(d13C), aes(x=WHage, y=d13C), color="#D55E00", method="loess", method.args = list(degree = 2), alpha=1, size=1, se=FALSE, span=0.05) +
  geom_line(data=cram09NA |> drop_na(d13C_adj), aes(x=Age..GTS2004., y=d13C_adj) , color="#56B4E9", size=1, alpha=1) +
  #geom_smooth(data=cram09NA |> drop_na(d13C_adj), aes(x=Age..GTS2004., y=d13C_adj) , color="#56B4E9", method="loess", method.args = list(degree = 1), alpha=1, size=1, se=FALSE, span=0.2) +
  geom_point(data=meckler_2022, aes(x=binage, y=d13Ccibavg), shape=24, color="#56B4E9", fill="white", size=4) +
  # key
  annotate("text", x = 60.8, y = -0.2, label = "South Atlantic - IODP 1262 (littler et al., 2014)", color="#D55E03", hjust=1, size=2.5) +
  annotate("text", x = 60.8, y = -0.6, label = "North Atlantic - IODP 1051, DSDP 384/401/550 (Cramer et al., 2009)", color="#56B4E3", hjust=1, size=2.5) +
  #annotate("shape", x = 60.8, y = -1, shape=24, color="#56B4E9", fill="white", size=4) +
  #annotate("shape", x = 60.6, y = -1, shape=25, color="#56B4E9", fill="white", size=4) +
  geom_point(aes(x=60.7, y=-1), shape=24, color="#56B4E9", fill="white", size=3) +
  geom_point(aes(x=60.6, y=-1), shape=25, color="#56B4E9", fill="white", size=3) +
  annotate("text", x = 60.5, y = -1, label = "North Atlantic - IODP 1407/1409 (Meckler et al., 2022)", color="#56B4E3", hjust=1, size=2.5) +
  # visually
  theme_classic() +
  guides(y ="axis_truncated") +
  theme(panel.background = element_rect(fill='transparent'), #transparent panel bg
        plot.background = element_rect(fill='transparent', color=NA)) + #transparent plot bg)
  theme(axis.line.x=element_blank(),
        axis.text.x=element_blank(),
        axis.ticks.x=element_blank(),
        axis.title.x=element_blank()) +
  theme(legend.position = "none") +
  coord_geo(xlim = c(xlimplots_lo,xlimplots_hi), height=unit(0,"line"), alpha=0, color="white")  # align

plot_d18Ob_NASA_ymin <- 1.5
plot_d18Ob_NASA_ymax <- -2

plot_d18Ob_NASA <- ggplot() +
  scale_x_continuous(limits=c(xlimplots_lo-2, xlimplots_hi+2), breaks=seq(xlimplots_lo,xlimplots_hi,1), position="top") +
  scale_y_reverse(limits=c(plot_d18Ob_NASA_ymin,plot_d18Ob_NASA_ymax), breaks=seq(plot_d18Ob_NASA_ymin-0.5,plot_d18Ob_NASA_ymax+0.5,-0.5), position="left") +
  labs(x="Age (Ma)", y=expression(paste(delta^{18},"O"["Cibicidoides"]," (\u2030 VPDB)"))) +
  # Markers
  annotate("rect", xmin = EECO_min, xmax = EECO_max, ymin = plot_d18Ob_NASA_ymin, ymax = plot_d18Ob_NASA_ymax, fill=episodecolor) +
  annotate("rect", xmin = ETM2_min, xmax = ETM2_max, ymin = plot_d18Ob_NASA_ymin, ymax = plot_d18Ob_NASA_ymax, fill=episodecolor) +
  annotate("rect", xmin = PETM_min, xmax = PETM_max, ymin = plot_d18Ob_NASA_ymin, ymax = plot_d18Ob_NASA_ymax, fill=episodecolor) +
  # cramer 2009 + Meckler 2022 North Atlantic || Littler South Atlantic
  geom_line(data=littler |> drop_na(d18O), aes(x=WHage, y=d18O), color="#D55E00", alpha=0.2, size=0.5) +
  geom_smooth(data=littler |> drop_na(d18O), aes(x=WHage, y=d18O), color="#D55E00", method="loess", method.args = list(degree = 2), alpha=1, size=1, se=FALSE, span=0.05) +
  geom_line(data=cram09NA  |> drop_na(d18O_adj), aes(x=Age..GTS2004., y=d18O_adj) , color="#56B4E9",  alpha=1, size=1) +
  geom_point(data=meckler_2022, aes(x=binage, y=d18Ocibavg), shape=25, color="#56B4E9", fill="white", size=4) +
  # visually
  theme_classic() +
  guides(y ="axis_truncated") +
  theme(panel.background = element_rect(fill='transparent'), #transparent panel bg
        plot.background = element_rect(fill='transparent', color=NA)) + #transparent plot bg)
  theme(axis.line.x=element_blank(),
        axis.text.x=element_blank(),
        axis.ticks.x=element_blank(),
        axis.title.x=element_blank()) +
```

```
  theme(legend.position = "none") +
  coord_geo(xlim = c(xlimplots_lo,xlimplots_hi), height=unit(0,"line"), alpha=0, color="white")  # align

plot_nd_ymin <- -18
plot_nd_ymax <- 0

plot_nd <- ggplot() +
  scale_x_continuous(limits=c(xlimplots_lo-5, xlimplots_hi+5), breaks=seq(xlimplots_lo,xlimplots_hi,1)) +
  scale_y_continuous(limits=c(plot_nd_ymin,plot_nd_ymax), breaks=seq(plot_nd_ymin+2,plot_nd_ymax-2,2), position="right") +
  labs(x="Age (Ma)", y=expression(paste(epsilon["Nd(t)"]))) +
  # Markers
  annotate("rect", xmin = EECO_min, xmax = EECO_max, ymin = plot_nd_ymin, ymax = plot_nd_ymax, fill=episodecolor) +
  annotate("text", x = (EECO_min + EECO_max)/2, y = plot_nd_ymin, vjust=-1, label = "EECO") +
  annotate("rect", xmin = ETM2_min, xmax = ETM2_max, ymin = plot_nd_ymin, ymax = plot_nd_ymax, fill=episodecolor) +
  annotate("text", x = (ETM2_min +ETM2_max)/2, y = plot_nd_ymin, vjust=-1, label = "ETM2") +
  annotate("rect", xmin = PETM_min, xmax = PETM_max, ymin = plot_nd_ymin, ymax = plot_nd_ymax, fill=episodecolor) +
  annotate("text", x = (PETM_min +PETM_max)/2, y = plot_nd_ymin, vjust=-1, label = "PETM") +
  # Batenburg / Martin
  geom_line(data=batenburg1267, aes(x = Age.Ma., y = ENd.t.), linewidth=1, color="#D55E00") +
  geom_point(data=batenburg1267, aes(x = Age.Ma., y = ENd.t.), size=2, shape=15, color="#D55E00") +
  geom_line(data=via1262, aes(x = Age, y = eNdt), linewidth=1, color="#D55E00", linetype="dashed") +
  geom_point(data=via1262, aes(x = Age, y = eNdt), size=2, shape=15, color="#D55E00") +
  geom_line(data=batenburg1403, aes(x = Age.Ma., y = ENd.t.), linewidth=1, color="#56B4E9") +
  geom_point(data=batenburg1403, aes(x = Age.Ma., y = ENd.t.), size=2, shape=15, color="#56B4E9") +
  geom_line(data=martinDR, aes(x = Age, y = eNdt), linewidth=1, color="#E69F00", linetype="dashed" ) +
  geom_point(data=martinDR, aes(x = Age, y = eNdt), size=2, shape=15, color="#E69F00") +
  # key
  geom_segment(aes(x = 55.2, y = -2, xend = 55.4, yend = -2), alpha=1, size=1, color="#D55E00", linetype="solid") +
  annotate("text", x = 55.5, y = -2, label = "IODP 1267 (Batenburg et al., 2018)", color="#D55E03", hjust=0, size=2.5) +
  geom_segment(aes(x = 55.2, y = -2.8, xend = 55.4, yend = -2.8), alpha=1, size=1, color="#D55E00", linetype="dashed") +
  annotate("text", x = 55.5, y = -2.8, label = "IODP 1262 (Via et al., 2006)", color="#D55E03", hjust=0, size=2.5) +
  geom_segment(aes(x = 55.2, y = -3.6, xend = 55.4, yend = -3.6), alpha=1, size=1, color="#56B4E9", linetype="solid") +
  annotate("text", x = 55.5, y = -3.6, label = "IODP 1403 (Batenburg et al., 2018)", color="#56B4E9", hjust=0, size=2.5) +
  geom_segment(aes(x = 55.2, y = -4.4, xend = 55.4, yend = -4.4), alpha=1, size=1, color="#E69F00", linetype="dashed") +
  annotate("text", x = 55.5, y = -4.4, label = "Demerara Rise (Martin et al., 2012)", color="#E69F00", hjust=0, size=2.5) +
  # visually
  theme_classic() +
  guides(y ="axis_truncated") +
  theme(panel.background = element_rect(fill='transparent'), #transparent panel bg
        plot.background = element_rect(fill='transparent', color=NA)) + #transparent plot bg)
  theme(legend.position = "none") +
  scale_colour_manual(values=cbPalette) +
  coord_geo(dat = list("Geomagnetic Polarity Chron", "Geomagnetic Polarity Subchron", "stages", "epochs"),
            xlim = c(xlimplots_lo,xlimplots_hi), ylim = c(plot_nd_ymin,plot_nd_ymax),
            pos = list("b", "b", "b", "b"),
            lab = list(TRUE ,FALSE, TRUE, TRUE),
            height=list(unit(0.8, "line"), unit(0.8, "line"), unit(1.0, "line"), unit(1.5, "line")),
            fill=list("white", c("black", "white"), NULL, NULL),
            abbrv = list(FALSE, TRUE, FALSE),
            size = list(2, 1, 3, 5),
            center_end_labels = TRUE)

# Below code creates a layout for the stacked plot
discussion_layout <- c(
  area(t = 1, l = 1, b = 6, r = 1),
  area(t = 6, l = 1, b = 11, r = 1),
  area(t = 11, l = 1, b = 16, r = 1),
  area(t = 16, l = 1, b = 24, r =1))

discussion_plots <- plot_T47 + plot_d13C_NASA + plot_d18Ob_NASA + plot_nd + plot_layout(design=discussion_layout)
print(discussion_plots)

# FIGURE 4.1 (Results)

plot_D47_ymin <- 0.59
plot_D47_ymax <- 0.67

plot_D47 <- ggplot() +
  scale_x_continuous(limits=c(xlimplots_lo, xlimplots_hi), breaks=seq(xlimplots_lo,xlimplots_hi,1), position="top") +
  scale_y_continuous(limits=c(plot_D47_ymin,plot_D47_ymax), breaks=seq(plot_D47_ymin+0.02,plot_D47_ymax-0.01,0.01)) +
  labs(x="Age (Ma)", y=expression(paste(Delta[47]," (I-CDES90 \u2030)"))) +
  # Markers
  annotate("rect", xmin = EECO_min, xmax = EECO_max, ymin = plot_D47_ymin, ymax = plot_D47_ymax, fill=episodecolor) +
  annotate("rect", xmin = ETM2_min, xmax = ETM2_max, ymin = plot_D47_ymin, ymax = plot_D47_ymax, fill=episodecolor) +
  annotate("rect", xmin = PETM_min, xmax = PETM_max, ymin = plot_D47_ymin, ymax = plot_D47_ymax, fill=episodecolor) +
  # this_study
  geom_errorbar(data=ALL_clumped |> filter(grepl("LP_", `bin_id`)), aes(x = binage, ymax = CI95upper, ymin = CI95lower), alpha=1,
  width=0, linetype="dashed", color="#D55E00") +
  geom_errorbar(data=ALL_clumped |> filter(grepl("LP_", `bin_id`)), aes(x = binage, ymax = CI68upper, ymin = CI68lower), alpha=1,
  width=0, size=1, linetype="solid", color="#D55E00") +
  geom_errorbarh(data=ALL_clumped |> filter(grepl("LP_", `bin_id`)), aes(xmin = binagemin, xmax = binagemax, y = D47), alpha=.2,
  size=5, height=0, linetype="solid", color="#D55E00") +
  geom_point(data=ALL_clumped |> filter(grepl("LP_", `bin_id`)), aes(x = binage, y = D47), size=3, shape=21, fill="white", color=
  "#D55E00") +
  geom_label(data=ALL_clumped |> filter(grepl("LP_", `bin_id`)), aes(x = binage, y = CI95upper, label=N), color="#D55E00", nudge_y=
  0.01, size=3, label.padding = unit(0.2, "lines"),label.r = unit(0, "lines")) +
  # visually
  theme_classic() +
  guides(y ="axis_truncated") +
  theme(legend.position = "none") +
  scale_colour_manual(values=cbPalette) +
  coord_geo(dat = list("epochs", "stages", "Geomagnetic Polarity Subchron", "Geomagnetic Polarity Chron"),
            xlim = c(xlimplots_lo,xlimplots_hi), ylim = c(plot_D47_ymin,plot_D47_ymax),
            pos = list("t", "t", "t", "t"),
            lab = list(TRUE, TRUE, FALSE, TRUE),
            height=list(unit(1.5, "line"), unit(1.0, "line"), unit(0.8, "line"), unit(0.8, "line")),
            fill=list(NULL, NULL, c("black", "white"), "white"),
            abbrv = list(FALSE, FALSE, TRUE, FALSE),
            size = list(5, 3, 1, 2),
```

```
            center_end_labels = TRUE)

plot_d13C_ymin <- -1.5
plot_d13C_ymax <- 3

plot_d13C <- ggplot() +
  scale_x_continuous(limits=c(xlimplots_lo+0.1, xlimplots_hi), breaks=seq(xlimplots_lo,xlimplots_hi,1), position="top") +
  scale_y_continuous(limits=c(plot_d13C_ymin,plot_d13C_ymax), breaks=seq(plot_d13C_ymin,plot_d13C_ymax-0.5,0.5), position="right")
  +
  labs(x="Age (Ma)", y=expression(paste(delta^{13},C[Nuttallides]," (\u2030 VPDB)"))) +
  # Markers
  annotate("rect", xmin = EECO_min, xmax = EECO_max, ymin = plot_d13C_ymin, ymax = plot_d13C_ymax, fill=episodecolor) +
  annotate("rect", xmin = ETM2_min, xmax = ETM2_max, ymin = plot_d13C_ymin, ymax = plot_d13C_ymax, fill=episodecolor) +
  annotate("rect", xmin = PETM_min, xmax = PETM_max, ymin = plot_d13C_ymin, ymax = plot_d13C_ymax, fill=episodecolor) +
  # littler
  geom_line(data=littler |> drop_na(d13C), aes(x=WHage, y=d13C), alpha=0.2, size=.5) +
  geom_line(data=archive_filter |> filter(bin_id == "LP_56.7"), aes(x=age, y=`Final d13C`), color="#D55E00", size=.5) +
  geom_line(data=archive_filter |> filter(bin_id == "LP_57.1"), aes(x=age, y=`Final d13C`), color="#D55E00", size=.5) +
  geom_line(data=archive_filter |> filter(bin_id == "LP_58.0"), aes(x=age, y=`Final d13C`), color="#D55E00", size=.5) +
  geom_line(data=archive_filter |> filter(bin_id == "LP_60.3"), aes(x=age, y=`Final d13C`), color="#D55E00", size=.5) +
  # visually
  theme_classic() +
  guides(y ="axis_truncated") +
  theme(panel.background = element_rect(fill='transparent'), #transparent panel bg
        plot.background = element_rect(fill='transparent', color=NA)) + #transparent plot bg)
  theme(axis.line.x=element_blank(),
        axis.text.x=element_blank(),
        axis.ticks.x=element_blank(),
        axis.title.x=element_blank()) +
  theme(legend.position = "none") +
  coord_geo(xlim = c(xlimplots_lo,xlimplots_hi), height=unit(0,"line"), alpha=0, color="white")  # align


plot_d18Ob_ymin <- 2
plot_d18Ob_ymax <- -1

plot_d18Ob <- ggplot() +
  scale_x_continuous(limits=c(xlimplots_lo, xlimplots_hi-0.1), breaks=seq(xlimplots_lo,xlimplots_hi,1), position="top") +
  scale_y_reverse(limits=c(plot_d18Ob_ymin,plot_d18Ob_ymax), breaks=seq(plot_d18Ob_ymin,plot_d18Ob_ymax,-0.5), position="left") +
  labs(x="Age (Ma)", y=expression(paste(delta^{18},O[Cibicidoides]," (\u2030 VPDB)"))) +
  # Markers
  annotate("rect", xmin = EECO_min, xmax = EECO_max, ymin = plot_d18Ob_ymin, ymax = plot_d18Ob_ymax, fill=episodecolor) +
  annotate("rect", xmin = ETM2_min, xmax = ETM2_max, ymin = plot_d18Ob_ymin, ymax = plot_d18Ob_ymax, fill=episodecolor) +
  annotate("rect", xmin = PETM_min, xmax = PETM_max, ymin = plot_d18Ob_ymin, ymax = plot_d18Ob_ymax, fill=episodecolor) +
  # littler
  geom_line(data=littler |> drop_na(d18Ocib), aes(x=WHage, y=d18Ocib), alpha=0.2, size=.5) +
  geom_line(data=archive_filter |> filter(bin_id == "LP_56.7"), aes(x=age, y=d18Ocib), color="#D55E00", size=.5) +
  geom_line(data=archive_filter |> filter(bin_id == "LP_57.1"), aes(x=age, y=d18Ocib), color="#D55E00", size=.5) +
  geom_line(data=archive_filter |> filter(bin_id == "LP_58.0"), aes(x=age, y=d18Ocib), color="#D55E00", size=.5) +
  geom_line(data=archive_filter |> filter(bin_id == "LP_60.3"), aes(x=age, y=d18Ocib), color="#D55E00", size=.5) +
  # visually
  theme_classic() +
  guides(y ="axis_truncated") +
  theme(panel.background = element_rect(fill='transparent'), #transparent panel bg
        plot.background = element_rect(fill='transparent', color=NA)) + #transparent plot bg)
  theme(axis.line.x=element_blank(),
        axis.text.x=element_blank(),
        axis.ticks.x=element_blank(),
        axis.title.x=element_blank()) +
  theme(legend.position = "none") +
  coord_geo(xlim = c(xlimplots_lo,xlimplots_hi), height=unit(0,"line"), alpha=0, color="white")  # align

plot_temp_ymin <- 4
plot_temp_ymax <- 24

plot_temp <- ggplot() +
  scale_x_continuous(limits=c(xlimplots_lo, xlimplots_hi), breaks=seq(xlimplots_lo,xlimplots_hi,1)) +
  scale_y_continuous(limits=c(plot_temp_ymin,plot_temp_ymax), breaks=seq(plot_temp_ymin,plot_temp_ymax-4,2), position="right") +
  labs(x="Age (Ma)", y="DST (°C)")+
  # Markers
  annotate("rect", xmin = EECO_min, xmax = EECO_max, ymin = plot_temp_ymin, ymax = plot_temp_ymax, fill=episodecolor) +
  annotate("rect", xmin = ETM2_min, xmax = ETM2_max, ymin = plot_temp_ymin, ymax = plot_temp_ymax, fill=episodecolor) +
  annotate("rect", xmin = PETM_min, xmax = PETM_max, ymin = plot_temp_ymin, ymax = plot_temp_ymax, fill=episodecolor) +
  # cenogrid
  geom_line(data=westerhold, aes(x = age, y=T_Marchitto), alpha=0.2, size=.5) +
  # this_study
  geom_errorbar(data=ALL_clumped |> filter(grepl("LP_", `bin_id`)), aes(x = binage, ymax = T_CI95upper, ymin = T_CI95lower), alpha=
  1, width=0, linetype="dashed", color="#D55E00") +
  geom_errorbar(data=ALL_clumped |> filter(grepl("LP_", `bin_id`)), aes(x = binage, ymax = T_CI68upper, ymin = T_CI68lower), alpha=
  1, width=0, size=1, linetype="solid", color="#D55E00") +
  geom_errorbarh(data=ALL_clumped |> filter(grepl("LP_", `bin_id`)), aes(xmin = binagemin, xmax = binagemax, y = T47_meinicke),
  alpha=.2, size=5, height=0, linetype="solid", color="#D55E00") +
  geom_point(data=ALL_clumped |> filter(grepl("LP_", `bin_id`)), aes(x = binage, y = T47_meinicke), size=3, shape=21, fill="white"
  , color="#D55E00") +
  geom_line(data=archive_filter |> filter(bin_id == "LP_56.7"), aes(x=age, y=T_marchitto), color="#D55E00", size=.5) +
  geom_line(data=archive_filter |> filter(bin_id == "LP_57.1"), aes(x=age, y=T_marchitto), color="#D55E00", size=.5) +
  geom_line(data=archive_filter |> filter(bin_id == "LP_58.0"), aes(x=age, y=T_marchitto), color="#D55E00", size=.5) +
  geom_line(data=archive_filter |> filter(bin_id == "LP_60.3"), aes(x=age, y=T_marchitto), color="#D55E00", size=.5) +
  # visually
  theme_classic() +
  guides(y ="axis_truncated") +
  theme(panel.background = element_rect(fill='transparent'), #transparent panel bg
        plot.background = element_rect(fill='transparent', color=NA)) + #transparent plot bg)
  theme(axis.line.x=element_blank(),
        axis.text.x=element_blank(),
        axis.ticks.x=element_blank(),
        axis.title.x=element_blank()) +
  theme(legend.position = "none") +
  coord_geo(xlim = c(xlimplots_lo,xlimplots_hi), height=unit(0,"line"), alpha=0, color="white")  # align
```

```r

plot_d18Osw_ymin <- 2.5 #2
plot_d18Osw_ymax <- -3 #-2

plot_d18Osw <- ggplot() +
  scale_x_continuous(limits=c(xlimplots_lo, xlimplots_hi), breaks=seq(xlimplots_lo,xlimplots_hi,1)) +
  scale_y_reverse(limits=c(plot_d18Osw_ymin, plot_d18Osw_ymax), breaks=seq(plot_d18Osw_ymin-0.5,plot_d18Osw_ymax+0.5,-.5), position="left") +
  labs(x="Age (Ma)", y=expression(paste(delta^{18},"O"["SW"]," (\u2030 VSMOW)"))) +
  # Markers
  annotate("rect", xmin = EECO_min, xmax = EECO_max, ymin = plot_d18Osw_ymin, ymax = plot_d18Osw_ymax, fill=episodecolor) +
  annotate("text", x = (EECO_min + EECO_max)/2, y = plot_d18Osw_ymin, vjust=-.5, label = "EECO") +
  annotate("rect", xmin = ETM2_min, xmax = ETM2_max, ymin = plot_d18Osw_ymin, ymax = plot_d18Osw_ymax, fill=episodecolor) +
  annotate("text", x = (ETM2_min +ETM2_max)/2, y = plot_d18Osw_ymin, vjust=-.5, label = "ETM2") +
  annotate("rect", xmin = PETM_min, xmax = PETM_max, ymin = plot_d18Osw_ymin, ymax = plot_d18Osw_ymax, fill=episodecolor) +
  annotate("text", x = (PETM_min +PETM_max)/2, y = plot_d18Osw_ymin, vjust=-.5, label = "PETM") +
  # lines and labels
  geom_hline(yintercept = d18Oicefree, linetype="dashed", size=1, alpha=0.2) +
  geom_text(show.legend=FALSE, aes(xlimplots_lo,d18Oicefree, hjust=-1, vjust = -.25, label = ("delta^{18}*O[ice-free]")), parse = TRUE) +
  geom_hline(yintercept = d18Omodern, linetype="solid", size=1, alpha=0.2) +
  geom_text(show.legend=FALSE, aes(xlimplots_lo,d18Omodern, hjust=-1, vjust = -.25, label = ("delta^{18}*O[modern]")), parse = TRUE) +
  geom_hline(yintercept = d18Oglacial, linetype="dashed", size=1, alpha=0.2) +
  geom_text(show.legend=FALSE, aes(xlimplots_lo,d18Oglacial, hjust=-1, vjust = -.25, label = ("delta^{18}*O[glacial]")), parse = TRUE) +
  # data
  geom_errorbar(data=ALL_clumped |> filter(grepl("LP_", `bin_id`)), aes(x = binage, ymax = d18Osw_CI95upper, ymin = d18Osw_CI95lower), alpha=1, width=0, linetype="dashed", color="#D55E00") +
  geom_errorbar(data=ALL_clumped |> filter(grepl("LP_", `bin_id`)), aes(x = binage, ymax = d18Osw_CI68upper, ymin = d18Osw_CI68lower), alpha=1, width=0, size=1, linetype="solid", color="#D55E00") +
  geom_point(data=ALL_clumped |> filter(grepl("LP_", `bin_id`)), aes(x = binage, y = d18Osw, shape=Site), size=3, shape=23, fill="white",color="#D55E00") +
  # visually
  theme_classic() +
  guides(y ="axis_truncated") +
  theme(panel.background = element_rect(fill='transparent'), #transparent panel bg
        plot.background = element_rect(fill='transparent', color=NA)) + #transparent plot bg)
  theme(legend.position = "none") +
  scale_colour_manual(values=cbPalette) +
  coord_geo(dat = list("Geomagnetic Polarity Chron", "Geomagnetic Polarity Subchron", "stages", "epochs"),
            xlim = c(xlimplots_lo,xlimplots_hi), ylim = c(plot_d18Osw_ymin,plot_d18Osw_ymax),
            pos = list("b", "b", "b", "b"),
            lab = list(TRUE ,FALSE, TRUE, TRUE),
            height=list(unit(0.8, "line"), unit(0.8, "line"), unit(1.0, "line"), unit(1.5, "line")),
            fill=list("white", c("black", "white"), NULL, NULL),
            abbrv = list(FALSE, TRUE, FALSE),
            size = list(2, 1, 3, 5),
            center_end_labels = TRUE)

results_layout <- c(
  area(t = 1, l = 1, b = 6, r = 1),
  area(t = 5, l = 1, b = 10, r = 1),
  area(t = 10, l = 1, b = 15, r = 1),
  area(t = 14, l = 1, b = 18, r = 1),
  area(t = 18, l = 1, b = 23, r = 1))

results_plots <- plot_D47 + plot_d13C + plot_d18Ob + plot_temp + plot_d18Osw + plot_layout(design=results_layout)
print(results_plots)



# select only relevant runs from archive (used for other plots) ----

archive_select <- archive |>
  filter(
    Run == 653|
      Run == 657|
      Run == 662|
      Run == 664|
      Run == 667|
      Run == 669|
      Run == 672|
      Run == 674|
      Run == 677|
      Run == 679|
      Run == 682|
      Run == 683|
      between(Run, 685, 697)) |>
  #filter(`49 parameter` < high49) |>
  #filter(`Sa m44` > lowintensity) |>
  #filter(between(`Final d18O`, d18Olo, d18Ohi)) |>
  mutate(
    `SA/STDcat` = case_when(
      `SA/STD` == "ETH-1" ~ "ETH-1",
      `SA/STD` == "ETH-2" ~ "ETH-2",
      `SA/STD` == "ETH-3" ~ "ETH-3",
      `SA/STD` == "IAEA-C2" ~ "IAEA-C2",
      `SA/STD` == "Merck" ~ "Merck",
      `SA/STD` == "ETH-4" ~ "ETH-4",
      TRUE ~ "Sample"))
#bin_id = str_extract(`SA/STD`, str_c(bins, collapse = "|")))

# FIGURE 5.5 (CO2 and temperatures)

plot_CO2_ymin <- -500
plot_CO2_ymax <- 5000

plot_CO2<- ggplot() +
```

```
    scale_x_continuous(limits=c(xlimplots_lo-1, xlimplots_hi+1), breaks=seq(xlimplots_lo,xlimplots_hi,1), position="top") +
    scale_y_continuous(limits=c(plot_CO2_ymin,plot_CO2_ymax), breaks=seq(plot_CO2_ymin+500,plot_CO2_ymax-1000,500)) +
    labs(x="Age (Ma)", y=expression(paste("Atmospheric CO"["2"]," (ppm)"))) +
    # Markers
    annotate("rect", xmin = EECO_min, xmax = EECO_max, ymin = plot_CO2_ymin, ymax = plot_CO2_ymax, fill=episodecolor) +
    annotate("rect", xmin = ETM2_min, xmax = ETM2_max, ymin = plot_CO2_ymin, ymax = plot_CO2_ymax, fill=episodecolor) +
    annotate("rect", xmin = PETM_min, xmax = PETM_max, ymin = plot_CO2_ymin, ymax = plot_CO2_ymax, fill=episodecolor) +
    annotate("rect", xmin = KPG_min, xmax = KPG_max, ymin = plot_CO2_ymin, ymax = plot_CO2_ymax, fill=episodecolor) +

    # paleoCO2
    geom_errorbar(data=paleoCO2, aes(x = age, ymin = co2_l, ymax = co2_h, color=proxy), alpha=.2, width=0.1, linetype="solid") +
    geom_errorbarh(data=paleoCO2, aes(xmin = age_l, xmax = age_h, y = co2, color=proxy), alpha=.2, height=50, linetype="solid") +
    geom_point(data=paleoCO2, aes(x = age, y = co2, color=proxy), alpha=.5, size=1) +
    #geom_line(data=paleoCO2, aes(x = age, y = co2, color=proxy), stat="smooth", alpha=1, size=2, span=1) +
    # Rae (2021)
    geom_line(data=rae, aes(x = age, y = xco2), alpha=0.3, size=2) +
    geom_errorbar(data=rae, aes(x = age, ymin = xco2_16pc, ymax = xco2_84pc), alpha=.2, width=0.1, linetype="solid") +
    geom_point(data=rae, aes(x = age, y = xco2), alpha=0.5, size=1) +
    # key
    annotate("text", x = 69.5, y = 4000, label = expression(paste(delta^{11},"B", " CO"["2"], " (Rae et al., 2021)")), color="black"
    , hjust=1, size=2.5) +
    annotate("text", x = 69.5, y = 3800, label = "Stomatal frequencies (Hoenisch, 2022)", color="#E69F00", hjust=1, size=2.5) +
    annotate("text", x = 69.5, y = 3600, label = expression(paste("Land plant", delta^{13},"C"," (Hoenisch, 2022)")), color="#D55E00"
    , hjust=1, size=2.5) +
    annotate("text", x = 69.5, y = 3400, label = expression(paste(delta^{11},"B", " CO"["2"], " (Hoenisch, 2022)")), color="#56B4E9"
    , hjust=1, size=2.5) +
    # visually
    theme_classic() +
    guides(y ="axis_truncated") +
    theme(legend.position = "none") +
    scale_colour_manual(values=cbPalette) +
    coord_geo(dat = list("epochs", "stages", "Geomagnetic Polarity Subchron", "Geomagnetic Polarity Chron"),
              xlim = c(xlimplots_lo,xlimplots_hi), ylim = c(plot_CO2_ymin,plot_CO2_ymax-500),
              pos = list("t", "t", "t", "t"),
              lab = list(TRUE, TRUE, FALSE, TRUE),
              height=list(unit(1.5, "line"), unit(1.0, "line"), unit(0.8, "line"), unit(0.8, "line")),
              fill=list(NULL, NULL, c("black", "white"), "white"),
              abbrv = list(FALSE, FALSE, TRUE, FALSE),
              size = list(4, 3, 1, 2),
              center_end_labels = TRUE)

plot_DSTSST_ymin <- 4
plot_DSTSST_ymax <- 48

plot_DSTSST <- ggplot() +
  scale_x_continuous(limits=c(xlimplots_lo-15, xlimplots_hi+5), breaks=seq(xlimplots_lo,xlimplots_hi,1), position="bottom") +
  scale_y_continuous(limits=c(plot_DSTSST_ymin,plot_DSTSST_ymax), breaks=seq(plot_DSTSST_ymin+2,plot_DSTSST_ymax-2,2), position=
  "right") +
  labs(x="Age (Ma)", y="Temperature (°C)") +
  # Markers
  annotate("rect", xmin = EECO_min, xmax = EECO_max, ymin = plot_DSTSST_ymin, ymax = plot_DSTSST_ymax, fill=episodecolor) +
  annotate("text", x = (EECO_min + EECO_max)/2, y = plot_DSTSST_ymin, vjust=-1, label = "EECO") +
  annotate("rect", xmin = ETM2_min, xmax = ETM2_max, ymin = plot_DSTSST_ymin, ymax = plot_DSTSST_ymax, fill=episodecolor) +
  annotate("text", x = (ETM2_min +ETM2_max)/2, y = plot_DSTSST_ymin, vjust=-1, label = "ETM2") +
  annotate("rect", xmin = PETM_min, xmax = PETM_max, ymin = plot_DSTSST_ymin, ymax = plot_DSTSST_ymax, fill=episodecolor) +
  annotate("text", x = (PETM_min +PETM_max)/2, y = plot_DSTSST_ymin, vjust=-1, label = "PETM") +
  annotate("rect", xmin = KPG_min, xmax = KPG_max, ymin = plot_DSTSST_ymin, ymax = plot_DSTSST_ymax, fill=episodecolor) +
  annotate("text", x = (KPG_min +KPG_max)/2, y = plot_DSTSST_ymin, vjust=-1, label = "K/Pg") +
  # cenogrid
  geom_line(data=westerhold, aes(x = age, y=T_Marchitto), alpha=0.2, size=0.5) +
  # SST
  geom_line(data=phanSST1262, aes(x = Age, y=SST), color="#D55E00", alpha=0.5, linewidth=1) +
  geom_point(data=phanSST1262, aes(x = Age, y=SST), color="#D55E00", alpha=0.5, size=2) +
  geom_line(data=cramwinckel18_tex |> filter(Location=="ODP Site 959"), aes(x=age , y=`SST (BAYSPAR)`), color="#E69F00", alpha=0.5
  , linewidth=1) +
  geom_point(data=cramwinckel18_tex |> filter(Location=="ODP Site 959"), aes(x=age , y=`SST (BAYSPAR)`), color="#E69F00", alpha=0.5
  , size=2) +
  geom_line(data=bijl09_tex, aes(x=`age(Ma)` , y=`T(kim)`), color="#339933", alpha=0.5, linewidth=1) +
  geom_point(data=bijl09_tex, aes(x=`age(Ma)` , y=`T(kim)`), color="#339933", alpha=0.5, size=2) +
  # DST
  geom_errorbar(data=ALL_clumped |> filter(grepl("Atlantic", `location`)), aes(x = binage, ymax = T_CI95upper, ymin = T_CI95lower,
  color=location), alpha=1, width=0, linetype="dashed") +
  geom_errorbar(data=ALL_clumped |> filter(grepl("Atlantic", `location`)), aes(x = binage, ymax = T_CI68upper, ymin = T_CI68lower,
  color=location), alpha=1, width=0, size=1, linetype="solid") +
  geom_errorbarh(data=ALL_clumped |> filter(grepl("Atlantic", `location`)), aes(xmin = binagemin, xmax = binagemax, y =
  T47_meinicke, color=location), alpha=.2, size=5, height=0, linetype="solid") +
  geom_point(data=ALL_clumped |> filter(grepl("Atlantic", `location`)), aes(x = binage, y = T47_meinicke, color=location), size=3,
  shape=21, fill="white") +
  # key
  geom_segment(aes(x = 68.5, y = 44, xend = 69.5, yend = 44), color="#E69F00", alpha=0.5, linewidth=1) +
  annotate("text", x = 68, y = 44, label = "SST TEX-86, Site 959 (Cramwinckel et al., 2018)", color="#E69F00", hjust=1, size=2.5,
  alpha=0.5) +
  geom_segment(aes(x = 68.5, y = 43, xend = 69.5, yend = 43), color="#339933", alpha=0.5, linewidth=1) +
  annotate("text", x = 68, y = 43, label = "SST TEX-86, Site 1172 (Bijl et al., 2009)", color="#339933", hjust=1, size=2.5, alpha=
  0.5) +
  geom_segment(aes(x = 68.5, y = 42, xend = 69.5, yend = 42), color="#D55E00", alpha=0.5, linewidth=1) +
  annotate("text", x = 68, y = 42, label = expression(paste("SST Planktonic ", delta^{18},"O, Site 1262 (Birch et al., 2016)")),
  color="#D55E00", hjust=1, size=2.5, alpha=0.5) +
  annotate("text", x = 68, y = 41, label = expression(paste("DST ", Delta["47"], " South Atlantic (this study)")), color="#D55E03"
  , hjust=1, size=2.5) +
  annotate("text", x = 68, y = 40, label = expression(paste("DST ", Delta["47"], " North Atlantic (Meckler et al., 2022)")), color=
  "#56B4E9", hjust=1, size=2.5) +
  geom_segment(aes(x = 68.5, y = 39, xend = 69.5, yend = 39), color="black", alpha=0.2, linewidth=0.5) +
  annotate("text", x = 68, y = 39, label = expression(paste("DST ", delta^{18},"O, CENOGRID (Westerhold et al., 2022)")), alpha=0.2
  , color="black", hjust=1, size=2.5) +
  # visually
  theme_classic() +
  guides(y ="axis_truncated") +
  theme(panel.background = element_rect(fill='transparent'), #transparent panel bg
```

```
      plot.background = element_rect(fill='transparent', color=NA)) + #transparent plot bg)
  theme(legend.position = "none") +
  scale_colour_manual(values=cbPalette) +
  coord_geo(dat = list("Geomagnetic Polarity Chron", "Geomagnetic Polarity Subchron", "stages", "epochs"),
            xlim = c(xlimplots_lo,xlimplots_hi), ylim = c(plot_DSTSST_ymin,plot_DSTSST_ymax),
            pos = list("b", "b", "b", "b"),
            lab = list(TRUE ,FALSE, TRUE, TRUE),
            height=list(unit(0.8, "line"), unit(0.8, "line"), unit(1.0, "line"), unit(1.5, "line")),
            fill=list("white", c("black", "white"), NULL, NULL),
            abbrv = list(FALSE, TRUE, FALSE),
            size = list(2, 1, 3, 4),
            center_end_labels = TRUE)

ESS_layout <- c(
  area(t = 1, l = 1, b = 10, r = 1),
  area(t = 10, l = 1, b = 26, r = 1))

ESS_plots <- plot_CO2 + plot_DSTSST + plot_layout(design=ESS_layout)
print(ESS_plots)

# δ¹□O of seawater ----

# Y-limits for this plot are shared with those for Figure 5.4

plot_clumped_temps_d18Osw <- ggplot() +
  scale_x_continuous(limits=c(xlimplots_lo-15, xlimplots_hi+5), breaks=seq(xlimplots_lo,xlimplots_hi,1), position="top") +
  scale_y_continuous(limits=c(plot_T47_ymin,plot_T47_ymax), breaks=seq(plot_T47_ymin+2,plot_T47_ymax-4,2)) +
  labs(x="Age (Ma)", y="DST (°C)") +
  # Markers
  annotate("rect", xmin = EECO_min, xmax = EECO_max, ymin = plot_T47_ymin, ymax = plot_T47_ymax, fill=episodecolor) +
  annotate("rect", xmin = ETM2_min, xmax = ETM2_max, ymin = plot_T47_ymin, ymax = plot_T47_ymax, fill=episodecolor) +
  annotate("rect", xmin = PETM_min, xmax = PETM_max, ymin = plot_T47_ymin, ymax = plot_T47_ymax, fill=episodecolor) +
  # data
  geom_errorbar(data=data_sel, aes(x = binage, ymax = T_CI95upper, ymin = T_CI95lower, color=location), alpha=1, width=0, linetype="dashed") +
  geom_errorbar(data=data_sel, aes(x = binage, ymax = T_CI68upper, ymin = T_CI68lower, color=location), alpha=1, width=0, size=1, linetype="solid") +
  geom_errorbarh(data=data_sel, aes(xmin = binagemin, xmax = binagemax, y = T47_meinicke, color=location), alpha=.2, size=5, height=0, linetype="solid") +
  geom_point(data=data_sel, aes(x = binage, y = T47_meinicke, color=location), size=3, shape=21, fill="white") +
  # key
  annotate("text", x = 46.2, y = 24, label = expression(paste(Delta["47"], " South Atlantic (this study)")), color="#D55E03", hjust=0, size=2.5) +
  annotate("text", x = 46.2, y = 22, label = expression(paste(Delta["47"], " North Atlantic (Meckler et al., 2022)")), color="#56B4E3", hjust=0, size=2.5) +
  # visually
  theme_classic() +
  guides(y ="axis_truncated") +
  theme(legend.position = "none") +
  scale_colour_manual(values=cbPalette) +
  coord_geo(dat = list("epochs", "stages", "Geomagnetic Polarity Subchron", "Geomagnetic Polarity Chron"),
            xlim = c(xlimplots_lo,xlimplots_hi), ylim = c(plot_T47_ymin,plot_T47_ymax),
            pos = list("t", "t", "t", "t"),
            lab = list(TRUE, TRUE, FALSE, TRUE),
            height=list(unit(1.5, "line"), unit(1.0, "line"), unit(0.8, "line"), unit(0.8, "line")),
            fill=list(NULL, NULL, c("black", "white"), "white"),
            abbrv = list(FALSE, FALSE, TRUE, FALSE),
            size = list(5, 3, 1, 2),
            center_end_labels = TRUE,
            skip = "C19")

plot_pH_ymin <- 7.0
plot_pH_ymin_cob <- 0.2
plot_pH_ymax <- 8.2
plot_pH_ymax_cot <- 0.2

plot_pH <- ggplot() +
  scale_x_continuous(limits=c(xlimplots_lo-10, xlimplots_hi+10), breaks=seq(xlimplots_lo,xlimplots_hi,2)) +
  scale_y_continuous(limits=c(plot_pH_ymin,plot_pH_ymax), breaks=seq(plot_pH_ymin+plot_pH_ymin_cob,plot_pH_ymax-plot_pH_ymax_cot, 0.2), position="right") +
  labs(x="Age (Ma)", y="seawater pH")+
  # Markers
  annotate("rect", xmin = EECO_min, xmax = EECO_max, ymin = plot_pH_ymin+plot_pH_ymin_cob, ymax = plot_pH_ymax-plot_pH_ymax_cot, fill=episodecolor) +
  annotate("rect", xmin = ETM2_min, xmax = ETM2_max, ymin = plot_pH_ymin+plot_pH_ymin_cob, ymax = plot_pH_ymax-plot_pH_ymax_cot, fill=episodecolor) +
  annotate("rect", xmin = PETM_min, xmax = PETM_max, ymin = plot_pH_ymin+plot_pH_ymin_cob, ymax = plot_pH_ymax-plot_pH_ymax_cot, fill=episodecolor) +
  # Rae pH
  geom_line(data=rae, aes(x = age, y=pH), linewidth=0.5, alpha=0.5, color="black") +
  geom_point(data=rae, aes(x = age, y=pH), alpha=0.8, size=2, shape=1) +
  # key
  annotate("text", x = 60.8, y = 7.7, label = expression(paste(delta^{11},"B", " seawater pH (Rae et al., 2021)")), color="black", hjust=1, size=2.5) +
  #visually
  theme_classic() +
  guides(y ="axis_truncated") +
  theme(legend.position = "none") +
  scale_colour_manual(values=cbPalette) +
  theme(panel.background = element_rect(fill='transparent'), #transparent panel bg
        plot.background = element_rect(fill='transparent', color=NA)) + #transparent plot bg)
  theme(axis.line.x=element_blank(),
        axis.text.x=element_blank(),
        axis.ticks.x=element_blank(),
        axis.title.x=element_blank()) +
  theme(legend.position = "none") +
  coord_geo(xlim = c(xlimplots_lo,xlimplots_hi), height=unit(0,"line"), alpha=0, color="white")

plot_d18Osw_disc <- ggplot() +
```

```
  scale_x_continuous(limits=c(xlimplots_lo, xlimplots_hi), breaks=seq(xlimplots_lo,xlimplots_hi,1)) +
  scale_y_reverse(limits=c(plot_d18Osw_ymin, plot_d18Osw_ymax), breaks=seq(plot_d18Osw_ymin-0.5,plot_d18Osw_ymax+0.5,-.5), position="left") +
  labs(x="Age (Ma)", y=expression(paste(delta^{18},"O"["SW"]," (\u2030 VSMOW)"))) +
  # Markers
  annotate("rect", xmin = EECO_min, xmax = EECO_max, ymin = plot_d18Osw_ymin, ymax = plot_d18Osw_ymax, fill=episodecolor) +
  annotate("text", x = (EECO_min + EECO_max)/2, y = plot_d18Osw_ymin, vjust=-.5, label = "EECO") +
  annotate("rect", xmin = ETM2_min, xmax = ETM2_max, ymin = plot_d18Osw_ymin, ymax = plot_d18Osw_ymax, fill=episodecolor) +
  annotate("text", x = (ETM2_min +ETM2_max)/2, y = plot_d18Osw_ymin, vjust=-.5, label = "ETM2") +
  annotate("rect", xmin = PETM_min, xmax = PETM_max, ymin = plot_d18Osw_ymin, ymax = plot_d18Osw_ymax, fill=episodecolor) +
  annotate("text", x = (PETM_min +PETM_max)/2, y = plot_d18Osw_ymin, vjust=-.5, label = "PETM") +
  # lines and labels
  geom_hline(yintercept = d18Oicefree, linetype="dashed", size=1, alpha=0.2) +
  geom_text(show.legend=FALSE, aes(xlimplots_lo,d18Oicefree, hjust=-1, vjust = -.25, label = ("delta^{18}*O[ice-free]")), parse = TRUE) +
  geom_hline(yintercept = d18Omodern, linetype="solid", size=1, alpha=0.2) +
  geom_text(show.legend=FALSE, aes(xlimplots_lo,d18Omodern, hjust=-1, vjust = -.25, label = ("delta^{18}*O[modern]")), parse = TRUE) +
  geom_hline(yintercept = d18Oglacial, linetype="dashed", size=1, alpha=0.2) +
  geom_text(show.legend=FALSE, aes(xlimplots_lo,d18Oglacial, hjust=-1, vjust = -.25, label = ("delta^{18}*O[glacial]")), parse = TRUE) +
  # d18O_sw values from litter + Cramer Mg/Ca. pH corrected: Cramer+zeebe & Cramer+Rathmann
  geom_smooth(data=littler |> drop_na(d18Ocib), aes(x=WHage, y=d18Osw_MgCa), se=FALSE, method="loess", span=0.01, alpha=0.5, size=0.5, color="#D55E00", , linetype="dashed") +
  geom_smooth(data=littler |> drop_na(d18Ocib), aes(x=WHage, y=d18Osw_MgCa_zeebe), se=FALSE, method="loess", span=0.01, alpha=0.5, size=0.5, color="#D55E00") +
  # data
  geom_errorbar(data=data_sel, aes(x = binage, ymax = d18Osw_CI95upper, ymin = d18Osw_CI95lower, color=location), alpha=0.4, width=0, linetype="dashed") +
  geom_errorbar(data=data_sel, aes(x = binage, ymax = d18Osw_CI68upper, ymin = d18Osw_CI68lower, color=location), alpha=0.4, width=0, size=1, linetype="solid") +
  geom_point(data=data_sel, aes(x = binage, y = d18Osw, color=location), size=3, shape=23, fill="white", alpha=0.4) +
  geom_point(data=data_sel, aes(x = binage, y = d18Osw_zeebe, color=location), size=4, shape=18) +
  # key
  annotate("text", x = 46.2, y = -2.2, label = expression(paste(Delta["47"], " + ", delta^{18},"O"["B"], " (this study) + pH correction (Zeebe, 2001)")), color="#D55E03", hjust=0, size=2.5) +
  annotate("text", x = 46.2, y = -1.9, label = expression(paste(Delta["47"], " + ", delta^{18},"O"["B"], " (Meckler et al., 2022) + pH correction (Zeebe, 2001)")), color="#56B4E3", hjust=0, size=2.5) +
  annotate("text", x = 60.0, y = -2.2, label = expression(paste("Mg/Ca (Cramer et al., 2011) + ", delta^{18},"O"["B"], " (Littler et al., 2014) + pH correction (Zeebe, 2001) ")), color="#D55E03", hjust=1, size=2.5) +
  annotate("text", x = 60.0, y = -1.9, label = expression(paste("Mg/Ca (Cramer et al., 2011) + ", delta^{18},"O"["B"], " (Littler et al., 2014) ")), color="#D55E03", hjust=1, size=2.5) +
  geom_segment(aes(x = 60.1, y = -2.2, xend = 60.8, yend = -2.2), alpha=1, size=0.5, color="#D55E00") +
  geom_segment(aes(x = 60.1, y = -1.9, xend = 60.8, yend = -1.9), alpha=1, size=0.5, color="#D55E00", linetype="dashed") +
  # visually
  theme_classic() +
  guides(y ="axis_truncated") +
  theme(panel.background = element_rect(fill='transparent'), #transparent panel bg
        plot.background = element_rect(fill='transparent', color=NA)) + #transparent plot bg)
  theme(legend.position = "none") +
  scale_colour_manual(values=cbPalette) +
  coord_geo(dat = list("Geomagnetic Polarity Chron", "Geomagnetic Polarity Subchron", "stages", "epochs"),
            xlim = c(xlimplots_lo,xlimplots_hi), ylim = c(plot_d18Osw_ymin,plot_d18Osw_ymax),
            pos = list("b", "b", "b", "b"),
            lab = list(TRUE ,FALSE, TRUE, TRUE),
            height=list(unit(0.8, "line"), unit(0.8, "line"), unit(1.0, "line"), unit(1.5, "line")),
            fill=list("white", c("black", "white"), NULL, NULL),
            abbrv = list(FALSE, TRUE, FALSE),
            size = list(2, 1, 3, 5),
            center_end_labels = TRUE)

plots_T_pH_d18Osw_layout <- c(
  area(t = 1, l = 1, b = 6, r = 1),
  area(t = 5, l = 1, b = 11, r = 1),
  area(t = 10, l = 1, b = 18, r = 1))

plots_T_pH_d18Osw <- plot_clumped_temps_d18Osw + plot_pH + plot_d18Osw_disc + plot_layout(design=plots_T_pH_d18Osw_layout)
print(plots_T_pH_d18Osw)

# Figure 5.6 (Earth System Sensitivity)

# subsetting data from All Clumped data
ESS <- ALL_clumped[c("binage", "T47_meinicke", "T_CI95upper", "T_CI95lower", "location")]

ESS <- ESS |>
  mutate(
    co2 = (approx(rae$age, rae$xco2, binage)$y), # look up CO2 value (interpolate) from Rae et al., 2021
    co2l = (approx(rae$age, rae$xco2_16pc, binage)$y),
    co2h = (approx(rae$age, rae$xco2_84pc, binage)$y),
    T47rel = T47_meinicke - 2, #relative to modern DSTs
    T47lrel = T_CI95lower - 2,
    T47hrel = T_CI95upper - 2,
    colour = case_when(
      binage < 3 ~ "#35236c",
      binage < 34 ~ "#9bb7d5",
      binage < 50 ~ "#fc7e3c",
      binage < 55 ~ "#b63931",
      TRUE ~ "#fc7e3c"))

co2values <- c(140,280,560,1120,2240)
text <- c("2°C/doubling","4°C/doubling","6°C/doubling","8°C/doubling","10°C/doubling")

sens_lines <- data.frame(co2values, text)

sens_lines <- sens_lines |>
  mutate(
    x2 = log2(co2values/280) * 2,
    x4 = log2(co2values/280) * 4,
    x6 = log2(co2values/280) * 6,
```

```
    x8 = log2(co2values/280) * 8,
    x10 = log2(co2values/280) * 10)

plot_ess <- ggplot() +
  scale_x_continuous(limits=c(140,4480), breaks=co2values, trans="log2") +
  scale_y_continuous(limits=c(-10,30), breaks=seq(-5,25,5)) +
  labs(y="DST anomaly (°C)", x="CO2 (ppm)")+
  # sensitivy lines
  geom_line(data=sens_lines, aes(x=co2values, y=x2), alpha=0.6, linetype="dashed") +
  geom_line(data=sens_lines, aes(x=co2values, y=x4), alpha=0.6, linetype="dashed") +
  geom_line(data=sens_lines, aes(x=co2values, y=x6), alpha=0.6, linetype="dashed") +
  geom_line(data=sens_lines, aes(x=co2values, y=x8), alpha=0.6, linetype="dashed") +
  geom_text(data=sens_lines, aes(x=2240, y=c(6, 12, 18, 24, 30)), label=text, nudge_x =0.35, nudge_y=0.7) +
  # data
  geom_errorbarh(data=ESS, aes(xmin=co2l, xmax=co2h, y=T47rel), color=ESS$colour) +
  geom_errorbar(data=ESS, aes(x=co2, ymin=T47lrel, ymax=T47hrel), color=ESS$colour) +
  geom_point(data=ESS, aes(x=co2, y=T47rel, shape=location), alpha =0.6, fill=ESS$colour, size=3) +
  geom_point(data=ESS |> filter(binage>55) |> filter(location=="South Atlantic"), aes(x=co2, y=T47rel, shape=location), fill=
  "#fc7e3c", alpha =1, size=4, stroke=1.5) +
  geom_point(data=ESS |> filter(binage>55) |> filter(location=="North Atlantic"), aes(x=co2, y=T47rel, shape=location), fill=
  "#fc7e3c", alpha =1, size=4, stroke=1.5) +
  # visually
  theme_classic() +
  scale_shape_manual(values = c(25,24,23,22,21)) +
  guides(y ="axis_truncated", x="axis_truncated") +
  theme(panel.background = element_rect(fill='transparent'), #transparent panel bg
        plot.background = element_rect(fill='transparent', color=NA)) + #transparent plot bg)
  theme(legend.position = "none") +
  coord_trans(ylim=c(-5,30), xlim=c(140, 4480))

print(plot_ess)


# Figure A.1

# Accepted Values (av) for (check)standards
ETH3av <- 0.6132
ETH2av <- 0.2085
ETH1av <- 0.2052
ETH4av <- 0.4505
IAEAC2av <- 0.6445
MERCKav <- 0.5151

plot_MERCK <- ggplot()+
  scale_x_continuous(limits=c(Trunmean_xmin,Trunmean_xmax+10), breaks=seq(Trunmean_xmin,Trunmean_xmax,5)) +
  scale_y_continuous(limits=c(0.40,0.70), breaks=seq(0.40,0.70,0.05)) +
  labs(x="Run", y=expression(paste(Delta[47],"  (I-CDES90 \u2030)"))) +
  geom_point(data=archive_runanalysis |> filter(bin_id == "Merck"), aes(x=Run, y=D47_runmean), shape=19, size=2, alpha=0.4) +
  geom_hline(yintercept = MERCKav, linetype="dashed", size=1, alpha=0.2) +
  geom_text(show.legend=FALSE, aes(Trunmean_xmax,MERCKav, hjust=-0.5, vjust = -0.4 , label = ("Merck"))) +
  # visually
  theme_classic() +
  theme(axis.line.x=element_blank(),
        axis.text.x=element_blank(),
        axis.ticks.x=element_blank(),
        axis.title.x=element_blank()) +
  guides(y ="axis_truncated", x="axis_truncated") +
  theme(panel.background = element_rect(fill='transparent'), #transparent panel bg
        plot.background = element_rect(fill='transparent', color=NA)) + #transparent plot bg)
  theme(legend.position = "none")

plot_IAEAC2 <- ggplot()+
  scale_x_continuous(limits=c(Trunmean_xmin,Trunmean_xmax+10), breaks=seq(Trunmean_xmin,Trunmean_xmax,5)) +
  scale_y_continuous(limits=c(0.50,0.80), breaks=seq(0.5,0.8,0.05)) +
  labs(x="Run", y=expression(paste(Delta[47],"  (I-CDES90 \u2030)"))) +
  geom_point(data=archive_runanalysis |> filter(bin_id == "IAEA-C2"), aes(x=Run, y=D47_runmean), shape=19, size=2, alpha=0.4) +
  geom_hline(yintercept = IAEAC2av, linetype="dashed", size=1, alpha=0.2) +
  geom_text(show.legend=FALSE, aes(Trunmean_xmax,IAEAC2av, hjust=-0.5, vjust = -0.4 , label = ("IAEA-C2"))) +
  # visually
  theme_classic() +
  theme(axis.line.x=element_blank(),
        axis.text.x=element_blank(),
        axis.ticks.x=element_blank(),
        axis.title.x=element_blank()) +
  guides(y ="axis_truncated", x="axis_truncated") +
  theme(panel.background = element_rect(fill='transparent'), #transparent panel bg
        plot.background = element_rect(fill='transparent', color=NA)) + #transparent plot bg)
  theme(legend.position = "none")

plot_ETH1 <- ggplot()+
  scale_x_continuous(limits=c(Trunmean_xmin,Trunmean_xmax+10), breaks=seq(Trunmean_xmin,Trunmean_xmax,5)) +
  scale_y_continuous(limits=c(0.05,0.35), breaks=seq(0.05,0.35,0.05)) +
  labs(x="Run", y=expression(paste(Delta[47],"  (I-CDES90 \u2030)"))) +
  geom_point(data=archive_runanalysis |> filter(bin_id == "ETH-1"), aes(x=Run, y=D47_runmean), shape=19, size=2, alpha=0.4) +
  geom_hline(yintercept = ETH1av, linetype="dashed", size=1, alpha=0.2) +
  geom_text(show.legend=FALSE, aes(Trunmean_xmax,ETH1av, hjust=-0.5, vjust = -0.4 , label = ("ETH-1"))) +
  # visually
  theme_classic() +
  theme(axis.line.x=element_blank(),
        axis.text.x=element_blank(),
        axis.ticks.x=element_blank(),
        axis.title.x=element_blank()) +
  guides(y ="axis_truncated", x="axis_truncated") +
  theme(panel.background = element_rect(fill='transparent'), #transparent panel bg
        plot.background = element_rect(fill='transparent', color=NA)) + #transparent plot bg)
  theme(legend.position = "none")

plot_ETH2 <- ggplot()+
  scale_x_continuous(limits=c(Trunmean_xmin,Trunmean_xmax+10), breaks=seq(Trunmean_xmin,Trunmean_xmax,5)) +
```

```
  scale_y_continuous(limits=c(0.05,0.35), breaks=seq(0.05,0.35,0.05)) +
  labs(x="Run", y=expression(paste(Delta[47]," (I-CDES90 \u2030)"))) +
  geom_point(data=archive_runanalysis |> filter(bin_id == "ETH-2"), aes(x=Run, y=D47_runmean), shape=19, size=2, alpha=0.4) +
  geom_hline(yintercept = ETH2av, linetype="dashed", size=1, alpha=0.2) +
  geom_text(show.legend=FALSE, aes(Trunmean_xmax,ETH2av, hjust=-0.5, vjust = -0.4 , label = ("ETH-2"))) +
  # visually
  theme_classic() +
  theme(axis.line.x=element_blank(),
        axis.text.x=element_blank(),
        axis.ticks.x=element_blank(),
        axis.title.x=element_blank()) +
  guides(y ="axis_truncated", x="axis_truncated") +
  theme(panel.background = element_rect(fill='transparent'), #transparent panel bg
        plot.background = element_rect(fill='transparent', color=NA)) + #transparent plot bg)
  theme(legend.position = "none")

plot_ETH3 <- ggplot()+
  scale_x_continuous(limits=c(Trunmean_xmin,Trunmean_xmax+10), breaks=seq(Trunmean_xmin,Trunmean_xmax,5)) +
  scale_y_continuous(limits=c(0.61,0.616), breaks=seq(0.61,0.616,0.001)) +
  labs(x="Run", y=expression(paste(Delta[47]," (I-CDES90 \u2030)"))) +
  geom_point(data=archive_runanalysis |> filter(bin_id == "ETH-3"), aes(x=Run, y=D47_runmean), shape=19, size=2, alpha=0.4) +
  geom_hline(yintercept = ETH3av, linetype="dashed", size=1, alpha=0.2) +
  geom_text(show.legend=FALSE, aes(Trunmean_xmax,ETH3av, hjust=-0.5, vjust = -0.4 , label = ("ETH-3"))) +
  # visually
  theme_classic() +
  theme(axis.line.x=element_blank(),
        axis.text.x=element_blank(),
        axis.ticks.x=element_blank(),
        axis.title.x=element_blank()) +
  guides(y ="axis_truncated", x="axis_truncated") +
  theme(panel.background = element_rect(fill='transparent'), #transparent panel bg
        plot.background = element_rect(fill='transparent', color=NA)) + #transparent plot bg)
  theme(legend.position = "none")

plot_ETH3SD <- ggplot()+
  scale_x_continuous(limits=c(Trunmean_xmin,Trunmean_xmax+10), breaks=seq(Trunmean_xmin,Trunmean_xmax,5)) +
  scale_y_continuous(limits=c(0.0,0.1), breaks=seq(0.0,0.1,0.02)) +
  labs(x="Run", y="ETH-3 external SD") +
  geom_bar(data=archive_runanalysis |> filter(bin_id == "ETH-3"), aes(x=Run, y=D47_runmeanSD), stat="identity", alpha=0.4, color=
  "#CC6666", fill="#CC6666") +
  # visually
  theme_classic() +
  guides(y ="axis_truncated", x="axis_truncated") +
  theme(panel.background = element_rect(fill='transparent'), #transparent panel bg
        plot.background = element_rect(fill='transparent', color=NA)) + #transparent plot bg)
  theme(legend.position = "none")

checkplots <- plot_MERCK + plot_IAEAC2 + plot_ETH1 + plot_ETH2 + plot_ETH3 + plot_ETH3SD + plot_layout(ncol=1, nrow=6)

print(checkplots)

# Subsetting Data Per Bin for Appendix plots

LP_60.3 <- filter(archive_select, bin_id == "LP_60.3")
LP_58.0 <- filter(archive_select, bin_id == "LP_58.0")
LP_57.1 <- filter(archive_select, bin_id == "LP_57.1")
LP_56.7 <- filter(archive_select, bin_id == "LP_56.7")

T_LP_60.3 <- ALL_clumped[ALL_clumped$bin_id == "LP_60.3",]$T47_meinicke
T_LP_58.0 <- ALL_clumped[ALL_clumped$bin_id == "LP_58.0",]$T47_meinicke
T_LP_57.1 <- ALL_clumped[ALL_clumped$bin_id == "LP_57.1",]$T47_meinicke
T_LP_56.7 <- ALL_clumped[ALL_clumped$bin_id == "LP_56.7",]$T47_meinicke

# Figure A.3 (Exploration of sub-binning)

LP_60.3_2bins <- archive_filter |>
  filter(bin_id == "LP_60.3") |>
  arrange(age) |>
  mutate(
    n = seq_along(age),
    subbin = case_when(
      n %% 2 == 1 ~ "2.A",
      n %% 2 == 0 ~ "2.B")) |>
  group_by(subbin) |>
  summarise(
    D47 = mean(`Final AFF`),
    extSD = sd(`Final AFF`),
    N = n(),
    SE = extSD/sqrt(N),
    CI95upper = D47 + qt(0.975, N-1) * SE, # 4 lines: Calculate upper and lower values for 95% and 68% CI
    CI95lower = D47 - qt(0.975, N-1) * SE,
    CI68upper = D47 + qt(0.840, N-1) * SE,
    CI68lower = D47 - qt(0.840, N-1) * SE,
    T47 = sqrt(slope/(D47-int))-C,
    T_CI95upper = sqrt(slope/(CI95lower-int))-C, # 4 lines: Calculate upper and lower temperatures associated with lower and upper
    CI's
    T_CI95lower = sqrt(slope/(CI95upper-int))-C,
    T_CI68upper = sqrt(slope/(CI68lower-int))-C,
    T_CI68lower = sqrt(slope/(CI68upper-int))-C)

LP_60.3_3bins <- archive_filter |>
  filter(bin_id == "LP_60.3") |>
  arrange(age) |>
  mutate(
    n = seq_along(age),
    subbin = case_when(
      n %% 3 == 1 ~ "3.A",
      n %% 3 == 2 ~ "3.B",
      n %% 3 == 0 ~ "3.C")) |>
```

```
    group_by(subbin) |>
    summarise(
      D47 = mean(`Final AFF`),
      extSD = sd(`Final AFF`),
      N = n(),
      SE = extSD/sqrt(N),
      CI95upper = D47 + qt(0.975, N-1) * SE, # 4 lines: Calculate upper and lower values for 95% and 68% CI
      CI95lower = D47 - qt(0.975, N-1) * SE,
      CI68upper = D47 + qt(0.840, N-1) * SE,
      CI68lower = D47 - qt(0.840, N-1) * SE,
      T47 = sqrt(slope/(D47-int))-C,
      T_CI95upper = sqrt(slope/(CI95lower-int))-C, # 4 lines: Calculate upper and lower temperatures associated with lower and upper CI's
      T_CI95lower = sqrt(slope/(CI95upper-int))-C,
      T_CI68upper = sqrt(slope/(CI68lower-int))-C,
      T_CI68lower = sqrt(slope/(CI68upper-int))-C)

  plot_LP_60.3_1bin <- ggplot() +
    scale_y_continuous(limits=c(5,30), breaks=seq(5,30,5)) +
    labs(y="DST (°C)", x="Bin" )+
    geom_hline(yintercept = T_LP_60.3, linetype="dashed", size=1, alpha=0.2, color=cbPalette[2]) +
    # bins
    geom_errorbar(data=ALL_clumped |> filter(bin_id == "LP_60.3"), aes(x = bin_id, ymax = T_CI95upper, ymin = T_CI95lower), alpha=1, width=0, linetype="dashed", color=cbPalette[2]) +
    geom_errorbar(data=ALL_clumped |> filter(bin_id == "LP_60.3"), aes(x = bin_id, ymax = T_CI68upper, ymin = T_CI68lower), alpha=1, width=0, size=1, linetype="solid", color=cbPalette[2]) +
    geom_point(data=ALL_clumped |> filter(bin_id == "LP_60.3"), aes(x = bin_id, y = T47_meinicke), size=3, shape=21, fill="white", color=cbPalette[2]) +
    geom_label_repel(data=ALL_clumped |> filter(bin_id == "LP_60.3"),
                     aes(x = bin_id, y = T_CI95upper, label=N), color=cbPalette[2],
                     nudge_y=.5, direction="y", segment.color = NA, size=3, label.padding = unit(0.1, "lines"),label.r = unit(0, "lines")) +
    # visually
    theme_classic() +
    guides(y ="axis_truncated", x="axis_truncated") +
    theme(panel.background = element_rect(fill='transparent'), #transparent panel bg
          plot.background = element_rect(fill='transparent', color=NA)) + #transparent plot bg)
    theme(axis.line.x=element_blank(),
          axis.text.x=element_blank(),
          axis.ticks.x=element_blank(),
          axis.title.x=element_blank()) +
    theme(legend.position = "none")

  plot_LP_60.3_2bins <- ggplot() +
    scale_y_continuous(limits=c(5,30), breaks=seq(5,30,5)) +
    labs(y="DST (°C)", x="Bin") +
    geom_hline(yintercept = T_LP_60.3, linetype="dashed", size=1, alpha=0.2, color=cbPalette[2]) +
    # bins
    geom_errorbar(data=LP_60.3_2bins, aes(x = subbin, ymax = T_CI95upper, ymin = T_CI95lower), alpha=1, width=0, linetype="dashed", color=cbPalette[1]) +
    geom_errorbar(data=LP_60.3_2bins, aes(x = subbin, ymax = T_CI68upper, ymin = T_CI68lower), alpha=1, width=0, size=1, linetype="solid", color=cbPalette[1]) +
    geom_point(data=LP_60.3_2bins, aes(x = subbin, y = T47), size=3, shape=21, fill="white", color=cbPalette[1]) +
    geom_label_repel(data=LP_60.3_2bins,
                     aes(x = subbin, y = T_CI95upper, label=N), color=cbPalette[1],
                     nudge_y=.5, direction="y", segment.color = NA, size=3, label.padding = unit(0.1, "lines"),label.r = unit(0, "lines")) +
    # visually
    theme_classic() +
    guides(y ="axis_truncated", x="axis_truncated") +
    theme(panel.background = element_rect(fill='transparent'), #transparent panel bg
          plot.background = element_rect(fill='transparent', color=NA)) + #transparent plot bg)
    theme(axis.line.x=element_blank(),
          axis.text.x=element_blank(),
          axis.ticks.x=element_blank(),
          axis.title.x=element_blank()) +
    theme(axis.line.y=element_blank(),
          axis.text.y=element_blank(),
          axis.ticks.y=element_blank(),
          axis.title.y=element_blank()) +
    theme(legend.position = "none")

  plot_LP_60.3_3bins <- ggplot() +
    scale_y_continuous(limits=c(5,30), breaks=seq(5,30,5)) +
    labs(y="DST (°C)", x="Bin") +
    geom_hline(yintercept = T_LP_60.3, linetype="dashed", size=1, alpha=0.2, color=cbPalette[2]) +
    # bins
    geom_errorbar(data=LP_60.3_3bins, aes(x = subbin, ymax = T_CI95upper, ymin = T_CI95lower), alpha=1, width=0, linetype="dashed", color=cbPalette[3]) +
    geom_errorbar(data=LP_60.3_3bins, aes(x = subbin, ymax = T_CI68upper, ymin = T_CI68lower), alpha=1, width=0, size=1, linetype="solid", color=cbPalette[3]) +
    geom_point(data=LP_60.3_3bins, aes(x = subbin, y = T47), size=3, shape=21, fill="white", color=cbPalette[3]) +
    geom_label_repel(data=LP_60.3_3bins,
                     aes(x = subbin, y = T_CI95upper, label=N), color=cbPalette[3],
                     nudge_y=.5, direction="y", segment.color = NA, size=3, label.padding = unit(0.1, "lines"),label.r = unit(0, "lines")) +
    # visually
    theme_classic() +
    guides(y ="axis_truncated", x="axis_truncated") +
    theme(panel.background = element_rect(fill='transparent'), #transparent panel bg
          plot.background = element_rect(fill='transparent', color=NA)) + #transparent plot bg)
    theme(axis.line.x=element_blank(),
          axis.text.x=element_blank(),
          axis.ticks.x=element_blank(),
          axis.title.x=element_blank()) +
    theme(axis.line.y=element_blank(),
          axis.text.y=element_blank(),
          axis.ticks.y=element_blank(),
          axis.title.y=element_blank()) +
```

```
  theme(legend.position = "none")

LP_58.0_2bins <- archive_filter |>
  filter(bin_id == "LP_58.0") |>
  arrange(age) |>
  mutate(
    n = seq_along(age),
    subbin = case_when(
      n %% 2 == 1 ~ "2.A",
      n %% 2 == 0 ~ "2.B")) |>
  group_by(subbin) |>
  summarise(
    D47 = mean(`Final AFF`),
    extSD = sd(`Final AFF`),
    N = n(),
    SE = extSD/sqrt(N),
    CI95upper = D47 + qt(0.975, N-1) * SE, # 4 lines: Calculate upper and lower values for 95% and 68% CI
    CI95lower = D47 - qt(0.975, N-1) * SE,
    CI68upper = D47 + qt(0.840, N-1) * SE,
    CI68lower = D47 - qt(0.840, N-1) * SE,
    T47 = sqrt(slope/(D47-int))-C,
    T_CI95upper = sqrt(slope/(CI95lower-int))-C, # 4 lines: Calculate upper and lower temperatures associated with lower and upper CI's
    T_CI95lower = sqrt(slope/(CI95upper-int))-C,
    T_CI68upper = sqrt(slope/(CI68lower-int))-C,
    T_CI68lower = sqrt(slope/(CI68upper-int))-C)

LP_58.0_3bins <- archive_filter |>
  filter(bin_id == "LP_58.0") |>
  arrange(age) |>
  mutate(
    n = seq_along(age),
    subbin = case_when(
      n %% 3 == 1 ~ "3.A",
      n %% 3 == 2 ~ "3.B",
      n %% 3 == 0 ~ "3.C")) |>
  group_by(subbin) |>
  summarise(
    D47 = mean(`Final AFF`),
    extSD = sd(`Final AFF`),
    N = n(),
    SE = extSD/sqrt(N),
    CI95upper = D47 + qt(0.975, N-1) * SE, # 4 lines: Calculate upper and lower values for 95% and 68% CI
    CI95lower = D47 - qt(0.975, N-1) * SE,
    CI68upper = D47 + qt(0.840, N-1) * SE,
    CI68lower = D47 - qt(0.840, N-1) * SE,
    T47 = sqrt(slope/(D47-int))-C,
    T_CI95upper = sqrt(slope/(CI95lower-int))-C, # 4 lines: Calculate upper and lower temperatures associated with lower and upper CI's
    T_CI95lower = sqrt(slope/(CI95upper-int))-C,
    T_CI68upper = sqrt(slope/(CI68lower-int))-C,
    T_CI68lower = sqrt(slope/(CI68upper-int))-C)

plot_LP_58.0_1bin <- ggplot() +
  scale_y_continuous(limits=c(5,30), breaks=seq(5,30,5)) +
  labs(y="DST (°C)", x="Bin" )+
  geom_hline(yintercept = T_LP_58.0, linetype="dashed", size=1, alpha=0.2, color=cbPalette[2]) +
  # bins
  geom_errorbar(data=ALL_clumped |> filter(bin_id == "LP_58.0"), aes(x = bin_id, ymax = T_CI95upper, ymin = T_CI95lower), alpha=1, width=0, linetype="dashed", color=cbPalette[2]) +
  geom_errorbar(data=ALL_clumped |> filter(bin_id == "LP_58.0"), aes(x = bin_id, ymax = T_CI68upper, ymin = T_CI68lower), alpha=1, width=0, size=1, linetype="solid", color=cbPalette[2]) +
  geom_point(data=ALL_clumped |> filter(bin_id == "LP_58.0"), aes(x = bin_id, y = T47_meinicke), size=3, shape=21, fill="white", color=cbPalette[2]) +
  geom_label_repel(data=ALL_clumped |> filter(bin_id == "LP_58.0"),
                   aes(x = bin_id, y = T_CI95upper, label=N), color=cbPalette[2],
                   nudge_y=.5, direction="y", segment.color = NA, size=3, label.padding = unit(0.1, "lines"),label.r = unit(0, "lines")) +
  # visually
  theme_classic() +
  guides(y ="axis_truncated", x="axis_truncated") +
  theme(panel.background = element_rect(fill='transparent'), #transparent panel bg
        plot.background = element_rect(fill='transparent', color=NA)) + #transparent plot bg)
  theme(axis.line.x=element_blank(),
        axis.text.x=element_blank(),
        axis.ticks.x=element_blank(),
        axis.title.x=element_blank()) +
  theme(legend.position = "none")

plot_LP_58.0_2bins <- ggplot() +
  scale_y_continuous(limits=c(5,30), breaks=seq(5,30,5)) +
  labs(y="DST (°C)", x="Bin") +
  geom_hline(yintercept = T_LP_58.0, linetype="dashed", size=1, alpha=0.2, color=cbPalette[2]) +
  # bins
  geom_errorbar(data=LP_58.0_2bins, aes(x = subbin, ymax = T_CI95upper, ymin = T_CI95lower), alpha=1, width=0, linetype="dashed", color=cbPalette[1]) +
  geom_errorbar(data=LP_58.0_2bins, aes(x = subbin, ymax = T_CI68upper, ymin = T_CI68lower), alpha=1, width=0, size=1, linetype="solid", color=cbPalette[1]) +
  geom_point(data=LP_58.0_2bins, aes(x = subbin, y = T47), size=3, shape=21, fill="white", color=cbPalette[1]) +
  geom_label_repel(data=LP_58.0_2bins,
                   aes(x = subbin, y = T_CI95upper, label=N), color=cbPalette[1],
                   nudge_y=.5, direction="y", segment.color = NA, size=3, label.padding = unit(0.1, "lines"),label.r = unit(0, "lines")) +
  # visually
  theme_classic() +
  guides(y ="axis_truncated", x="axis_truncated") +
  theme(panel.background = element_rect(fill='transparent'), #transparent panel bg
        plot.background = element_rect(fill='transparent', color=NA)) + #transparent plot bg)
  theme(axis.line.x=element_blank(),
```

```
        axis.text.x=element_blank(),
        axis.ticks.x=element_blank(),
        axis.title.x=element_blank()) +
  theme(axis.line.y=element_blank(),
        axis.text.y=element_blank(),
        axis.ticks.y=element_blank(),
        axis.title.y=element_blank()) +
  theme(legend.position = "none")

plot_LP_58.0_3bins <- ggplot() +
  scale_y_continuous(limits=c(5,30), breaks=seq(5,30,5)) +
  labs(y="DST (°C)", x="Bin") +
  geom_hline(yintercept = T_LP_58.0, linetype="dashed", size=1, alpha=0.2, color=cbPalette[2]) +
  # bins
  geom_errorbar(data=LP_58.0_3bins, aes(x = subbin, ymax = T_CI95upper, ymin = T_CI95lower), alpha=1, width=0, linetype="dashed",
  color=cbPalette[3]) +
  geom_errorbar(data=LP_58.0_3bins, aes(x = subbin, ymax = T_CI68upper, ymin = T_CI68lower), alpha=1, width=0, size=1, linetype=
  "solid", color=cbPalette[3]) +
  geom_point(data=LP_58.0_3bins, aes(x = subbin, y = T47), size=3, shape=21, fill="white", color=cbPalette[3]) +
  geom_label_repel(data=LP_58.0_3bins,
                   aes(x = subbin, y = T_CI95upper, label=N), color=cbPalette[3],
                   nudge_y=.5, direction="y", segment.color = NA, size=3, label.padding = unit(0.1, "lines"),label.r = unit(0,
                   "lines")) +
  # visually
  theme_classic() +
  guides(y ="axis_truncated", x="axis_truncated") +
  theme(panel.background = element_rect(fill='transparent'), #transparent panel bg
        plot.background = element_rect(fill='transparent', color=NA)) + #transparent plot bg)
  theme(axis.line.x=element_blank(),
        axis.text.x=element_blank(),
        axis.ticks.x=element_blank(),
        axis.title.x=element_blank()) +
  theme(axis.line.y=element_blank(),
        axis.text.y=element_blank(),
        axis.ticks.y=element_blank(),
        axis.title.y=element_blank()) +
  theme(legend.position = "none")

LP_57.1_2bins <- archive_filter |>
  filter(bin_id == "LP_57.1") |>
  arrange(age) |>
  mutate(
    n = seq_along(age),
    subbin = case_when(
      n %% 2 == 1 ~ "2.A",
      n %% 2 == 0 ~ "2.B")) |>
  group_by(subbin) |>
  summarise(
    D47 = mean(`Final AFF`),
    extSD = sd(`Final AFF`),
    N = n(),
    SE = extSD/sqrt(N),
    CI95upper = D47 + qt(0.975, N-1) * SE, # 4 lines: Calculate upper and lower values for 95% and 68% CI
    CI95lower = D47 - qt(0.975, N-1) * SE,
    CI68upper = D47 + qt(0.840, N-1) * SE,
    CI68lower = D47 - qt(0.840, N-1) * SE,
    T47 = sqrt(slope/(D47-int))-C,
    T_CI95upper = sqrt(slope/(CI95lower-int))-C, # 4 lines: Calculate upper and lower temperatures associated with lower and upper
    CI's
    T_CI95lower = sqrt(slope/(CI95upper-int))-C,
    T_CI68upper = sqrt(slope/(CI68lower-int))-C,
    T_CI68lower = sqrt(slope/(CI68upper-int))-C)

LP_57.1_3bins <- archive_filter |>
  filter(bin_id == "LP_57.1") |>
  arrange(age) |>
  mutate(
    n = seq_along(age),
    subbin = case_when(
      n %% 3 == 1 ~ "3.A",
      n %% 3 == 2 ~ "3.B",
      n %% 3 == 0 ~ "3.C")) |>
  group_by(subbin) |>
  summarise(
    D47 = mean(`Final AFF`),
    extSD = sd(`Final AFF`),
    N = n(),
    SE = extSD/sqrt(N),
    CI95upper = D47 + qt(0.975, N-1) * SE, # 4 lines: Calculate upper and lower values for 95% and 68% CI
    CI95lower = D47 - qt(0.975, N-1) * SE,
    CI68upper = D47 + qt(0.840, N-1) * SE,
    CI68lower = D47 - qt(0.840, N-1) * SE,
    T47 = sqrt(slope/(D47-int))-C,
    T_CI95upper = sqrt(slope/(CI95lower-int))-C, # 4 lines: Calculate upper and lower temperatures associated with lower and upper
    CI's
    T_CI95lower = sqrt(slope/(CI95upper-int))-C,
    T_CI68upper = sqrt(slope/(CI68lower-int))-C,
    T_CI68lower = sqrt(slope/(CI68upper-int))-C)

plot_LP_57.1_1bin <- ggplot() +
  scale_y_continuous(limits=c(5,30), breaks=seq(5,30,5)) +
  labs(y="DST (°C)", x="Bin" )+
  geom_hline(yintercept = T_LP_57.1, linetype="dashed", size=1, alpha=0.2, color=cbPalette[2]) +
  # bins
  geom_errorbar(data=ALL_clumped |> filter(bin_id == "LP_57.1"), aes(x = bin_id, ymax = T_CI95upper, ymin = T_CI95lower), alpha=1,
  width=0, linetype="dashed", color=cbPalette[2]) +
  geom_errorbar(data=ALL_clumped |> filter(bin_id == "LP_57.1"), aes(x = bin_id, ymax = T_CI68upper, ymin = T_CI68lower), alpha=1,
  width=0, size=1, linetype="solid", color=cbPalette[2]) +
  geom_point(data=ALL_clumped |> filter(bin_id == "LP_57.1"), aes(x = bin_id, y = T47_meinicke), size=3, shape=21, fill="white",
```

```
  color=cbPalette[2]) +
  geom_label_repel(data=ALL_clumped |> filter(bin_id == "LP_57.1"),
                   aes(x = bin_id, y = T_CI95upper, label=N), color=cbPalette[2],
                   nudge_y=.5, direction="y", segment.color = NA, size=3, label.padding = unit(0.1, "lines"),label.r = unit(0,
                   "lines")) +
  # visually
  theme_classic() +
  guides(y ="axis_truncated", x="axis_truncated") +
  theme(panel.background = element_rect(fill='transparent'), #transparent panel bg
        plot.background = element_rect(fill='transparent', color=NA)) + #transparent plot bg)
  theme(axis.line.x=element_blank(),
        axis.text.x=element_blank(),
        axis.ticks.x=element_blank(),
        axis.title.x=element_blank()) +
  theme(legend.position = "none")

plot_LP_57.1_2bins <- ggplot() +
  scale_y_continuous(limits=c(5,30), breaks=seq(5,30,5)) +
  labs(y="DST (°C)", x="Bin") +
  geom_hline(yintercept = T_LP_57.1, linetype="dashed", size=1, alpha=0.2, color=cbPalette[2]) +
  # bins
  geom_errorbar(data=LP_57.1_2bins, aes(x = subbin, ymax = T_CI95upper, ymin = T_CI95lower), alpha=1, width=0, linetype="dashed",
  color=cbPalette[1]) +
  geom_errorbar(data=LP_57.1_2bins, aes(x = subbin, ymax = T_CI68upper, ymin = T_CI68lower), alpha=1, width=0, size=1, linetype=
  "solid", color=cbPalette[1]) +
  geom_point(data=LP_57.1_2bins, aes(x = subbin, y = T47), size=3, shape=21, fill="white", color=cbPalette[1]) +
  geom_label_repel(data=LP_57.1_2bins,
                   aes(x = subbin, y = T_CI95upper, label=N), color=cbPalette[1],
                   nudge_y=.5, direction="y", segment.color = NA, size=3, label.padding = unit(0.1, "lines"),label.r = unit(0,
                   "lines")) +
  # visually
  theme_classic() +
  guides(y ="axis_truncated", x="axis_truncated") +
  theme(panel.background = element_rect(fill='transparent'), #transparent panel bg
        plot.background = element_rect(fill='transparent', color=NA)) + #transparent plot bg)
  theme(axis.line.x=element_blank(),
        axis.text.x=element_blank(),
        axis.ticks.x=element_blank(),
        axis.title.x=element_blank()) +
  theme(axis.line.y=element_blank(),
        axis.text.y=element_blank(),
        axis.ticks.y=element_blank(),
        axis.title.y=element_blank()) +
  theme(legend.position = "none")

plot_LP_57.1_3bins <- ggplot() +
  scale_y_continuous(limits=c(5,30), breaks=seq(5,30,5)) +
  labs(y="DST (°C)", x="Bin") +
  geom_hline(yintercept = T_LP_57.1, linetype="dashed", size=1, alpha=0.2, color=cbPalette[2]) +
  # bins
  geom_errorbar(data=LP_57.1_3bins, aes(x = subbin, ymax = T_CI95upper, ymin = T_CI95lower), alpha=1, width=0, linetype="dashed",
  color=cbPalette[3]) +
  geom_errorbar(data=LP_57.1_3bins, aes(x = subbin, ymax = T_CI68upper, ymin = T_CI68lower), alpha=1, width=0, size=1, linetype=
  "solid", color=cbPalette[3]) +
  geom_point(data=LP_57.1_3bins, aes(x = subbin, y = T47), size=3, shape=21, fill="white", color=cbPalette[3]) +
  geom_label_repel(data=LP_57.1_3bins,
                   aes(x = subbin, y = T_CI95upper, label=N), color=cbPalette[3],
                   nudge_y=.5, direction="y", segment.color = NA, size=3, label.padding = unit(0.1, "lines"),label.r = unit(0,
                   "lines")) +
  # visually
  theme_classic() +
  guides(y ="axis_truncated", x="axis_truncated") +
  theme(panel.background = element_rect(fill='transparent'), #transparent panel bg
        plot.background = element_rect(fill='transparent', color=NA)) + #transparent plot bg)
  theme(axis.line.x=element_blank(),
        axis.text.x=element_blank(),
        axis.ticks.x=element_blank(),
        axis.title.x=element_blank()) +
  theme(axis.line.y=element_blank(),
        axis.text.y=element_blank(),
        axis.ticks.y=element_blank(),
        axis.title.y=element_blank()) +
  theme(legend.position = "none")

LP_56.7_2bins <- archive_filter |>
  filter(bin_id == "LP_56.7") |>
  arrange(age) |>
  mutate(
    n = seq_along(age),
    subbin = case_when(
      n %% 2 == 1 ~ "2.A",
      n %% 2 == 0 ~ "2.B")) |>
  group_by(subbin) |>
  summarise(
    D47 = mean(`Final AFF`),
    extSD = sd(`Final AFF`),
    N = n(),
    SE = extSD/sqrt(N),
    CI95upper = D47 + qt(0.975, N-1) * SE, # 4 lines: Calculate upper and lower values for 95% and 68% CI
    CI95lower = D47 - qt(0.975, N-1) * SE,
    CI68upper = D47 + qt(0.840, N-1) * SE,
    CI68lower = D47 - qt(0.840, N-1) * SE,
    T47 = sqrt(slope/(D47-int))-C,
    T_CI95upper = sqrt(slope/(CI95lower-int))-C, # 4 lines: Calculate upper and lower temperatures associated with lower and upper
    CI's
    T_CI95lower = sqrt(slope/(CI95upper-int))-C,
    T_CI68upper = sqrt(slope/(CI68lower-int))-C,
    T_CI68lower = sqrt(slope/(CI68upper-int))-C)

```

```
LP_56.7_3bins <- archive_filter |>
  filter(bin_id == "LP_56.7") |>
  arrange(age) |>
  mutate(
    n = seq_along(age),
    subbin = case_when(
      n %% 3 == 1 ~ "3.A",
      n %% 3 == 2 ~ "3.B",
      n %% 3 == 0 ~ "3.C")) |>
  group_by(subbin) |>
  summarise(
    D47 = mean(`Final AFF`),
    extSD = sd(`Final AFF`),
    N = n(),
    SE = extSD/sqrt(N),
    CI95upper = D47 + qt(0.975, N-1) * SE, # 4 lines: Calculate upper and lower values for 95% and 68% CI
    CI95lower = D47 - qt(0.975, N-1) * SE,
    CI68upper = D47 + qt(0.840, N-1) * SE,
    CI68lower = D47 - qt(0.840, N-1) * SE,
    T47 = sqrt(slope/(D47-int))-C,
    T_CI95upper = sqrt(slope/(CI95lower-int))-C, # 4 lines: Calculate upper and lower temperatures associated with lower and upper CI's
    T_CI95lower = sqrt(slope/(CI95upper-int))-C,
    T_CI68upper = sqrt(slope/(CI68lower-int))-C,
    T_CI68lower = sqrt(slope/(CI68upper-int))-C)

plot_LP_56.7_1bin <- ggplot() +
  scale_y_continuous(limits=c(5,30), breaks=seq(5,30,5)) +
  labs(y="DST (°C)", x="Bin" )+
  geom_hline(yintercept = T_LP_56.7, linetype="dashed", size=1, alpha=0.2, color=cbPalette[2]) +
  # bins
  geom_errorbar(data=ALL_clumped |> filter(bin_id == "LP_56.7"), aes(x = bin_id, ymax = T_CI95upper, ymin = T_CI95lower), alpha=1, width=0, linetype="dashed", color=cbPalette[2]) +
  geom_errorbar(data=ALL_clumped |> filter(bin_id == "LP_56.7"), aes(x = bin_id, ymax = T_CI68upper, ymin = T_CI68lower), alpha=1, width=0, size=1, linetype="solid", color=cbPalette[2]) +
  geom_point(data=ALL_clumped |> filter(bin_id == "LP_56.7"), aes(x = bin_id, y = T47_meinicke), size=3, shape=21, fill="white", color=cbPalette[2]) +
  geom_label_repel(data=ALL_clumped |> filter(bin_id == "LP_56.7"),
                   aes(x = bin_id, y = T_CI95upper, label=N), color=cbPalette[2],
                   nudge_y=.5, direction="y", segment.color = NA, size=3, label.padding = unit(0.1, "lines"),label.r = unit(0, "lines")) +
  # visually
  theme_classic() +
  guides(y ="axis_truncated", x="axis_truncated") +
  theme(panel.background = element_rect(fill='transparent'), #transparent panel bg
        plot.background = element_rect(fill='transparent', color=NA)) + #transparent plot bg)
  theme(axis.line.x=element_blank(),
        axis.text.x=element_blank(),
        axis.ticks.x=element_blank(),
        axis.title.x=element_blank()) +
  theme(legend.position = "none")

plot_LP_56.7_2bins <- ggplot() +
  scale_y_continuous(limits=c(5,30), breaks=seq(5,30,5)) +
  labs(y="DST (°C)", x="Bin") +
  geom_hline(yintercept = T_LP_56.7, linetype="dashed", size=1, alpha=0.2, color=cbPalette[2]) +
  # bins
  geom_errorbar(data=LP_56.7_2bins, aes(x = subbin, ymax = T_CI95upper, ymin = T_CI95lower), alpha=1, width=0, linetype="dashed", color=cbPalette[1]) +
  geom_errorbar(data=LP_56.7_2bins, aes(x = subbin, ymax = T_CI68upper, ymin = T_CI68lower), alpha=1, width=0, size=1, linetype="solid", color=cbPalette[1]) +
  geom_point(data=LP_56.7_2bins, aes(x = subbin, y = T47), size=3, shape=21, fill="white", color=cbPalette[1]) +
  geom_label_repel(data=LP_56.7_2bins,
                   aes(x = subbin, y = T_CI95upper, label=N), color=cbPalette[1],
                   nudge_y=.5, direction="y", segment.color = NA, size=3, label.padding = unit(0.1, "lines"),label.r = unit(0, "lines")) +
  # visually
  theme_classic() +
  guides(y ="axis_truncated", x="axis_truncated") +
  theme(panel.background = element_rect(fill='transparent'), #transparent panel bg
        plot.background = element_rect(fill='transparent', color=NA)) + #transparent plot bg)
  theme(axis.line.x=element_blank(),
        axis.text.x=element_blank(),
        axis.ticks.x=element_blank(),
        axis.title.x=element_blank()) +
  theme(axis.line.y=element_blank(),
        axis.text.y=element_blank(),
        axis.ticks.y=element_blank(),
        axis.title.y=element_blank()) +
  theme(legend.position = "none")

plot_LP_56.7_3bins <- ggplot() +
  scale_y_continuous(limits=c(5,30), breaks=seq(5,30,5)) +
  labs(y="DST (°C)", x="Bin") +
  geom_hline(yintercept = T_LP_56.7, linetype="dashed", size=1, alpha=0.2, color=cbPalette[2]) +
  # bins
  geom_errorbar(data=LP_56.7_3bins, aes(x = subbin, ymax = T_CI95upper, ymin = T_CI95lower), alpha=1, width=0, linetype="dashed", color=cbPalette[3]) +
  geom_errorbar(data=LP_56.7_3bins, aes(x = subbin, ymax = T_CI68upper, ymin = T_CI68lower), alpha=1, width=0, size=1, linetype="solid", color=cbPalette[3]) +
  geom_point(data=LP_56.7_3bins, aes(x = subbin, y = T47), size=3, shape=21, fill="white", color=cbPalette[3]) +
  geom_label_repel(data=LP_56.7_3bins,
                   aes(x = subbin, y = T_CI95upper, label=N), color=cbPalette[3],
                   nudge_y=.5, direction="y", segment.color = NA, size=3, label.padding = unit(0.1, "lines"),label.r = unit(0, "lines")) +
  # visually
  theme_classic() +
  guides(y ="axis_truncated", x="axis_truncated") +
  theme(panel.background = element_rect(fill='transparent'), #transparent panel bg
```

```
        plot.background = element_rect(fill='transparent', color=NA)) + #transparent plot bg)
  theme(axis.line.x=element_blank(),
        axis.text.x=element_blank(),
        axis.ticks.x=element_blank(),
        axis.title.x=element_blank()) +
  theme(axis.line.y=element_blank(),
        axis.text.y=element_blank(),
        axis.ticks.y=element_blank(),
        axis.title.y=element_blank()) +
  theme(legend.position = "none")

plots_LP_allbindivision <- plot_LP_56.7_1bin + plot_LP_56.7_2bins + plot_LP_56.7_3bins + plot_LP_57.1_1bin + plot_LP_57.1_2bins + plot_LP_57.1_3bins +  plot_LP_58.0_1bin + plot_LP_58.0_2bins + plot_LP_58.0_3bins + plot_LP_60.3_1bin + plot_LP_60.3_2bins + plot_LP_60.3_3bins  + plot_layout(ncol=6, nrow=2)

print(plots_LP_allbindivision)

# Figure A.2 (Evolution of temperature and confidence intervals with increasing number of replicates)

LP_60.3 <- LP_60.3 |>
  rename(
    D47 = `Final AFF`) |>
  mutate(
    n = seq_along(D47),
    m = cumsum(D47)/n,
    m2 = cumsum(D47*D47)/n,
    v = (m2 - m*m) * (n/(n-1)),
    cumSD = sqrt(v),
    SE = cumSD/sqrt(n),
    CI95upper = m + qt(0.975, n-1) * SE, # 4 lines: Calculate upper and lower values for 95% and 68% CI
    CI95lower = m - qt(0.975, n-1) * SE,
    CI68upper = m + qt(0.840, n-1) * SE,
    CI68lower = m - qt(0.840, n-1) * SE,
    T47 =  sqrt(slope/(m-int))-C,
    T_CI95upper = sqrt(slope/(CI95lower-int))-C, # 4 lines: Calculate upper and lower temperatures associated with lower and upper CI's
    T_CI95lower = sqrt(slope/(CI95upper-int))-C,
    T_CI68upper = sqrt(slope/(CI68lower-int))-C,
    T_CI68lower = sqrt(slope/(CI68upper-int))-C)

LP_58.0 <- LP_58.0 |>
  rename(
    D47 = `Final AFF`) |>
  mutate(
    n = seq_along(D47),
    m = cumsum(D47)/n,
    m2 = cumsum(D47*D47)/n,
    v = (m2 - m*m) * (n/(n-1)),
    cumSD = sqrt(v),
    SE = cumSD/sqrt(n),
    CI95upper = m + qt(0.975, n-1) * SE, # 4 lines: Calculate upper and lower values for 95% and 68% CI
    CI95lower = m - qt(0.975, n-1) * SE,
    CI68upper = m + qt(0.840, n-1) * SE,
    CI68lower = m - qt(0.840, n-1) * SE,
    T47 =  sqrt(slope/(m-int))-C,
    T_CI95upper = sqrt(slope/(CI95lower-int))-C, # 4 lines: Calculate upper and lower temperatures associated with lower and upper CI's
    T_CI95lower = sqrt(slope/(CI95upper-int))-C,
    T_CI68upper = sqrt(slope/(CI68lower-int))-C,
    T_CI68lower = sqrt(slope/(CI68upper-int))-C)

LP_57.1 <- LP_57.1 |>
  rename(
    D47 = `Final AFF`) |>
  mutate(
    n = seq_along(D47),
    m = cumsum(D47)/n,
    m2 = cumsum(D47*D47)/n,
    v = (m2 - m*m) * (n/(n-1)),
    cumSD = sqrt(v),
    SE = cumSD/sqrt(n),
    CI95upper = m + qt(0.975, n-1) * SE, # 4 lines: Calculate upper and lower values for 95% and 68% CI
    CI95lower = m - qt(0.975, n-1) * SE,
    CI68upper = m + qt(0.840, n-1) * SE,
    CI68lower = m - qt(0.840, n-1) * SE,
    T47 =  sqrt(slope/(m-int))-C,
    T_CI95upper = sqrt(slope/(CI95lower-int))-C, # 4 lines: Calculate upper and lower temperatures associated with lower and upper CI's
    T_CI95lower = sqrt(slope/(CI95upper-int))-C,
    T_CI68upper = sqrt(slope/(CI68lower-int))-C,
    T_CI68lower = sqrt(slope/(CI68upper-int))-C)

LP_56.7 <- LP_56.7 |>
  rename(
    D47 = `Final AFF`) |>
  mutate(
    n = seq_along(D47),
    m = cumsum(D47)/n,
    m2 = cumsum(D47*D47)/n,
    v = (m2 - m*m) * (n/(n-1)),
    cumSD = sqrt(v),
    SE = cumSD/sqrt(n),
    CI95upper = m + qt(0.975, n-1) * SE, # 4 lines: Calculate upper and lower values for 95% and 68% CI
    CI95lower = m - qt(0.975, n-1) * SE,
    CI68upper = m + qt(0.840, n-1) * SE,
    CI68lower = m - qt(0.840, n-1) * SE,
    T47 =  sqrt(slope/(m-int))-C,
    T_CI95upper = sqrt(slope/(CI95lower-int))-C, # 4 lines: Calculate upper and lower temperatures associated with lower and upper CI's
```

```
      T_CI95lower = sqrt(slope/(CI95upper-int))-C,
      T_CI68upper = sqrt(slope/(CI68lower-int))-C,
      T_CI68lower = sqrt(slope/(CI68upper-int))-C)



plot_LP_60.3 <- ggplot() +
  scale_x_continuous(limits=c(0,101), breaks=seq(0,101,10)) +
  scale_y_continuous(limits=c(-1000,1000), breaks=seq(-10,50,10)) +
  coord_trans(ylim=c(-10,50)) +
  labs(y="DST (°C)", x="Number of replicates")+
  #data
  geom_ribbon(data=LP_60.3, aes(x=n, ymin=T_CI95lower, ymax=T_CI95upper), alpha=.2, fill=cbPalette[1]) +
  geom_ribbon(data=LP_60.3, aes(x=n, ymin=T_CI68lower, ymax=T_CI68upper), alpha=.4, fill=cbPalette[1]) +
  geom_line(data=LP_60.3, aes(x=n, y=T47), linewidth=1, color=cbPalette[1]) +
  # visually
  theme_classic() +
  scale_shape_manual(values = c(25,24,23,22,21)) +
  guides(y ="axis_truncated", x="axis_truncated") +
  theme(panel.background = element_rect(fill='transparent'), #transparent panel bg
        plot.background = element_rect(fill='transparent', color=NA)) + #transparent plot bg)
  theme(legend.position = "none")

plot_LP_58.0 <- ggplot() +
  scale_x_continuous(limits=c(0,101), breaks=seq(0,101,10)) +
  scale_y_continuous(limits=c(-1000,1000), breaks=seq(-10,50,10)) +
  coord_trans(ylim=c(-10,50)) +
  labs(y="DST (°C)", x="Number of replicates")+
  #data
  geom_ribbon(data=LP_58.0, aes(x=n, ymin=T_CI95lower, ymax=T_CI95upper), alpha=.2, fill=cbPalette[2]) +
  geom_ribbon(data=LP_58.0, aes(x=n, ymin=T_CI68lower, ymax=T_CI68upper), alpha=.4, fill=cbPalette[2]) +
  geom_line(data=LP_58.0, aes(x=n, y=T47), linewidth=1, color=cbPalette[2]) +
  # visually
  theme_classic() +
  scale_shape_manual(values = c(25,24,23,22,21)) +
  guides(y ="axis_truncated", x="axis_truncated") +
  theme(panel.background = element_rect(fill='transparent'), #transparent panel bg
        plot.background = element_rect(fill='transparent', color=NA)) + #transparent plot bg)
  theme(legend.position = "none")

plot_LP_57.1 <- ggplot() +
  scale_x_continuous(limits=c(0,101), breaks=seq(0,101,10)) +
  scale_y_continuous(limits=c(-1000,1000), breaks=seq(-10,50,10)) +
  coord_trans(ylim=c(-10,50)) +
  labs(y="DST (°C)", x="Number of replicates")+
  #data
  geom_ribbon(data=LP_57.1, aes(x=n, ymin=T_CI95lower, ymax=T_CI95upper), alpha=.2, fill=cbPalette[3]) +
  geom_ribbon(data=LP_57.1, aes(x=n, ymin=T_CI68lower, ymax=T_CI68upper), alpha=.4, fill=cbPalette[3]) +
  geom_line(data=LP_57.1, aes(x=n, y=T47), linewidth=1, color=cbPalette[3]) +
  # visually
  theme_classic() +
  scale_shape_manual(values = c(25,24,23,22,21)) +
  guides(y ="axis_truncated", x="axis_truncated") +
  theme(panel.background = element_rect(fill='transparent'), #transparent panel bg
        plot.background = element_rect(fill='transparent', color=NA)) + #transparent plot bg)
  theme(legend.position = "none")

plot_LP_56.7 <- ggplot() +
  scale_x_continuous(limits=c(0,101), breaks=seq(0,101,10)) +
  scale_y_continuous(limits=c(-1000,1000), breaks=seq(-10,50,10)) +
  coord_trans(ylim=c(-10,50)) +
  labs(y="DST (°C)", x="Number of replicates")+
  #data
  geom_ribbon(data=LP_56.7, aes(x=n, ymin=T_CI95lower, ymax=T_CI95upper), alpha=.2, fill=cbPalette[4]) +
  geom_ribbon(data=LP_56.7, aes(x=n, ymin=T_CI68lower, ymax=T_CI68upper), alpha=.4, fill=cbPalette[4]) +
  geom_line(data=LP_56.7, aes(x=n, y=T47), linewidth=1, color=cbPalette[4]) +
  # visually
  theme_classic() +
  scale_shape_manual(values = c(25,24,23,22,21)) +
  guides(y ="axis_truncated", x="axis_truncated") +
  theme(panel.background = element_rect(fill='transparent'), #transparent panel bg
        plot.background = element_rect(fill='transparent', color=NA)) + #transparent plot bg)
  theme(legend.position = "none")

plots_LP <- plot_LP_56.7 + plot_LP_57.1 + plot_LP_58.0 + plot_LP_60.3+ plot_layout(ncol=2, nrow=2)
print(plots_LP)

# end of file ----
```

Bibliography

Agterhuis, T., Ziegler, M., de Winter, N. J., & Lourens, L. J. (2022). Warm deep-sea temperatures across eocene thermal maximum 2 from clumped isotope thermometry. *Communications Earth & Environment*, *3*(1), 1–9. https://doi.org/10.1038/s43247-022-00350-8

Anagnostou, E., John, E. H., Edgar, K. M., Foster, G. L., Ridgwell, A., Inglis, G. N., Pancost, R. D., Lunt, D. J., & Pearson, P. N. (2016). Changing atmospheric CO2 concentration was the primary driver of early cenozoic climate. *Nature*, *533*(7603), 380–384. https://doi.org/10.1038/nature17423

Anderson, N. T., Kelson, J. R., Kele, S., Daëron, M., Bonifacie, M., Horita, J., Mackey, T. J., John, C. M., Kluge, T., Petschnig, P., Jost, A. B., Huntington, K. W., Bernasconi, S. M., & Bergmann, K. D. (2021). A unified clumped isotope thermometer calibration (0.5–1,100°c) using carbonate-based standardization. *Geophysical Research Letters*, *48*(7), e2020GL092069. https://doi.org/10.1029/2020GL092069

Arrhenius, S. (1896). XXXI. *On the influence of carbonic acid in the air upon the temperature of the ground. The London, Edinburgh, and Dublin Philosophical Magazine and Journal of Science*, *41*(251), 237–276. https://doi.org/10.1080/14786449608620846

Barker, S., Cacho, I., Benway, H., & Tachikawa, K. (2005). Planktonic foraminiferal mg/ca as a proxy for past oceanic temperatures: A methodological overview and data compilation for the last glacial maximum. *Quaternary Science Reviews*, *24*(7), 821–834. https://doi.org/10.1016/j.quascirev.2004.07.016

Barnet, J. S. K., Littler, K., Westerhold, T., Kroon, D., Leng, M. J., Bailey, I., Röhl, U., & Zachos, J. C. (2019). A high-fidelity benthic stable isotope record of late cretaceous–early eocene climate change and carbon-cycling. *Paleoceanography and Paleoclimatology*, *34*(4), 672–691. https://doi.org/10.1029/2019PA003556

Batenburg, S. J., Voigt, S., Friedrich, O., Osborne, A. H., Bornemann, A., Klein, T., Pérez-Díaz, L., & Frank, M. (2018). Major intensification of atlantic overturning circulation at the onset of paleogene greenhouse warmth. *Nature Communications*, *9*(1), 4954. https://doi.org/10.1038/s41467-018-07457-7

Berends, C. J., de Boer, B., & van de Wal, R. S. W. (2021). Reconstructing the evolution of ice sheets, sea level, and atmospheric CO_2 during the past 3.6 million years. *Climate of the Past*, *17*(1), 361–377. https://doi.org/10.5194/cp-17-361-2021

Bernasconi, S. M., Daëron, M., Bergmann, K. D., Bonifacie, M., Meckler, A. N., Affek, H. P., Anderson, N., Bajnai, D., Barkan, E., Beverly, E., Blamart, D., Burgener, L., Calmels, D., Chaduteau, C., Clog, M., Davidheiser-Kroll, B., Davies, A., Dux, F., Eiler, J., … Ziegler, M. (2021). InterCarb: A community effort to improve interlaboratory standardization of the carbonate clumped isotope thermometer using carbonate standards. *Geochemistry, Geophysics, Geosystems*, *22*(5), e2020GC009588. https://doi.org/10.1029/2020GC009588

Bijl, P. K., Schouten, S., Sluijs, A., Reichart, G.-J., Zachos, J. C., & Brinkhuis, H. (2009). Early palaeogene temperature evolution of the southwest pacific ocean. *Nature*, *461*(7265), 776–779. https://doi.org/10.1038/nature08399

Binczewska, A., Polovodova Asteman, I., & Farmer, E. J. (2014). Foraminifers (benthic). In J. Harff, M. Meschede, S. Petersen, & J. Thiede (Eds.), *Encyclopedia of marine geosciences* (pp. 1–8). Springer Netherlands. https://doi.org/10.1007/978-94-007-6644-0_60-1

Birch, H. S., Coxall, H. K., Pearson, P. N., Kroon, D., & Schmidt, D. N. (2016). Partial collapse of the marine carbon pump after the cretaceous-paleogene boundary. *Geology*, *44*(4), 287–290. https://doi.org/10.1130/G37581.1

Brand, W. A., Assonov, S. S., & Coplen, T. B. (2010). Correction for the 17O interference in (13C) measurements when analyzing CO2 with stable isotope mass spectrometry (IUPAC Technical Report). *Pure and Applied Chemistry*, *82*(8), 1719–1733. https://doi.org/10.1351/PAC-REP-09-01-05

Brassell, S. C., Eglinton, G., Marlowe, I. T., Pflaumann, U., & Sarnthein, M. (1986). Molecular stratigraphy: A new tool for climatic assessment. *Nature*, *320*(6058), 129–133. https://doi.org/10.1038/320129a0

Broecker, W. S. (1982). Tracers in the sea.

Caballero, R., & Huber, M. (2013). State-dependent climate sensitivity in past warm climates and its implications for future climate projections. *Proceedings of the National Academy of Sciences*, *110*(35), 14162–14167. https://doi.org/10.1073/pnas.1303365110

Coogan, L., Daëron, M., & Gillis, K. (2019). Seafloor weathering and the oxygen isotope ratio in seawater: Insight from whole-rock 18o and carbonate 18o and 47 from the troodos ophiolite. *Earth and Planetary Science Letters*, *508*, 41–50. https://doi.org/10.1016/j.epsl.2018.12.014

Cramer, B. S., Miller, K. G., Barrett, P. J., & Wright, J. D. (2011). Late cretaceous–neogene trends in deep ocean temperature and continental ice volume: Reconciling records of benthic foraminiferal geochemistry (18o and mg/ca) with sea level history. *Journal of Geophysical Research: Oceans*, *116*. https://doi.org/10.1029/2011JC007255

Cramer, B. S., Toggweiler, J. R., Wright, J. D., Katz, M. E., & Miller, K. G. (2009). Ocean overturning since the late cretaceous: Inferences from a new benthic foraminiferal isotope compilation. *Paleoceanography*, *24*(4). https://doi.org/10.1029/2008PA001683

Cramwinckel, M. J., Huber, M., Kocken, I. J., Agnini, C., Bijl, P. K., Bohaty, S. M., Frieling, J., Goldner, A., Hilgen, F. J., Kip, E. L., Peterse, F., van der Ploeg, R., Röhl, U., Schouten, S., & Sluijs, A. (2018). Synchronous tropical and polar temperature evolution in the eocene. *Nature*, *559*(7714), 382–386. https://doi.org/10.1038/s41586-018-0272-2

Cui, L., & Wang, X. (2014). Determination of clumped isotopes in carbonate using isotope ratio mass spectrometer: Effects of extraction potential and long-term stability. *International Journal of Mass Spectrometry*, *372*, 46–50. https://doi.org/10.1016/j.ijms.2014.08.006

Daëron, M., Blamart, D., Peral, M., & Affek, H. (2016). Absolute isotopic abundance ratios and the accuracy of 47 measurements. *Chemical Geology*, *442*, 83–96. https://doi.org/10.1016/j.chemgeo.2016.08.014

Davies, A., Gréselle, B., Hunter, S. J., Baines, G., Robson, C., Haywood, A. M., Ray, D. C., Simmons, M. D., & van Buchem, F. S. P. (2020). Assessing the impact of aquifer-eustasy on short-term cretaceous sea-level. *Cretaceous Research*, *112*, 104445. https://doi.org/10.1016/j.cretres.2020.104445

de Bar, M. W., Rampen, S. W., Hopmans, E. C., Sinninghe Damsté, J. S., & Schouten, S. (2019). Constraining the applicability of organic paleotemperature proxies for the last 90 myrs. *Organic Geochemistry*, *128*, 122–136. https://doi.org/10.1016/j.orggeochem.2018.12.005

DeConto, R. M., & Pollard, D. (2003). Rapid cenozoic glaciation of antarctica induced by declining atmospheric CO2. *Nature*, *421*(6920), 245–249. https://doi.org/10.1038/nature01290

Dinarès-Turell, J., Westerhold, T., Pujalte, V., Röhl, U., & Kroon, D. (2014). Astronomical calibration of the danian stage (early paleocene) revisited: Settling chronologies of sedimentary records across the

atlantic and pacific oceans. *Earth and Planetary Science Letters*, *405*, 119–131. https://doi.org/10.1016/j.epsl.2014.08.027

Eiler, J. M. (2007). "clumped-isotope" geochemistry—the study of naturally-occurring, multiply-substituted isotopologues. *Earth and Planetary Science Letters*, *262*(3), 309–327. https://doi.org/10.1016/j.epsl.2007.08.020

Epstein, S., Buchsbaum, R., Lowenstam, H., & Urey, H. C. (1951). CARBONATE-WATER ISOTOPIC TEMPERATURE SCALE. *Bull. Geol. Soc. Am.*, *Vol: 62*. https://doi.org/10.1130/0016-7606(1951)62[417:CITS]2.0.CO;2

Epstein, S., Buchsbaum, R., Lowenstam, H. A., & Urey, H. C. (1953). REVISED CARBONATE-WATER ISOTOPIC TEMPERATURE SCALE. *Geological Society of America Bulletin*, *64*(11), 1315. https://doi.org/10.1130/0016-7606(1953)64[1315:RCITS]2.0.CO;2

Evans, D., & Müller, W. (2012). Deep time foraminifera mg/ca paleothermometry: Nonlinear correction for secular change in seawater mg/ca. *Paleoceanography*, *27*(4). https://doi.org/10.1029/2012PA002315

Eyring, V., Gillett, N., Achuta Rao, K., Barimalala, R., Barreiro Parrillo, M., Bellouin, N., Cassou, C., Durack, Y., Kosaka, S., McGregor, S., Min, S., Morgenstern, O., & Sun, Y. (2021). Chapter 3: Human influence on the climate system. *Human Influence on the Climate System. In Climate Change 2021: The Physical Science Basis. Contribution of Working Group I to the Sixth Assessment Report of the Intergovernmental Panel on Climate Change*, 423–552. https://doi.org/10.1017/9781009157896.005

France-Lanord, C., & Derry, L. A. (1997). Organic carbon burial forcing of the carbon cycle from himalayan erosion. *Nature*, *390*(6655), 65–67. https://doi.org/10.1038/36324

Frew, R. D., Dennis, P. F., Heywood, K. J., Meredith, M. P., & Boswell, S. M. (2000). The oxygen isotope composition of water masses in the northern north atlantic. *Deep Sea Research Part I: Oceanographic Research Papers*, *47*(12), 2265–2286. https://doi.org/10.1016/S0967-0637(00)00023-6

Friedlingstein, P., Jones, M. W., O'Sullivan, M., Andrew, R. M., Hauck, J., Peters, G. P., Peters, W., Pongratz, J., Sitch, S., Le Quéré, C., Bakker, D. C. E., Canadell, J. G., Ciais, P., Jackson, R. B., Anthoni, P., Barbero, L., Bastos, A., Bastrikov, V., Becker, M., … Zaehle, S. (2019). Global carbon budget 2019. *Earth System Science Data*, *11*(4), 1783–1838. https://doi.org/10.5194/essd-11-1783-2019

Gerlach, T. (2011). Volcanic versus anthropogenic carbon dioxide. *Eos, Transactions American Geophysical Union*, *92*(24), 201–202. https://doi.org/10.1029/2011EO240001

Ghosh, P., Adkins, J., Affek, H., Balta, B., Guo, W., Schauble, E. A., Schrag, D., & Eiler, J. M. (2006). 13c–18o bonds in carbonate minerals: A new kind of paleothermometer. *Geochimica et Cosmochimica Acta*, *70*(6), 1439–1456. https://doi.org/10.1016/j.gca.2005.11.014

Goudsmit-Harzevoort, B., Lansu, A., Baatsen, M. L. J., von der Heydt, A. S., de Winter, N. J., Zhang, Y., Abe-Ouchi, A., de Boer, A., Chan, W.-L., Donnadieu, Y., Hutchinson, D. K., Knorr, G., Ladant, J.-B., Morozova, P., Niezgodzki, I., Steinig, S., Tripati, A., Zhang, Z., Zhu, J., & Ziegler, M. (2023). The relationship between the global mean deep-sea and surface temperature during the early eocene. *Paleoceanography and Paleoclimatology*, *38*(3), e2022PA004532. https://doi.org/10.1029/2022PA004532

Gulev, S., Thorne, P., Ahn, J., Dentener, F., Domingues, C. M., Gerland, S., Gong, D., Kaufman, D., Nnamchi, H., Quaas, J., Rivera, J., Sathyendranath, S., Smith, S., Trewin, B., von Schuckmann, K., & Vose, R. (2021). Chapter 2: Changing state of the climate system. *Changing State of the Climate System. In Climate Change 2021: The Physical Science Basis. Contribution of Working Group I to the Sixth Assessment Report of the Intergovernmental Panel on Climate Change*, 287–422. https://doi.org/10.1017/9781009157896.004

Hansen, J., Jerram, D. A., McCAFFREY, K., & Passey, S. R. (2009). The onset of the north atlantic igneous province in a rifting perspective. *Geological Magazine*, *146*(3), 309–325. https://doi.org/10.1017/S0016756809006347

Hansen, J., Sato, M., Russell, G., & Kharecha, P. (2013). Climate sensitivity, sea level and atmospheric carbon dioxide. *Philosophical Transactions of the Royal Society A: Mathematical, Physical and Engineering Sciences*, *371*(2001), 20120294. https://doi.org/10.1098/rsta.2012.0294

He, B., Olack, G. A., & Colman, A. S. (2012). Pressure baseline correction and high-precision CO2 clumped-isotope (Δ47) measurements in bellows and micro-volume modes. *Rapid Communications in Mass Spectrometry*, *26*(24), 2837–2853. https://doi.org/10.1002/rcm.6436

Hoenisch, B. (2022, November 22). Paleo-CO2 data archive. https://doi.org/10.5281/zenodo.7348638

Holbourn, A., Henderson, A. S., & MacLeod, N. (2013, May 14). *Atlas of benthic foraminifera* (1st ed.). Wiley. https://doi.org/10.1002/9781118452493

Hotinski, R. M., & Toggweiler, J. R. (2003). Impact of a tethyan circumglobal passage on ocean heat transport and "equable" climates: TETHYAN CIRCUMGLOBAL PASSAGE IMPACT. *Paleoceanography*, *18*(1), n/a–n/a. https://doi.org/10.1029/2001PA000730

Hu, B., Radke, J., Schlüter, H.-J., Heine, F. T., Zhou, L., & Bernasconi, S. M. (2014). A modified procedure for gas-source isotope ratio mass spectrometry: The long-integration dual-inlet (LIDI) methodology and implications for clumped isotope measurements. *Rapid Communications in Mass Spectrometry*, *28*(13), 1413–1425. https://doi.org/10.1002/rcm.6909

Huntington, K. W., Eiler, J. M., Affek, H. P., Guo, W., Bonifacie, M., Yeung, L. Y., Thiagarajan, N., Passey, B., Tripati, A., Daëron, M., & Came, R. (2009). Methods and limitations of 'clumped' CO2 isotope (Δ47) analysis by gas-source isotope ratio mass spectrometry. *Journal of Mass Spectrometry*, *44*(9), 1318–1329. https://doi.org/10.1002/jms.1614

Huntington, K. W., & Petersen, S. V. (2023). Frontiers of carbonate clumped isotope thermometry. *Annual Review of Earth and Planetary Sciences*, *51*(1), annurev–earth–031621–085949. https://doi.org/10.1146/annurev-earth-031621-085949

Inglis, G. N., Bragg, F., Burls, N. J., Cramwinckel, M. J., Evans, D., Foster, G. L., Huber, M., Lunt, D. J., Siler, N., Steinig, S., Tierney, J. E., Wilkinson, R., Anagnostou, E., de Boer, A. M., Dunkley Jones, T., Edgar, K. M., Hollis, C. J., Hutchinson, D. K., & Pancost, R. D. (2020). Global mean surface temperature and climate sensitivity of the early eocene climatic optimum (EECO), paleocene–eocene thermal maximum (PETM), and latest paleocene. *Climate of the Past*, *16*(5), 1953–1968. https://doi.org/10.5194/cp-16-1953-2020

Jaffrés, J. B. D., Shields, G. A., & Wallmann, K. (2007). The oxygen isotope evolution of seawater: A critical review of a long-standing controversy and an improved geological water cycle model for the past 3.4 billion years. *Earth-Science Reviews*, *83*(1), 83–122. https://doi.org/10.1016/j.earscirev.2007.04.002

Katz, M. E., Katz, D. R., Wright, J. D., Miller, K. G., Pak, D. K., Shackleton, N. J., & Thomas, E. (2003). Early cenozoic benthic foraminiferal isotopes: Species reliability and interspecies correction factors: EARLY CENOZOIC BENTHIC FORAM ISOTOPE CORRECTION FACTORS. *Paleoceanography*, *18*(2), n/a–n/a. https://doi.org/10.1029/2002PA000798

Kennett, J. P. (1977). Cenozoic evolution of antarctic glaciation, the circum-antarctic ocean, and their impact on global paleoceanography. *Journal of Geophysical Research (1896-1977)*, *82*(27), 3843–3860. https://doi.org/10.1029/JC082i027p03843

Kim, S.-T., Mucci, A., & Taylor, B. E. (2007). Phosphoric acid fractionation factors for calcite and aragonite between 25 and 75 °c: Revisited. *Chemical Geology*, *246*(3), 135–146. https://doi.org/10.1016/j.chemgeo.2007.08.005

Knutti, R., Rugenstein, M. A. A., & Hegerl, G. C. (2017). Beyond equilibrium climate sensitivity. *Nature Geoscience*, *10*(10), 727–736. https://doi.org/10.1038/ngeo3017

Kocken, I. J., Müller, I. A., & Ziegler, M. (2019). Optimizing the use of carbonate standards to minimize uncertainties in clumped isotope data. *Geochemistry, Geophysics, Geosystems*, *20*(11), 5565–5577. https://doi.org/10.1029/2019GC008545

Kocken, I. J. (2022, December 21). *Clumped isotope thermometry in deep time palaeoceanography* [dr.]. Utrecht University. https://doi.org/10.33540/1425

Laskar, J., Fienga, A., Gastineau, M., & Manche, H. (2011). La2010: A new orbital solution for the long-term motion of the earth. *Astronomy & Astrophysics*, *532*, A89. https://doi.org/10.1051/0004-6361/201116836

Lear, C. H., Mawbey, E. M., & Rosenthal, Y. (2010). Cenozoic benthic foraminiferal mg/ca and li/ca records: Toward unlocking temperatures and saturation states. *Paleoceanography*, *25*(4). https://doi.org/10.1029/2009PA001880

Levitus, S., Antonov, J. I., Boyer, T. P., Baranova, O. K., Garcia, H. E., Locarnini, R. A., Mishonov, A. V., Reagan, J. R., Seidov, D., Yarosh, E. S., & Zweng, M. M. (2012). World ocean heat content and thermosteric sea level change (0–2000 m), 1955–2010. *Geophysical Research Letters*, *39*(10). https://doi.org/10.1029/2012GL051106

Lisiecki, L. E., & Raymo, M. E. (2005). A pliocene-pleistocene stack of 57 globally distributed benthic δ^{18} o records: PLIOCENE-PLEISTOCENE BENTHIC STACK. *Paleoceanography*, *20*(1), n/a–n/a. https://doi.org/10.1029/2004PA001071

Littler, K., Röhl, U., Westerhold, T., & Zachos, J. C. (2014). A high-resolution benthic stable-isotope record for the south atlantic: Implications for orbital-scale changes in late paleocene–early eocene climate and carbon cycling. *Earth and Planetary Science Letters*, *401*, 18–30. https://doi.org/10.1016/j.epsl.2014.05.054

Marchitto, T., Curry, W., Lynch-Stieglitz, J., Bryan, S., Cobb, K., & Lund, D. (2014). Improved oxygen isotope temperature calibrations for cosmopolitan benthic foraminifera. *Geochimica et Cosmochimica Acta*, *130*, 1–11. https://doi.org/10.1016/j.gca.2013.12.034

Martin, E. E., MacLeod, K. G., Jiménez Berrocoso, A., & Bourbon, E. (2012). Water mass circulation on demerara rise during the late cretaceous based on nd isotopes. *Earth and Planetary Science Letters*, *327-328*, 111–120. https://doi.org/10.1016/j.epsl.2012.01.037

Masson-Delmotte, V., Zhai, P., Pirani, A., Connors, S. L., Péan, C., Chen, Y., Goldfarb, L., Gomis, M. I., Matthews, J. B. R., Berger, S., Huang, M., Yelekçi, O., Yu, R., Zhou, B., Lonnoy, E., Maycock, T. K., Waterfield, T., & Leitzell, K. (2021). Working group i contribution to the sixth assessment report of the intergovernmental panel on climate change.

McCrea, J. M. (1950). On the isotopic chemistry of carbonates and a paleotemperature scale. *The Journal of Chemical Physics*, *18*(6), 849–857. https://doi.org/10.1063/1.1747785

Meckler, A. N., Sexton, P. F., Piasecki, A. M., Leutert, T. J., Marquardt, J., Ziegler, M., Agterhuis, T., Lourens, L. J., Rae, J. W. B., Barnet, J., Tripati, A., & Bernasconi, S. M. (2022). Cenozoic evolution of deep ocean temperature from clumped isotope thermometry. *Science*, *377*(6601), 86–90. https://doi.org/10.1126/science.abk0604

Meckler, A. N., Ziegler, M., Millán, M. I., Breitenbach, S. F. M., & Bernasconi, S. M. (2014). Long-term performance of the kiel carbonate device with a new correction scheme for clumped isotope measurements. *Rapid Communications in Mass Spectrometry*, *28*(15), 1705–1715. https://doi.org/10.1002/rcm.6949

Meinicke, N., Ho, S., Hannisdal, B., Nürnberg, D., Tripati, A., Schiebel, R., & Meckler, A. (2020). A robust calibration of the clumped isotopes to temperature relationship for foraminifers. *Geochimica et Cosmochimica Acta*, *270*, 160–183. https://doi.org/10.1016/j.gca.2019.11.022

Meinicke, N., Reimi, M. A., Ravelo, A. C., & Meckler, A. N. (2021). Coupled mg/ca and clumped isotope measurements indicate lack of substantial mixed layer cooling in the western pacific warm pool during the last $\sim$5 million years. *Paleoceanography and Paleoclimatology*, *36*(8), e2020PA004115. https://doi.org/10.1029/2020PA004115

Miller, K., Mountain, G., Wright, J., & Browning, J. (2011). A 180-million-year record of sea level and ice volume variations from continental margin and deep-sea isotopic records. *Oceanography*, *24*(2), 40–53. https://doi.org/10.5670/oceanog.2011.26

Miller, K. G., Kominz, M. A., Browning, J. V., Wright, J. D., Mountain, G. S., Katz, M. E., Sugarman, P. J., Cramer, B. S., Christie-Blick, N., & Pekar, S. F. (2005). The phanerozoic record of global sea-level change. *Science*, *310*(5752), 1293–1298. https://doi.org/10.1126/science.1116412

Miller, K. G., Wright, J. D., & Browning, J. V. (2005). Visions of ice sheets in a greenhouse world. *Marine Geology*, *217*(3), 215–231. https://doi.org/10.1016/j.margeo.2005.02.007

Müller, I. A., Fernandez, A., Radke, J., van Dijk, J., Bowen, D., Schwieters, J., & Bernasconi, S. M. (2017). Carbonate clumped isotope analyses with the long-integration dual-inlet (LIDI) workflow: Scratching at the lower sample weight boundaries. *Rapid Communications in Mass Spectrometry*, *31*(12), 1057–1066. https://doi.org/10.1002/rcm.7878

Pearson, P. N., & Palmer, M. R. (2000). Atmospheric carbon dioxide concentrations over the past 60 million years. *Nature*, *406*(6797), 695–699. https://doi.org/10.1038/35021000

Peral, M., Daëron, M., Blamart, D., Bassinot, F., Dewilde, F., Smialkowski, N., Isguder, G., Bonnin, J., Jorissen, F., Kissel, C., Michel, E., Vázquez Riveiros, N., & Waelbroeck, C. (2018). Updated calibration of the clumped isotope thermometer in planktonic and benthic foraminifera. *Geochimica et Cosmochimica Acta*, *239*, 1–16. https://doi.org/10.1016/j.gca.2018.07.016

Pérez-Díaz, L., & Eagles, G. (2017). South atlantic paleobathymetry since early cretaceous. *Scientific Reports*, *7*(1), 11819. https://doi.org/10.1038/s41598-017-11959-7

Peterse, F., van der Meer, J., Schouten, S., Weijers, J. W. H., Fierer, N., Jackson, R. B., Kim, J.-H., & Sinninghe Damsté, J. S. (2012). Revised calibration of the MBT–CBT paleotemperature proxy based on branched tetraether membrane lipids in surface soils. *Geochimica et Cosmochimica Acta*, *96*, 215–229. https://doi.org/10.1016/j.gca.2012.08.011

Rae, J. W., Zhang, Y. G., Liu, X., Foster, G. L., Stoll, H. M., & Whiteford, R. D. (2021). Atmospheric CO_2 over the past 66 million years from marine archives. *Annual Review of Earth and Planetary Sciences*, *49*(1), 609–641. https://doi.org/10.1146/annurev-earth-082420-063026

Rathmann, S., & Kuhnert, H. (2008). Carbonate ion effect on mg/ca, sr/ca and stable isotopes on the benthic foraminifera oridorsalis umbonatus off namibia. *Marine Micropaleontology*, *66*(2), 120–133. https://doi.org/10.1016/j.marmicro.2007.08.001

Ravelo, A. C., & Hillaire-Marcel, C. (2007). Chapter eighteen the use of oxygen and carbon isotopes of foraminifera in paleoceanography. In *Developments in marine geology* (pp. 735–764, Vol. 1). Elsevier. https://doi.org/10.1016/S1572-5480(07)01023-8

Raymo, M. E., Ruddiman, W. F., & Froelich, P. N. (1988). Influence of late cenozoic mountain building on ocean geochemical cycles. *Geology*, *16*(7), 649–653. https://doi.org/10.1130/0091-7613(1988)016<0649:IOLCMB>2.3.CO;2

Rohling, E. J., Rohling, E. J., Sluijs, A., Dijkstra, H. A., Köhler, P., van de Wal, R. S. W., von der Heydt, A. S., Beerling, D. J., Berger, A., Bijl, P. K., Crucifix, M., DeConto, R., Drijfhout, S. S., Fedorov, A., Foster, G. L., Ganopolski, A., Hansen, J., Hönisch, B., Hooghiemstra, H., … PALAEOSENS Project Members. (2012). Making sense of palaeoclimate sensitivity. *Nature*, *491*(7426), 683–691. https://doi.org/10.1038/nature11574

Rohling, E. J. (2017). *The oceans: A deep history*. Princeton University Press.

Rohling, E. J., & Bigg, G. R. (1998). Paleosalinity and δ18o: A critical assessment. *Journal of Geophysical Research: Oceans*, *103*, 1307–1318. https://doi.org/10.1029/97JC01047

Sames, B., Wagreich, M., Conrad, C. P., & Iqbal, S. (2020). Aquifer-eustasy as the main driver of short-term sea-level fluctuations during cretaceous hothouse climate phases. *Geological Society, London, Special Publications*, *498*(1), 9–38. https://doi.org/10.1144/SP498-2019-105

Schouten, S., Hopmans, E. C., Schefuß, E., & Sinninghe Damsté, J. S. (2002). Distributional variations in marine crenarchaeotal membrane lipids: A new tool for reconstructing ancient sea water temperatures? *Earth and Planetary Science Letters*, *204*(1), 265–274. https://doi.org/10.1016/S0012-821X(02)00979-2

Seneviratne, S., Zhang, X., Adnan, M., Badi, W., Dereczynski, C., Di Luca, A., Ghosh, S., Iskander, I., Kossin, J., Lewis, S., Otto, F., Pinto, I., Satoh, M., Vicente-Serrano, S., Wehner, M., & Zhou, B. (2021). Chapter 11: Weather and climate extreme events in a changing climate. *Weather and Climate Extreme Events in a Changing Climate. In Climate Change 2021: The Physical Science Basis. Contribution of Working Group I to the Sixth Assessment Report of the Intergovernmental Panel on Climate Change*, 1513–1766. https://doi.org/10.1017/9781009157896.013

Shackleton, N. J. (1974). ATTAINMENT OF ISOTOPIC EQUILIBRIUM BETWEEN OCEAN WATER AND THE BENTHONIC FORAMINIFERA GENUS UVIGERINA : ISOTOPIC CHANGES IN THE OCEAN DURING THE LAST GLACIAL, 7.

Spencer, C., & Kim, S.-T. (2015). Carbonate clumped isotope paleothermometry: A review of recent advances in CO2 gas evolution, purification, measurement and standardization techniques. *Geosciences Journal*, *19*(2), 357–374. https://doi.org/10.1007/s12303-015-0018-1

Stevens, B., Sherwood, S. C., Bony, S., & Webb, M. J. (2016). Prospects for narrowing bounds on earth's equilibrium climate sensitivity. *Earth's Future*, *4*(11), 512–522. https://doi.org/10.1002/2016EF000376

Tierney, J. E., Poulsen, C. J., Montañez, I. P., Bhattacharya, T., Feng, R., Ford, H. L., Hönisch, B., Inglis, G. N., Petersen, S. V., Sagoo, N., Tabor, C. R., Thirumalai, K., Zhu, J., Burls, N. J., Foster, G. L., Goddéris, Y., Huber, B. T., Ivany, L. C., Kirtland Turner, S., … Zhang, Y. G. (2020). Past climates inform our future. *Science*, *370*(6517), eaay3701. https://doi.org/10.1126/science.aay3701

Torfstein, A., & Steinberg, J. (2020). The oligo–miocene closure of the tethys ocean and evolution of the proto-mediterranean sea. *Scientific Reports*, *10*(1), 13817. https://doi.org/10.1038/s41598-020-70652-4

Uchikawa, J., & Zeebe, R. E. (2010). Examining possible effects of seawater pH decline on foraminiferal stable isotopes during the paleocene-eocene thermal maximum: PETM FORAM ISOTOPES BIASED BY OCEAN pH? *Paleoceanography*, *25*(2). https://doi.org/10.1029/2009PA001864

Uenzelmann-Neben, G., Weber, T., Grützner, J., & Thomas, M. (2017). Transition from the cretaceous ocean to cenozoic circulation in the western south atlantic — a twofold reconstruction. *Tectonophysics*, *716*, 225–240. https://doi.org/10.1016/j.tecto.2016.05.036

Usdowski, E., & Hoefs, J. (1993). Oxygen isotope exchange between carbonic acid, bicarbonate, carbonate, and water: A re-examination of the data of McCrea (1950) and an expression for the overall partitioning of oxygen isotopes between the carbonate species and water. *Geochimica et Cosmochimica Acta*, *57*(15), 3815–3818. https://doi.org/10.1016/0016-7037(93)90159-T

van der Ploeg, R., Cramwinckel, M. J., Kocken, I. J., Leutert, T. J., Bohaty, S. M., Fokkema, C. D., Hull, P. M., Meckler, A. N., Middelburg, J. J., Müller, I. A., Penman, D. E., Peterse, F., Reichart, G.-J., Sexton, P. F., Vahlenkamp, M., De Vleeschouwer, D., Wilson, P. A., Ziegler, M., & Sluijs, A. (2023). North atlantic surface ocean warming and salinization in response to middle eocene greenhouse warming. *Science Advances*, *9*(4), eabq0110. https://doi.org/10.1126/sciadv.abq0110

Via, R. K., & Thomas, D. J. (2006). Evolution of atlantic thermohaline circulation: Early oligocene onset of deep-water production in the north atlantic. *Geology*, *34*(6), 441–444. https://doi.org/10.1130/G22545.1

Wallmann, K. (2001). Controls on the cretaceous and cenozoic evolution of seawater composition, atmospheric CO2 and climate. *Geochimica et Cosmochimica Acta*, *65*(18), 3005–3025. https://doi.org/10.1016/S0016-7037(01)00638-X

Wang, Z., Schauble, E. A., & Eiler, J. M. (2004). Equilibrium thermodynamics of multiply substituted isotopologues of molecular gases. *Geochimica et Cosmochimica Acta*, *68*(23), 4779–4797. https://doi.org/10.1016/j.gca.2004.05.039

Watson, A. J., Schuster, U., Shutler, J. D., Holding, T., Ashton, I. G. C., Landschützer, P., Woolf, D. K., & Goddijn-Murphy, L. (2020). Revised estimates of ocean-atmosphere CO2 flux are consistent with ocean carbon inventory. *Nature Communications*, *11*(1), 1–6. https://doi.org/10.1038/s41467-020-18203-3

Weijers, J. W. H., Schouten, S., Sluijs, A., Brinkhuis, H., & Sinninghe Damsté, J. S. (2007). Warm arctic continents during the palaeocene–eocene thermal maximum. *Earth and Planetary Science Letters*, *261*(1), 230–238. https://doi.org/10.1016/j.epsl.2007.06.033

Westerhold, T., Marwan, N., Drury, A. J., Liebrand, D., Agnini, C., Anagnostou, E., Barnet, J. S. K., Bohaty, S. M., De Vleeschouwer, D., Florindo, F., Frederichs, T., Hodell, D. A., Holbourn, A. E., Kroon, D., Lauretano, V., Littler, K., Lourens, L. J., Lyle, M., Pälike, H., … Zachos, J. C. (2020). An astronomically dated record of earth's climate and its predictability over the last 66 million years. *Science*, *369*(6509), 1383–1387. https://doi.org/10.1126/science.aba6853

Westerhold, T., Röhl, U., Frederichs, T., Agnini, C., Raffi, I., Zachos, J. C., & Wilkens, R. H. (2017). Astronomical calibration of the ypresian timescale: Implications for seafloor spreading rates and the chaotic behavior of the solar system? *Climate of the Past*, *13*(9), 1129–1152. https://doi.org/10.5194/cp-13-1129-2017

Westerhold, T., Röhl, U., Raffi, I., Fornaciari, E., Monechi, S., Reale, V., Bowles, J., & Evans, H. F. (2008). Astronomical calibration of the paleocene time. *Palaeogeography, Palaeoclimatology, Palaeoecology*, *257*(4), 377–403. https://doi.org/10.1016/j.palaeo.2007.09.016

Westerhold, T., Röhl, U., Wilkens, R. H., Gingerich, P. D., Clyde, W. C., Wing, S. L., Bowen, G. J., & Kraus, M. J. (2018). Synchronizing early eocene deep-sea and continental records – cyclostratigraphic age models for the bighorn basin coring project drill cores. *Climate of the Past*, *14*(3), 303–319. https://doi.org/10.5194/cp-14-303-2018

Zachos, J., Pagani, M., Sloan, L., Thomas, E., & Billups, K. (2001). Trends, rhythms, and aberrations in global climate 65 ma to present. *Science*, *292*(5517), 686–693. https://doi.org/10.1126/science.1059412

Zachos, J., Kroon, D., Blum, P., & et al. (Eds.). (2004, June 21). *Proceedings of the ocean drilling program, 208 initial reports* (Vol. 208). Ocean Drilling Program. https://doi.org/10.2973/odp.proc.ir.208.2004

Zeebe, R. E. (2001). Seawater pH and isotopic paleotemperatures of cretaceous oceans. *Palaeogeography, Palaeoclimatology, Palaeoecology*, *170*(1), 49–57. https://doi.org/10.1016/S0031-0182(01)00226-7

Zeebe, R. E., & Zachos, J. C. (2007). Reversed deep-sea carbonate ion basin gradient during paleocene-eocene thermal maximum. *Paleoceanography*, *22*(3). https://doi.org/10.1029/2006PA001395

Zhang, Y., Huck, T., Lique, C., Donnadieu, Y., Ladant, J.-B., Rabineau, M., & Aslanian, D. (2020). Early eocene vigorous ocean overturning and its contribution to a warm southern ocean. *Climate of the Past*, *16*(4), 1263–1283. https://doi.org/10.5194/cp-16-1263-2020